UNIVERSITY OF OKLAHOMA

GRADUATE COLLEGE

HOST-GUEST COMPLEXATION OF BENZYL AND XYLYL AMMONIUM GUESTS WITH CUCURBIT[7]URIL FOR SHUTTLE ROTAXANES

A DISSERTATION

SUBMITTED TO THE GRADUATE FACULTY

in partial fulfillment of the requirements for the

Degree of

DOCTOR OF PHILOSOPHY

By

JUSTIN TRAVIS GARRETT
Norman, Oklahoma
2017

HOST-GUEST COMPLEXATION OF BENZYL AND XYLYL AMMONIUM GUESTS WITH CUCURBIT[7]URIL FOR SHUTTLE ROTAXANES

A DISSERTATION APPROVED FOR THE
DEPARTMENT OF CHEMISTRY AND BIOCHEMISTRY

BY

_____
Dr. Ronald Halterman, Chair

_____
Dr. Daniel Glatzhofer

_____
Dr. Kenneth Nicholas

_____
Dr. Wai Tak Yip

_____
Dr. Lloyd Bumm

© Copyright by JUSTIN TRAVIS GARRETT 2017
All Rights Reserved.

I dedicate this work to my wife, Haley Garrett,
and to my parents Roger and Karen Garrett.

Acknowledgements

First and foremost, I need to thank my amazing wife Haley for always being by my side by loving, supporting, and encouraging me throughout this journey. She is the best thing that has ever happened to me and has always kept me grounded and focused on what is important in life, and I am extremely grateful for her love and support. I would also like to thank my parents for their love and always believing in me and encouraging me to be the best I can be no matter what.

The work presented here would not have been possible without the vision and guidance of my advisor Dr. Ronald Halterman. I am sincerely grateful for his friendship, mentoring, and encouragement.

I would like to thank the members of my doctoral advisory committee Dr. Daniel Glatzhofer, Dr. Ken Nicholas, Dr. Wai Tak Yip, and Dr. Lloyd Bumm and all of the University of Oklahoma, Department of Chemistry and Biochemistry faculty for their advice and encouragement throughout the years. I would like to thank Dr. Steven Foster for his help with Mass Spectrometry, his friendship and inspiring conversations. I would also like to thank Dr. Susan Nimmo for her assistance with NMR spectroscopy. I express thanks to Louis Redfern for his encouragement and working along side of me in my research. I would also like to give thanks to all of my friends without listing their names for their encouragement.

Table of Contents

Acknowledgements iv

List of Tables viii

List of Figures ix

Abstract xviii

Chapter 1: Introduction 1

1.1 Mechanically Interlocked Molecules (MIMs) 3

1.2 Cucurbiturils 5

1.3 Research Focus 12

1.4 References 19

Chapter 2: Host-Guest Binding of N-Substituted Benzylammonium Guests with Cucurbit[7]uril 24

2.1 Introduction to Host-Guest Chemistry and Association Constants 24

2.2 Specific Aims 30

2.3 Synthesis 33

2.4 Results and Discussion 34

2.5 Conclusion 40

2.6 Experimental 40

2.7 References 61

Chapter 3: Development and Analysis of Stoppering Groups for Viologen Rotaxanes 64

3.1 Introduction to Rotaxanes 64

3.2 Specific Aims 72

3.3 Synthesis 73

3.4 Results and Discussion 75

3.4.1 Theoretical Investigations of Bis(3,5-diisopropoxybenzyl)-4,4'-bipyridinium Dibromide with Cucurbit[7]uril 76

3.4.2 Spectroscopic Investigations of Bis(3,5-dimethoxybenzyl)-4,4'-bipyridinium Dibromide with Cucurbit[7]uril 78

3.4.3 Spectroscopic Investigations of Bis(3,5-diisopropoxybenzyl)-4,4'-bipyridinium Dibromide with Cucurbit[7]uril 80

3.5 Conclusion 84

3.6 Experimental 85

3.7 References 96

Chapter 4: Investigation of Stopper Effectiveness of Cucurbit[7]uril Shuttle Rotaxanes 99

4.1 Introduction 99

4.2 Specific Aims 102

4.3 Synthesis 104

4.4 Results and Discussion 106

4.4.1 Spectroscopic Investigations of 1-(3,5-diisopropoxybenzyl)-4-(4-((diisopropylamino)methyl)benzyloxymethyl)-1,2,3-triazole with Cucurbit[7]uril 107

4.4.2 Spectroscopic Investigations of *p*-Bis(isopropylaminomethyl)benzene with Cucurbit[7]uril 111

4.4.3 Spectroscopic Investigations of *p*-Bis(diisopropylaminomethyl) benzene with Cucurbit[7]uril 112

4.4.4 Determination of Binding Constants of Bis-(N-substituted)-xylenediamines 116

4.5 Conclusion 119

4.6 Future Directions 120

4.7 Experimental 122

4.8 References 139

List of Tables

Table 1.1 Dimensions and aqueous solubilities of CB[n]..... 7

Table 2.1 1:1 Absolute binding constant values (K_a) for (Guest: CB[7])..... 38

Table 4.1 1:1 Absolute binding constant values (K_a) for (Guest: CB[7])..... 118

List of Figures

Figure 1.1 a) fluorescence-on response due to CB[7] binding to viologen-dyad, b) fluorescence off-on shuttle rotaxane molecular sensor, c) shuttling of CB[7] between docking sites on a rotaxane induced by external stimuli. 2

Figure 1.2 Cartoon representation of a) [2]catenane, b) [2]rotaxane, c) molecular knot, d) Borromean Rings.....3

Figure 1.3 Sauvage's Cu^1 catenane synthesis using a 1,10-phenanthroline-based thread (17) and a 1,10-phenanthroline-containing ring (19). Formation of 18-Cu^1 from 17 and 19 is quantitative, subsequent ring closure gives catenane 20-Cu^1 in 42% yield.....5

Figure 1.4 Syntheisis of Cucurbituril.....6

Figure 1.5 a) Internal complex of methyl viologen (MV2+) and CB[7], b) partial 1H-NMR spectra of MV2+ in the presence of 1 equivalent of CB[7], c) partial 1H-NMR spectra of MV2+ in the absence of CB[7].....10

Figure 1.6 External complex of benzyl viologen and CB[7].....10

Figure 1.7 pH-controlled shuttling of CB[7] between viologen and carboxylic acid terminated pseudorotaxane.....11

Figure 1.8 Guest compounds used by the Isaacs group to study binding affinity with CB[7].....12

Figure 1.9 Cartoon representation of a surface attached molecular sensing rotaxane....14

Figure 1.10 Analogs of bulky benzyl ammonium stopper (top), and competitive binding of CB[7] with ammonium stopper and silane (bottom).....16

Figure 1.11 Host-guest interactions of CB[7] and bis(3,5-dimethoxybenzyl)-viologen (top) and bis(3,5-diisopropoxybenzyl)-viologen (bottom).....17

Figure 1.12 Synthesis of model rotaxane using Copper (Cu)-catalyzed Azide-Alkyne cycloaddition CuAAC "Click chemistry" (top) and investigation of ammonium stopper stability to CB[7](bottom).....18

Figure 2.1 Molecular recognition between host molecule and selected complimentary guest molecule to form a host-guest supramolecular complex.....24

Figure 2.2 Line drawing of various reported macrocyclic hosts. 2a) crown ether, 2b) cryptand, 2c) cyclophane, 2d) calix[4]arene, 2e) resorcin[4]arene, 2f) bridged resorcin[4]arene, 2g) beta-cyclodextrin, 2h) cucurbit[7]uril.....26

Figure 2.3 Preparation of Cucurbiturils from glycoluril and paraformaldehyde under acidic conditions.....27

Figure 2.4 External complexation of benzylviologen 1^{2+} and CB[7].....28

Figure 2.5 Selected guests dimethylviologen 10, p-xylyenediamine 20, and trimethylsilylpropanoic acid 12 used by the Isaacs group to study binding affinity with CB[7].....28

Figure 2.6 Proposed benzyl amine stoppers.....31

Figure 2.7 Width dimensions of a) triisopropylsilyl group, b) paraquat-cyclophane, c) diisopropyl amino group, d) CB[7].....32

Figure 2.8 Cartoon representation of the competitive binding of CB[7] (orange rectangle) between benzyl ammonium A and viologen-dyad B.....32

Figure 2.9 Synthetic scheme of benzyl amine stoppers 4-((diisopropylamino)methyl)benzyl alcohol (2.1a), 4-((diisopropyl-

amino)methyl)benzyl methyl ether (2.2b), 4-((diisopropylamino)methyl)benzyl propargyl ether (2.3c).....34

Figure 2.10 Line drawing of 2.4d 3-(Trimethylsilyl)propanoic-2,2,3,3-d4 acid $(Me)_3SiCD_2CD_2COOH$ (TMSP) and 1:1 binding constant with CB[7].....35

Figure 2.11 Equations outlining concentrations of unbound and bound guests with CB[7]. Using the concentration of all species allow for calculation of K_{rel} and the absolute K_a for the competing guest.....37

Figure 2.12 ^{1}H NMR (400 MHz, $CDCl_3$) spectrum of methyl 4-(bromomethyl)benzoate.....42

Figure 2.13 ^{13}C NMR (101 MHz, $CDCl_3$) spectrum of methyl 4-(bromomethyl)benzoate.....42

Figure 2.14 ^{1}H NMR (300 MHz, $CDCl_3$) spectrum of methyl 4-((diisopropylamino)methyl)benzoate.....44

Figure 2.15 ^{13}C NMR (75 MHz, $CDCl_3$) spectrum of methyl 4-((diisopropylamino)methyl)benzoate.....44

Figure 2.16 ^{1}H NMR (300 MHz, $CDCl_3$) spectrum of 2.1a 4-((diisopropylamino)methyl)benzyl alcohol.....46

Figure 2.17 ^{13}C NMR (101 MHz, $CDCl_3$) spectrum of 2.1a 4-((diisopropylamino)methyl)benzyl alcohol.....46

Figure 2.18 ^{1}H NMR (300 MHz, $CDCl_3$) spectrum of 4-((diisopropylamino)methyl)benzyl methyl ether.....48

Figure 2.19 ^{13}C NMR (75 MHz, $CDCl_3$) spectrum of 4-((diisopropylamino)methyl)benzyl methyl ether.....48

Figure 2.20 ^{1}H NMR (300 MHz, $CDCl_3$) spectrum of 4-((diisopropylamino)methyl)benzyl propargyl ether.....50

Figure 2.21 ^{13}C NMR (101 MHz, $CDCl_3$) spectrum of 4-((diisopropylamino)methyl)benzyl propargyl ether.....50

Figure 2.22 ^{1}H NMR (300 MHz, D_2O) spectrum of Cucurbit[7]uril.....52

Figure 2.23 ^{13}C NMR (126 MHz, D_2O) spectrum of Cucurbit[7]uril.....52

Figure 2.24 ^{1}H-NMR (500 MHz, $Na(O_2CCD_3)$-buffered D_2O (pD = 4.45)) spectrum 1 of competitive binding of 2.1a, 2.4d, and CB[7].....54

Figure 2.25 ^{1}H-NMR (500 MHz, $Na(O_2CCD_3)$-buffered D_2O (pD = 4.45)) spectrum 2 of competitive binding of 2.1a, 2.4d, and CB[7].....54

Figure 2.26 ^{1}H-NMR (500 MHz, $Na(O_2CCD_3)$-buffered D_2O (pD = 4.45)) spectrum 3 of competitive binding of 2.1a, 2.4d, and CB[7].....55

Figure 2.27 ^{1}H-NMR (500 MHz, $Na(O_2CCD_3)$-buffered D_2O (pD = 4.45)) spectrum 1 of competitive binding of 2.2b, 2.4d, and CB[7].....56

Figure 2.28 ^{1}H-NMR (500 MHz, $Na(O_2CCD_3)$-buffered D_2O (pD = 4.45)) spectrum 2 of competitive binding of 2.2b, 2.4d, and CB[7].....57

Figure 2.29 ^{1}H-NMR (500 MHz, $Na(O_2CCD_3)$-buffered D_2O (pD = 4.45)) spectrum 3 of competitive binding of 2.2b, 2.4d, and CB[7].....57

Figure 2.30 ^{1}H-NMR (500 MHz, $Na(O_2CCD_3)$-buffered D_2O (pD = 4.45)) spectrum 1 of competitive binding of 2.3c, 2.4d, and CB[7].....59

Figure 2.31 ^{1}H-NMR (500 MHz, $Na(O_2CCD_3)$-buffered D_2O (pD = 4.45)) spectrum 2 of competitive binding of 2.3c, 2.4d, and CB[7].....59

Figure 2.32 ^{1}H-NMR (500 MHz, Na(O_2CCD_3)-buffered D_2O (pD = 4.45)) spectrum 3 of competitive binding of 2.3c, 2.4d, and CB[7].....60

Figure 3.1 Cartoon representation of rotaxane, pseudorotaxane, semirotaxane.....64

Figure 3.2 Cartoon representation of the construction of rotaxanes.....66

Figure 3.3 Cartoon representation of the types of molecular mobility of rotaxanes.....67

Figure 3.4 Paraquat-cyclophane rotaxane from Stoddart et. al.....68

Figure 3.5 Paraquat-cyclophane shuttles mediated by pH and electrochemical oxidation from Stoddart and Kaifer et. al.....69

Figure 3.6 Molecular switch based cucurbit[6]uril rotaxane by Tuncel and co-workers.....70

Figure 3.7 Fluorescence-On CB[7] viologen-dyad pseudorotaxane from Singh and Halterman.....71

Figure 3.8 Figure of proposed viologen rotaxane stoppers, (left) bis(3,5-dimethoxybenzyl)-4,4'-bipyridinium dibromide 3.1A, (right) bis(3,5-diisopropoxybenzyl)-4,4'-bipyridinium dibromide 3.2B.....73

Figure 3.9 Synthetic scheme for the syntheisis of 3.1A bis(3,5-dimethoxybenzyl)-4,4'-bipyridinium dibromide..... 74

Figure 3.10 Synthetic scheme for the syntheisis of 3.2B bis(3,5-diisopropoxybenzyl)-4,4'-bipyridinium dibromide.....75

Figure 3.11 External complexation of 3.2B with CB[7].....76

Figure 3.12 Internal Complexation of 3.2B with CB[7].....77

Figure 3.13 ^{1}H-NMR spectra (400 MHz, D_2O) of CB[7] (top), bis(3,5-dimethoxybenzyl)-4,4'-bipyridinium dibromide 3.1A in the presence of 1:1 (middle) and absence of CB[7] (bottom).....78

Figure 3.14 ^{1}H-NMR spectra of (400 MHz, D_2O) of bis(3,5-dimethoxybenzyl)-4,4'-bipyridinium dibromide 3.1A with CB[7] and adamantylammonium (0 to 1 equivalent).....80

Figure 3.15 ^{1}H-NMR spectra of (400 MHz, D_2O) of bis(3,5-diisopropoxybenzyl)-4,4'-bipyridinium dibromide 3.2B with CB[7] (0 to 1 equivalent at times 1 min to 8d).....82

Figure 3.16 ^{1}H NMR spectra of (400 MHz, D_2O) of bis(3,5-diisopropoxybenzyl)-4,4'-bipyridinium dibromide 3.2B with CB[7] (0 to 1 equivalent at times 1 min to 8 d and after heating at 80 °C for 24 h).....83

Figure 3.17 ^{1}H NMR (400 MHz, $CDCl_3$) spectrum of isopropyl 3,5-diiso-propoxybenzoate.....86

Figure 3.18 ^{13}C NMR (101 MHz, $CDCl_3$) spectrum of isopropyl 3,5-diiso-propoxybenzoate.....86

Figure 3.19 ^{1}H NMR (500 MHz, $CDCl_3$) spectrum of 3,5-diisopropoxybenzyl alcohol.....88

Figure 3.20 ^{13}C NMR (126 MHz, $CDCl_3$) spectrum of 3,5-diisopropoxybenzyl alcohol.....88

Figure 3.21 ^{1}H NMR (500 MHz, $CDCl_3$) spectrum of 3,5-diisopropoxybenzyl bromide.....90

Figure 3.22 ^{13}C NMR (126 MHz, $CDCl_3$) spectrum of 3,5-diisopropoxybenzyl bromide.....90

Figure 3.23 ^{1}H NMR (400 MHz, D_2O) spectrum of bis(3,5-dimethoxybenzyl)-4,4'-bipyridinium dibromide.....91

Figure 3.24 ^{1}H NMR (400 MHz, D_2O) spectrum of bis(3,5-diisopropoxybenzyl)-4,4'-bipyridinium dibromide.....93

Figure 4.1 Schematic depiction of differential "chemical nose" based sensing array using imprinted polymers.....100

Figure 4.2 Schematic of proposed surface-attached fluorescence-on sensor.....101

Figure 4.3 Synthetic scheme of copper(I)-catalyzed azide-alkyne cycloaddition (Cu-AAC).....103

Figure 4.4 Proposed model rotaxane (top), model rotaxane with two docking sites for CB[7] shuttling.....104

Figure 4.5 Synthetic scheme of 1-(3,5-diisopropoxybenzyl)-4-(4-((diisopropyl-amino)methyl)benzyloxymethyl)-1,2,3-triazole 4.2b.....105

Figure 4.6 Synthetic scheme *p*-bis(isopropylaminomethyl)benzene 4.3c, and *p*-bis-(diisopropylaminomethyl)benzene 4.4d.....106

Figure 4.7 ^{1}H NMR spectra of (500 MHz, D_2O) of 1-(3,5-diisopropoxybenzyl)-4-(4-((diisopropylamino)methyl)benzyloxymethyl)-1,2,3-triazole 4.2b with CB[7] (0 to 1 equivalent at times 1 min to 48 h).....108

Figure 4.8 ^{1}H NMR spectra of (500 MHz, D_2O) of 1-(3,5-diisopropoxybenzyl)-4-(4-((diisopropylamino)methyl)benzyloxymethyl)-1,2,3-triazole 4.2b with CB[7] and adamantylammonium (0 to 1 equivalent).....110

Figure 4.9 ^{1}H NMR spectra of (500 MHz, D_2O) of *p*-bis(isopropylaminomethyl)benzene 4.3c with CB[7] (0 to 2 equivalents).....112

Figure 4.10 ^{1}H NMR spectra of (500 MHz, D_2O) of *p*-bis(diisopropylaminomethyl)benzene 4.4d with CB[7] (0 to 2 equivalents)....114

Figure 4.11 ^{1}H NMR spectra of (500 MHz, D_2O) of *p*-bis(diisopropyl-aminomethyl)benzene 4.4d with CB[7] and adamantylammonium (0 to 1 equivalent).....115

Figure 4.12 Line drawing of (trimethylsilyl)methylamine $(Me)_3SiCH_2NH_2$ 4.5e.....116

Figure 4.13 Equations outlining concentrations of bound and unbound guests with CB[7]. Using the concentrations of all species allow for calculationd of K_{rel} and the absolute K_a for the competing guest.....118

Figure 4.14 ^{1}H NMR (500 MHz, D_2O DCl) spectrum of *p*-bis(isopropylaminomethyl)-benzene.....123

Figure 4.15 ^{13}C NMR (75 MHz, $CDCl_3$) spectrum of *p*-bis(isopropylaminomethyl)-benzene.....123

Figure 4.16 ^{1}H NMR (500 MHz, D_2O DCl) spectrum of *p*-Bis(diisopropylaminomethyl)-benzene.....125

Figure 4.17 ^{13}C NMR (101 MHz, $CDCl_3$) spectrum of *p*-bis(diisopropylaminomethyl-benzene.....125

Figure 4.18 ^{1}H NMR (400 MHz, $CDCl_3$) spectrum of 3,5-diisopropoxybenzyl azide.....127

Figure 4.19 ^{13}C NMR (101 MHz, $CDCl_3$) spectrum of 3,5-diisopropoxybenzyl azide.....127

Figure 4.20 ^{1}H NMR (500 MHz, $CDCl_3$) spectrum of 1-(3,5-diisopropoxybenzyl)-4-(4-((diisopropylamino)methyl)benzyloxymethyl)-1,2,3-triazole.....129

Figure 4.21 ^{13}C NMR (126 MHz, $CDCl_3$) spectrum of 1-(3,5-diisopropoxybenzyl)-4-(4-((diisopropylamino)methyl)benzyloxymethyl)-1,2,3-triazole.....129

Figure 4.22 ^{1}H NMR (500 MHz, $Na(O_2CCD_3)$-buffered D_2O (pD = 4.45)) spectrum 1 of competitive binding of 4.3c, 4.5e, and CB[7].....131

Figure 4.23 ^{1}H NMR (500 MHz, $Na(O_2CCD_3)$-buffered D_2O (pD = 4.45)) spectrum 2 of competitive binding of 4.3c, 4.5e, and CB[7].....131

Figure 4.24 ^{1}H NMR (500 MHz, $Na(O_2CCD_3)$-buffered D_2O (pD = 4.45)) spectrum 3 of competitive binding of 4.3c, 4.5e, and CB[7].....132

Figure 4.25 ^{1}H NMR (500 MHz, $Na(O_2CCD_3)$-buffered D_2O (pD = 4.45)) spectrum 1 of competitive binding of 4.4d, 4.5e, and CB[7].....134

Figure 4.26 ^{1}H NMR (500 MHz, $Na(O_2CCD_3)$-buffered D_2O (pD = 4.45)) spectrum 2 of competitive binding of 4.4d, 4.5e, and CB[7].....134

Figure 4.27 ^{1}H NMR (500 MHz, $Na(O_2CCD_3)$-buffered D_2O (pD = 4.45)) spectrum 3 of competitive binding of 4.4d, 4.5e, and CB[7].....135

Abstract

Bistable rotaxanes are considered to be important design elements of molecular devices for a wide range of applications, such as controlled drug release, molecular machines, and molecular sensors and shuttles. The interest in molecular shuttles comes from the possibility of achieving controlled submolecular motion of their components with respect to each other. Cucurbiturils have become highly attractive for such applications due to their affinity to form host–guest complexes with ammonium and diammonium salts and have also been used for the construction of supramolecular assemblies that demonstrate intriguing structural, and functional properties. However, little research has been conducted to explore the use of cucurbituril, in particular cucurbit[7]uril (CB[7]), as a molecular shuttle within a rotaxane based molecular sensor. Our aim was targeted to expand the scope of CB[7] host-guest chemistry for shuttle rotaxanes (i) by developing suitable binding guests equipped with efficient stoppers and (ii) by investigating rotaxane formation under mild conditions.

A series of benzyl ammonium analogues incorporating bulky end groups (diisopropyl) and variable groups at the para position were synthesized for usage as suitable rotaxane binding stoppers. The host-guest complexes between CB[7] and the benzyl ammonium analogues were analyzed in competition binding experiments with NMR spectroscopy. The 1:1 equilibrium binding constants show binding affinities of $K_a \cong 10^5\ M^{-1}$.

Supramolecular complexes between CB[7] and select 4,4'-dipyridiunium dications (viologens) containing sizeable end groups were explored with the intent to sterically block CB[7] from forming a full inclusion complex. When the larger end

groups (3,5-diisopropoxybenzyl) were present, the CB[7] could only form a transient complex at the periphery even after heating to 80 °C for 24 h.

Lastly, rotaxane formation with a benzyl ammonium stopper containing a terminal alkyne and a benzyl azide *via* copper (Cu)-catalyzed azide-alkyne cycloaddition (CuAAC) was explored to provide a model rotaxane to examine stopper efficiency against CB[7] encapsulation. The CB[7] was shown to pass over the bulky end groups of the benzyl ammonium resulting in the formation of an inclusion complex. Xylyl diammonium analogues containing various sizes of endgroups were also explored to confirm stoppering efficiency against CB[7]. Host-guest complexes with CB[7] and the xylyl diammonium analogues were analyzed in competition binding experiments and had shown strong binding affinities with 1:1 equilibrium binding constants of $K_a \cong 10^9\ M^{-1}$.

Chapter 1: Introduction

Imagine a world where humankind could manipulate and control the self-organization and motion of groups of molecular systems, in particular mechanical devices powered by synthetic molecular switches. However, before this ambition can be fully achieved we must understand and overcome the challenges of constructing machine-like assemblies by controlling the spatial organization of switchable molecules, the barriers that regulate the relative motions of the switchable components, and the interface with the environment in which the individual switchable assemblies interact. The potential applications for molecular devices in which sophisticated functionalities can be acquired by convenient and reversible processes, under mild conditions, could only be limited to one's ingenuity and resourcefulness.

Our group has previously demonstrated a fluorescence-on response due to binding of cucurbit[7]uril (CB[7]) to a viologen quencher tethered to a fluorophore BODIPY-dyad pseudorotaxane (Figure 1.1a).[29] This novel approach to fluorescence-on response by disrupting the aggregation of fluorophore-quencher could be utilized toward the development of a molecular device, in particular a molecular sensor shuttle rotaxane. A sensor based on this approach would possess two docking sites for CB[7] to shuttle between, one site for binding with analytes and another site responsible for the fluorescence signal (Figure 1.1b). In this case, the shuttling of CB[7] causes the switching on/off mechanism for the fluorescence response. Therefore, as the sensor binds with an analyte, it induces host-guest shuttling to disrupt fluorophore-quencher aggregation allowing for a fluorescence-on response.

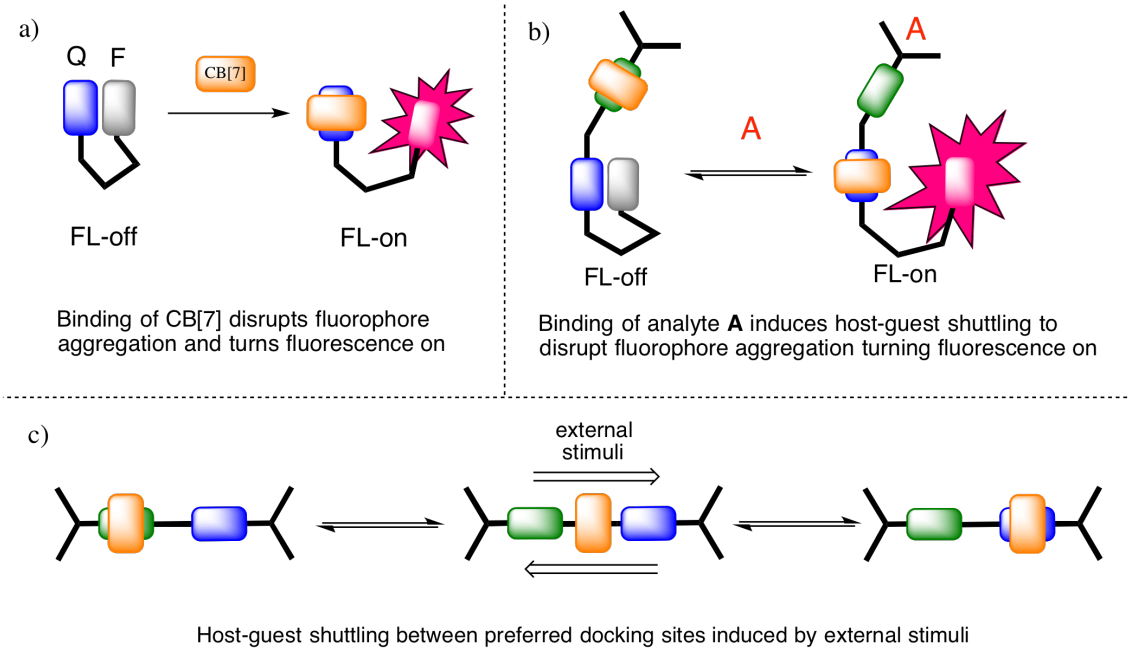

Figure 1.1 a) Fluorescence-on response due to CB[7] binding to viologen-dyad, b) fluorescence off-on shuttle rotaxane molecular sensor, c) shuttling of CB[7] between docking sites on a rotaxane induced by external stimuli.

In the next phase of this work we can gain added utility by shuttling the CB[7] between two docking sites in response to an external stimuli. The focus of the work presented in this dissertation is to determine the binding and stoppering abilities of various CB[7]-axle constructs for the assembly of a shuttle rotaxane with competitive binding sites (Figure 1.1c). In order to understand the challenges and significance of our contributions, a literature background concerning mechanically interlocked molecules and cucurbituril chemistry is presented in Chapter I. Chapter II focuses on the synthesis and competitive binding of benzyl ammonium guests with cucurbit[7]uril. A discussion on rotaxane synthesis and preparation of bulky stoppers of CB[7] viologen rotaxane is presented in Chapter III. In Chapter IV, rotaxane formation via Copper (Cu)-catalyzed azide-alkyne cycloaddition CuACC "Click chemistry", and stoppering efficiency from a CB[7] host, is presented.

1.1 Mechanically Interlocked Molecules (MIMs)

For more than half a century, chemists have been intrigued by the challenge of building interlocked architectures in the form of mechanically interlocked molecules (MIMs) and molecular machines which include catenanes, rotaxanes, molecular knots, and molecular Borromean rings (Figure 1.2).[1] Work in this has been recognized with the 2016 Nobel Prize in Chemistry to Bernard L. Feringa, Jean-Pierre Sauvage, and J. Fraser Stoddart.[2] Catenanes, derived from the Latin word *catena* which means "chain", are mechnically bonded molecules which contain two or more ring shaped molecules linked together analogous to chain links[3]. The term rotaxane is derived from the Latin words *rota* meaning "wheel" and *axle* meaning "axis".[3] Rotaxanes consist of at least 2 components, a bead-like macrocycle or wheel that is threaded over a linear axle-like molecule with stoppering groups that prevents unthreading of the macrocycle. The components of each system are not connected covalently, therefore, a mechanical bond holds them together.

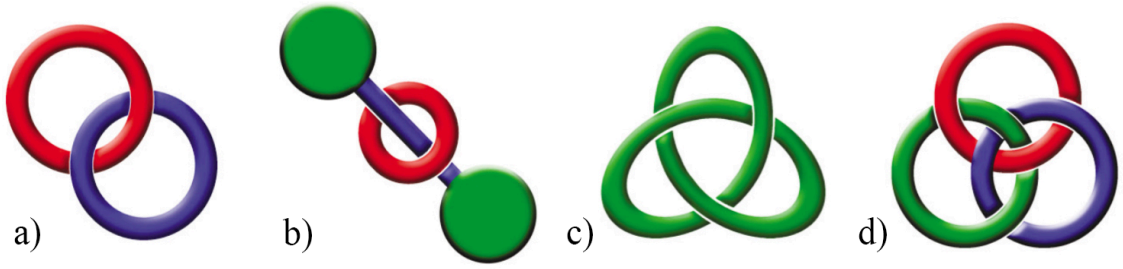

Figure 1.2 Cartoon representation of a) [2]catenane, b) [2]rotaxane, c) molecular knot, d) Borromean Rings. Adapted from Stoddart.[1]

MIM's based on molecular recognition and self-assembly have gained quite an interest due to their dynamic features and prospective components to access molecular-scale devices and machines. However, the interlocked molecules can be synthetically

challenging targets, to a great extent because of the complexity in attempting to assemble two or more independent molecules in space so that a mechanical bond can be formed. The earliest attempt to synthesize catenanes and rotaxanes, by Wasserman in 1960 and by Harrison in 1967 respectively, was dependent on statistical probability and suffered from very low yields of the final products.[4,5] Even after the covalent bond directed syntheses developed by Schill and others, access to these molecules suffered from long synthetic routes and the overall yields were not drastically improved.[6] These early attempts were inefficient in producing mechanically interlocked compounds, primarily due to minimal interactions between the components that bring them together in order to make the final covalent bond. Sauvage and co-workers discovered a key breakthrough in the synthesis of MIMs through molecular recognition by demonstrating a non-covalent template method for the synthesis of a [2]catenane. Sauvage untilized a Cu(I) ion to form a complex of a 1,10-phenanthroline-based thread and a 1,10-phenanthroline-containing ring, followed by the covalent bond cyclization of the threaded component to form the target catenane in high yield (Figure 1.3).[7] Following the establishment of such template-directed syntheses, based on metal-ligand coordination, many other noncovalent bonding interactions—ie. donor-acceptor,[8] hydrogen bonding,[9] hydrophobic interactions,[10] etc. have been used in the construction of MIMs in high yields. These developments in the field can be seen in a wide range of template designs and higher order interlocked structures by Sauvage, Stoddart, Leigh, Harada, Beer among others.[11]

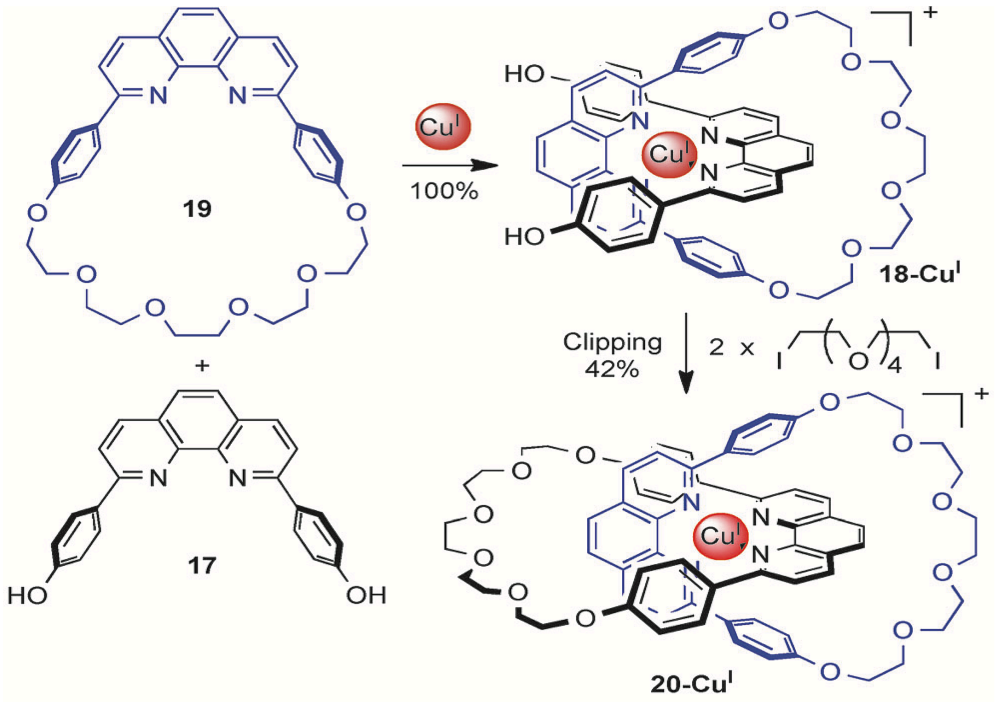

Figure 1.3 Sauvage's Cu^1 catenane synthesis using a 1,10-phenanthroline-based thread (17) and a 1,10-phenanthroline-containing ring (19). Formation of 18-Cu^1 from 17 and 19 is quantitative, subsequent ring closure gives catenane 20-Cu^1 in 42% yield. Adapted from Leigh.[7]

1.2 Cucurbiturils

Cucurbiturils are stable macrocyclic molecules consisting of methylene-bridged glycoluril oligomers. Researchers are particularly interested in these compounds due to their molecular container properties giving rise to the ability to bind or include other molecules within their cavity. The cucurbituril name is derived from the Latin word *cucurbitaceae* which resembles the shape to that of a pumpkin.[12, 13] The naming systems for cucurbit[n]urils (CB[*n*]) is to easily distinguish between each homologue, where *n* referes to the numbers of glycoluril units found within the macrocycle (Figure 1.4).

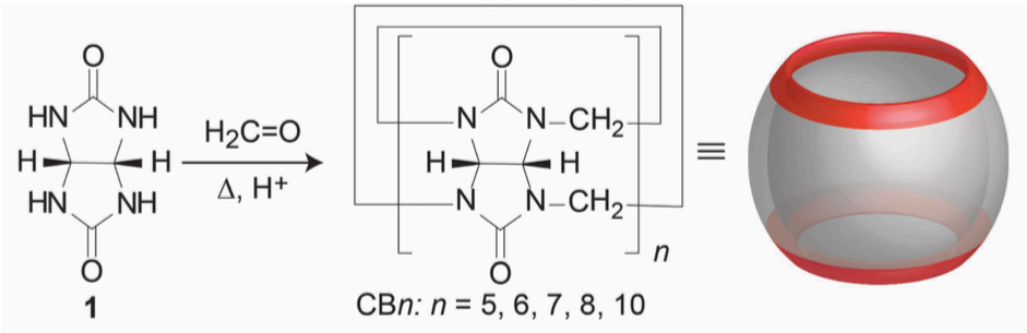

Figure 1.4 Syntheisis of Cucurbituril. Adapted from Nau.[13]

Behrend and coworkers first synthesized these compounds in 1905 by the acid-catalyzed condensation reaction between glycoluril and formaldehyde and was known as "Behrend's polymer".[14] It wasn't until 1981 that Mock and coworkers had reinvestigated Behrend's report and characterized the product's structure by IR and NMR spectroscopy, and X-ray crystallography. The results of these analyses suggested the substance was comprised of a macrocyclic structure containing six glycoluril units bridged by twelve methylene units to give cucurbit[6]uril or CB[6].[12]

Once the structure of cucurbituril (CB) was established, Mock recognized its potential as a macrocyclic host and began to study its binding properties.[15] The barrel-like structure of CB[n] bears two sets of polar hydrophilic portals lined with ureidyl carbonyl groups and a hydrophobic central cavity. The carbonyl rims allow for the formation of molecular inclusion complexes through strong ion-dipole interactions, while the neutral hydrophobic moiety sits within the CB[n] cavity making this an excellent receptor for cations.[12,16] In contrast to other macrocyclic hosts such as cyclodextrin and calixarene that have only one bridge connecting the subunits, cucurbiturils have two linkers connecting each subunit. This gives CB[n] a distinctively rigid structure which bestows a high level of self-assembly allowing it to strongly and

selectively bind to guest molecules. Initially, cucurbiturils were limited to binding metal cations, and small aliphatic and aromatic guests that could fit within the hydrophobic cavities. Years later, this limitation was overcome by the research groups of Kim and Day when they reported a convenient synthesis and isolation procedure for many homologues of cucurbituril (CB[5]–CB[10]).[17] Through this work of Kim and Day, various cucurbituril oligomers have gained popularity with a large number of research groups.

The discovery of these new additions to the CB[n] family enhanced the applicabilities of cucurbiturils. The bigger cavity size of the larger CB's enables them to form 1:1 binary complexes and 1:1:1 heteroternary complexes based on their larger cavity volumes in addition to increased solubility. Cucurbiturils all have a standard height of 9.1 Å, although their portal diameter, cavity diameter and volume vary consistently with ring size (Table 1.1). It is important to note that the portal size of CB[n] is approximately 2 Å narrower than the cavity diameter, which causes constrictive binding that produces a greater steric barrier to guest association and dissociation.[18]

Table 1.1 Dimensions and aqueous solubilities of CB[n].[17a, 18a, 19, 20]

Host	Portal Diameter (Å)	Cavity Diameter (Å)	Height (Å)	Cavity Volume (Å^3)	Solubility in Water (mM)
CB[5]	2.4	4.4	9.1	82	20-30
CB[6]	3.9	5.8	9.1	164	<0.01
CB[7]	5.4	7.3	9.1	279	20-30
CB[8]	6.9	8.8	9.1	479	<0.01
CB[10]	9.5-10.6	11.3-12.4	9.1	870	<0.01

The solubilities of CB's in aqueous solvents range from 0.01 mM for CB[6] and CB[8] to that of 20–30 mM for CB[7] and CB[5] as seen in Table 1.1.[17a,18a,19,20] However the solubilities increase dramatically for CB[5]–CB[8] in concentrated aqueous acid. An outstanding feature of CB[5]–CB[8] is their ability to remain stable in the presence of high temperatures in which thermal gravimetric analysis shows this to exceed 370 °C for all homologues.[18a] Another important factor to note is their toxicity *in vitro* and *in vivo* are negligible. These hosts are well documented to form inclusion complexes with cationic organic moieties through ion-dipole, hydrogen bonding, and hydrophobic interactions.

Mock and coworkers established CB[6] as a host and reported its high binding affinity for aliphatic ammonium species.[15] Mock and Tuncel examined the shuttling effects of CB[6] from one docking site to another through external stimuli by pH.[21] This work opened pathways for CB[n] applications in catalysis, and molecular switches and shuttles.[21,22]

Due to the small cavity size of CB[6], the applications are limited to inclusion of small guests only, such as metal cations, aliphatic (ammonium and diammonium) guests, some aromatic guests such as toluene and *para*-substituted phenyl rings, and is unable to bind with *ortho* and *meta*-substituted phenyl rings.[18a,19,23] However, CB[7] has an optimal portal size and cavity making it a more ideal candidate for practical applications. As a host, CB[7] is able to bind with a wide variety of guests, including most aliphatic and aromatic compounds, ferrocenes, adamantanes particularly when an ammonium site is presented, and metal cations.[18a,19,24] Numerous research groups such

as Macartney, Nau, Kaifer, and Isaacs, among many others have rigorously investigated CB[n] in order to probe applications in catalysis, drug delivery, biological sensors and molecular shuttles.

Kaifer and coworkers have studied the mode of binding of CB[7] with 4,4'-dipyridiunium dications (viologens) containing aromatic and aliphatic substituents using NMR spectroscopy.[25] Data obtained from these studies showed that when viologens contained short alkyl chains, CB[7] would encapsulate the viologen core to form a stable inclusion complex. In this case the aromatic bipyridinium units fit snuggly within the hydrophobic cavity of the macrocycle, while the ammonium cations are surrounded by the rimmed carbonyl portal of CB[7].[25a,b] The ^{1}H-NMR spectra (Figure 1.5 b) of the 1:1 host-guest inclusion complex with CB[7] and methyl viologen (MV^{2+}) shows the upfield chemical shift of the *beta*-protons of the viologen unit confirming full inclusion within CB[7]. Alternately CB[7] would form external complexes with one of the benzyl or longer alkyl chain substituents of viologen (Figure 1.6).[25c] Evidence for the formation of these 1:1 external host-guest complexes was supported by the upfield shifting of the aromatic protons of the benzylic moiety and those of the aliphatic moiety indicating the enclusion of the substituents within the macrocyclic host. These studies provide the needed insight into creating designed complexes.

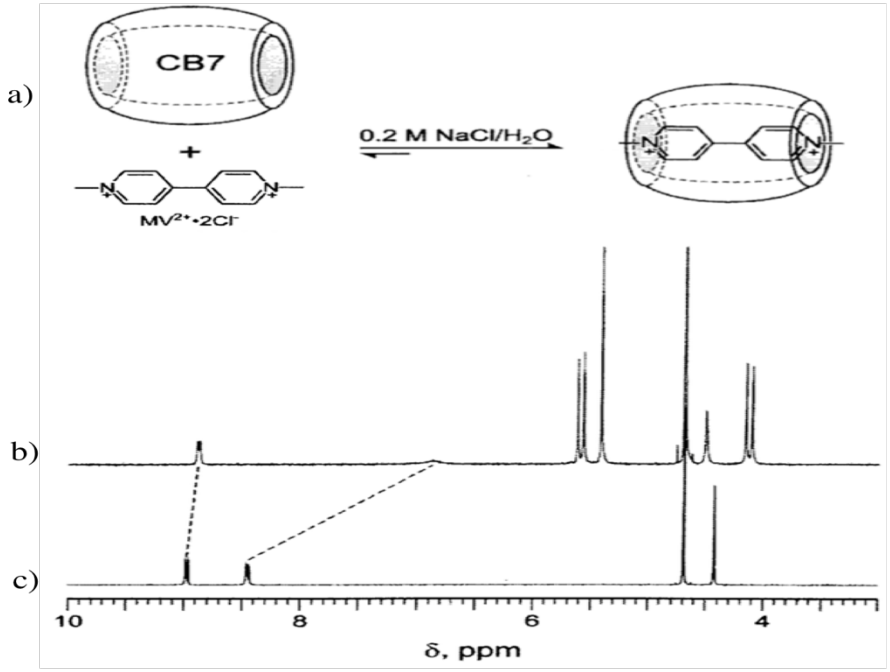

Figure 1.5 a) Internal complex of methyl viologen (MV^{2+}) and CB[7], b) partial ^{1}H-NMR spectra of MV^{2+} in the presence of 1 equivalent of CB[7], c) partial ^{1}H-NMR spectra of MV^{2+} in the absence of CB[7].[25a]

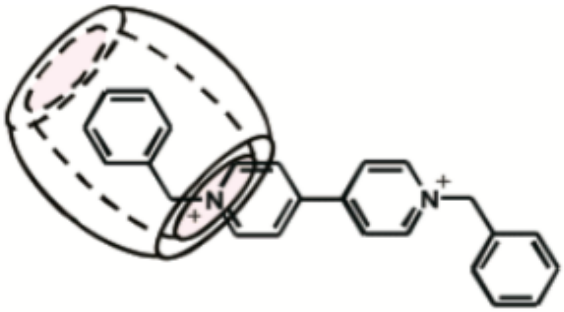

Figure 1.6 External complex of benzyl viologen and CB[7].[25c]

More recently the Kaifer group has developed a molecular shuttle based on a pH controlled viologen psuedorotaxane with CB[7] (Figure 1.7).[26] In this system the viologen species contained aliphatic sidearms terminated with carboxylic acid groups. Upon CB[7] complexation under acidic conditions the macrocycle resides over the aliphatic alkyl chain showing an upfield shift of the alkyl protons in the ^{1}H-NMR

spectra. At higher pH and subsequent deprotonation of the carboxylic acid groups the CB[7] host will shuttle from the alkyl chains to encapsulating the viologen core shifting the *beta*-protons of the bipyridinium unit in the ^{1}H-NMR spectra as seen in their previous studies.

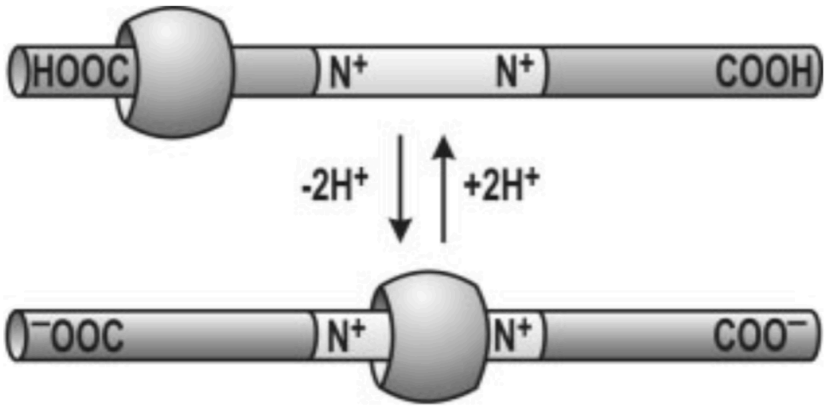

Figure 1.7 pH-controlled shuttling of CB[7] between viologen and carboxylic acid terminated pseudorotaxane .[26]

Isaacs and coworkers have published reports detailing the formation of 1:1 host-guest inclusion complexes with CB[7] and a wide selection of guest molecules (Figure 1.8).[24] From these studies they were able to determine the equilibrium binding constants (K_a) of the guests by utilizing ^{1}H-NMR competition experiments in aqueous solutions, where the guests were allowed to compete for a limiting quantity of CB[7]. Data obtained from this work gives binding constant ranges from 10^4 M^{-1} to 10^{12} M^{-1} and more recently obtained values of 10^{17} M^{-1} with diamantane diammonium ion in D_2O.[24,27] This high-affinity binding and selectivity with CB[7] is largely due to the combination of electrostatic, hydrophobic, and steric interactions.[24,28]

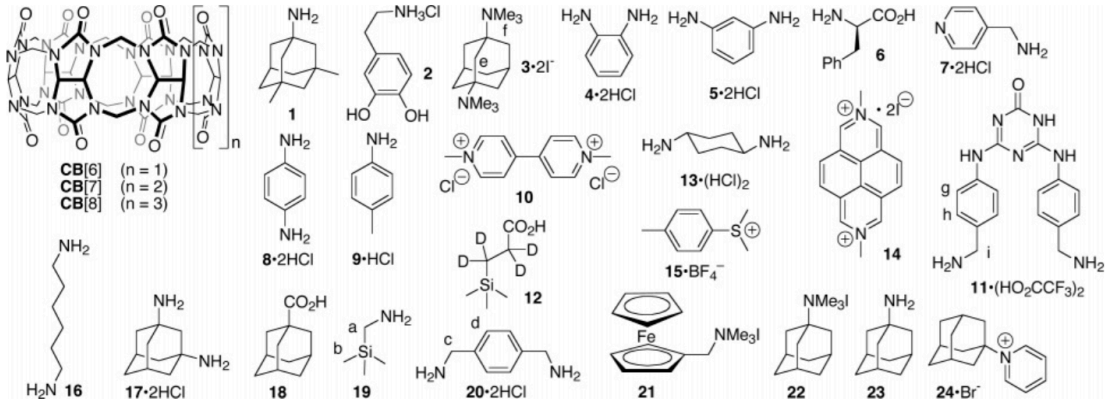

Figure 1.8 Guest compounds used by the Isaacs group to study binding affinity with CB[7]. Adapted from Isaacs and co workers.[24]

Researchers have identified that the synthetic properties of CB[7] can have a significant impact on the physical and chemical properties of a guest undergoing complexation.[18a,19] These effects can involve changes in the guest's solubility, physical structure, pKa values, chemical stability and reactivity, spectroscopic analyses.[22c] These resulting impacts unfold a variety of applications for CB[7], including self-sorting systems, molecular switches, molecular machines, chemical sensing, drug delivery, and molecular catalysis within and between guests.[22b,c] Despite the fact that CB[7] has a vital role in each of these applications, the research described herein is best applied to self-sorting systems, molecular switches and chemical sensing.

1.3 Research Focus

Our group is specifically interested in the design and synthesis of a mechanically interlocked molecular sensing rotaxane that uses cucurbit[7]uril as a shuttle to communicate between two cationic docking sites in aqueous systems. The shuttling effect is mediated by external stimuli, such as pH or biomolecular interaction.

The components of the proposed molecular sensor are illustrated in Figure 1.9. Initially, CB[7] (orange rectangle) encapsulates a strong binding ammonium sensing receptor (green rectangle) with a binding affinity toward CB[7] that is ideally 100-1000 fold higher than any other potential binding site on the molecular sensor. This high binding affinity ensures that CB[7] will spend most of its time interacting with the receptor unit through supramolecular interaction. Additionally the cationic site must contain a bulky end group and a variable biomolecule recognition (R) group to stopper and prevent CB[7] from dethreading. Next, if a minimal amount of CB[7] dissociates and shuttles across the axle to the second weaker docking site, a viologen (blue rectangle), the cationic receptor is available to bind with biomolecule analytes. The binding affinity of the CB[7] and receptor may be reduced from the incoming steric bulk and electronic interactions of the biomolecule analyte. As CB[7] shuttles to the secondary viologen docking site it interrupts any photoinduced electron transfer (PET) or fluorescence quenching effect between the viologen-dyad fluorescent reporter, which allows the dyad to be revealed to elicit a fluorescence-on response. It is expected that various biomolecule analytes would interact with the molecular sensor with differentiation in that the fluorescence increase from the baseline can be measured with high sensitivity for each type of analyte. The advantages of this system are that by changing the variable recognition group, while maintaining the core structure of the shuttle rotaxane, a variety of novel sensors could be assembled to accommodate specific analytes. This system could also be adapted for solution-based sensing or covalently attached to a recoverable surface for future use.

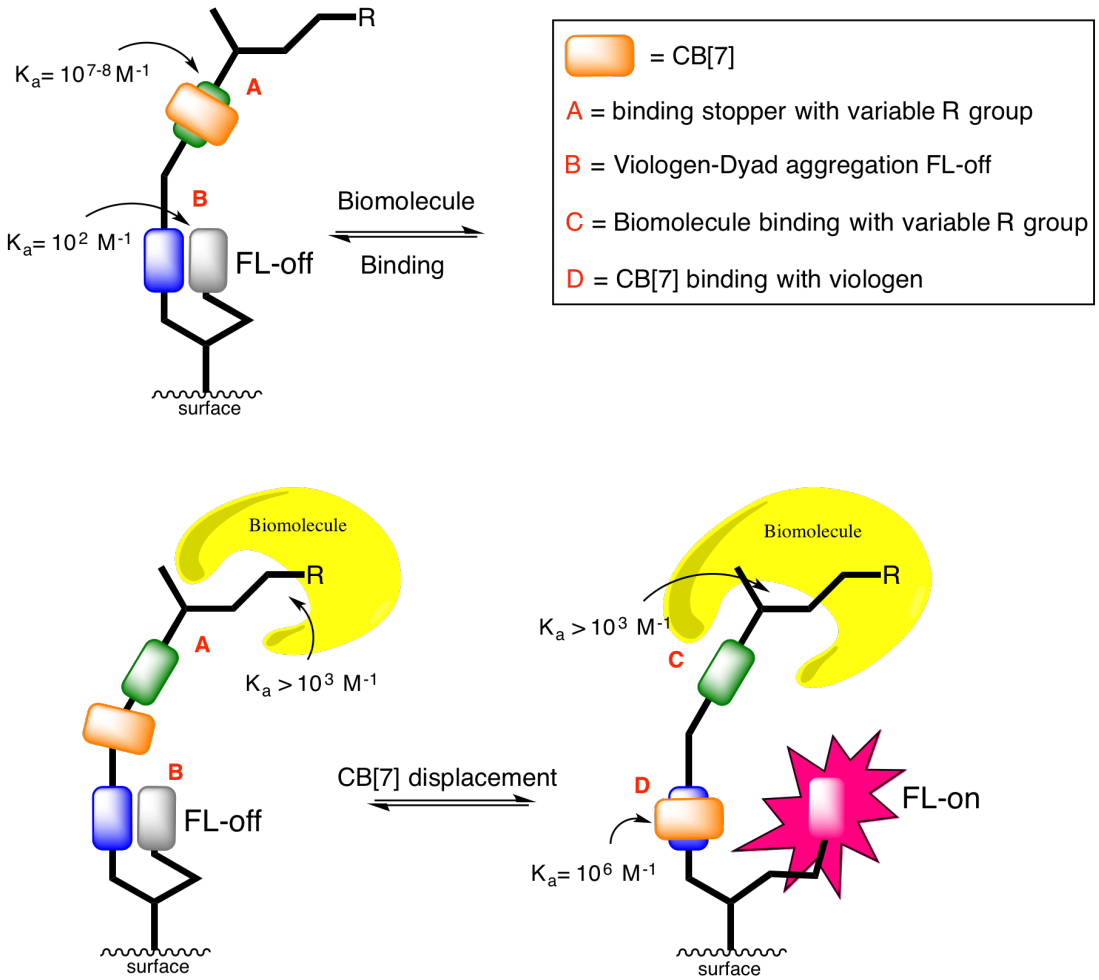

FL-on if biomolecule binding strong enough and close enough to displace CB[7]

Figure 1.9 Cartoon representation of a surface attached molecular sensing rotaxane.

Our group has recently established a viologen-fluorophore dyad reporter that is readily accessible to be incorporated into the above mentioned shuttle rotaxane.[29] However, to be considered a true or full rotaxane it must contain bulky endgroups which prevent the unthreading of cucurbit[7]uril. In particular, the body of this work focuses on the synthetic development and binding properties of the cationic binding stopper, the collection of host-guest inclusion data, and rotaxane formation. To the best of our knowledge, little is exploited on synthesis of CB[7] rotaxane based molecular

sensors. Therefore, it is advantageous to develop new synthetic strategies for the construction of shuttle rotaxanes. Thus, our goal was to first understand the behavior and binding affinity of CB[7] complexation of a binding stopper. Secondly, to transfer the knowledge gained from the binding studies to the synthesis of a supramolecular rotaxane to determine stopper efficacy and CB[7] shuttling between two docking sites. Consequently, in order to achieve the goals mentioned above we need to address the following objectives: to develop synthetic methodology of a cationic (ammonium) binding stopper, determine and acquire binding constant data of cationic binding stopper through competitive binding experiments, assemble a bulky non-binding stopper and determine stopper efficiency against CB[7], utilize the developed methodology for the assembly of a shuttle rotaxane and determine stopper efficacy of ammonium binding stopper against CB[7].

The work presented in this dissertation describes our efforts towards the development of a CB[7] shuttle rotaxane based molecular sensor. In Chapter 2, a series of monocationic para-substituted bulky benzyl ammonium rotaxane stoppers were synthesized and their host-guest association with CB[7] was explored (Figure 1.10). Two main structural features of the benzyl ammonium guests that were incorporated were the large branched aliphatic stoppering groups, as well as varying the nature of the terminal substituents that were *para* to the ammonium group. The nature of the terminal substituent could either assist in, or hinder the binding affinity of, the CB[7] from full enclusion of the molecule. Additionally, the terminal substituent is transformed into a reactive alkyne group allowing for connectivity of an extension linker or second stopper by Copper (Cu)-catalyzed Azide-Alkyne cycloaddition CuAAC. The properties of the

binding between the benzyl ammonium guests and the CB[7] host were studied in the presence of a competitive binder, and their binding constants were measured.

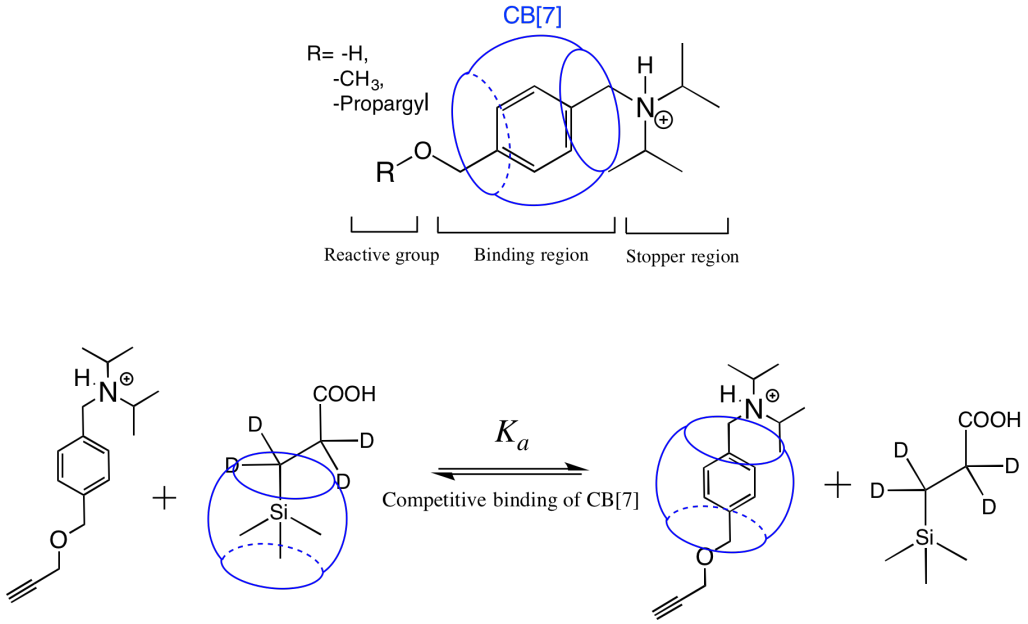

Figure 1.10 Analogs of bulky benzyl ammonium stopper (top), and competitive binding of CB[7] with ammonium stopper and silane (bottom).

Chapter 3 presents the continual efforts to develop a bulky non-binding stopper for CB[7] viologen rotaxanes (Figure 1.11). A particular bis(3,5-dimethoxybenzyl)-viologen guest previously synthesized by our group was reexamined as to its ability to prevent CB[7] from threading over the end groups to form a rotaxane. This inspiration was attributed to preliminary data for this viologen showing unclear and conflicting results with recently published data from another group. Throughout our study great care was taken in replicating the experiments, and therefore confirming the published results by CB[7] forming a full inclusion complex with the bis(3,5-dimethoxybenzyl)-viologen guest. Furthermore, in the presence of a stronger binder, CB[7] was shown to decomplex with the viologen and instead form a full inclusion complex with the

stronger binder. A bulkier bis(3,5-diisopropoxybenzyl)-viologen guest was then synthesized and its host-guest inclusion was studied. The larger guest showed transient (external) complexation with CB[7], and the bulkier groups prevented slippage of CB[7] to bind with the viologen core.

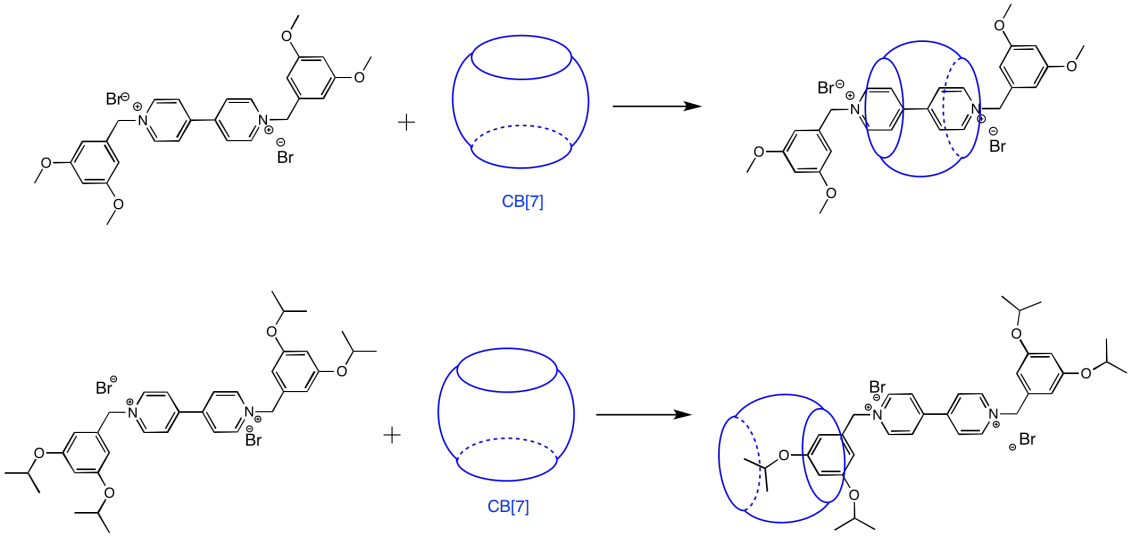

Figure 1.11 Host-guest interactions of CB[7] and bis(3,5-dimethoxybenzyl)-viologen (top) and bis(3,5-diisopropoxybenzyl)-viologen (bottom).

Lastly, Chapter 4 focuses on rotaxane formation by Copper (Cu)-catalyzed Azide-Alkyne cycloaddition CuAAC "Click chemistry". The appeal of Click chemistry lies in the great success to perform the reaction under mild aqueous conditions, having high functional group tolerance, and generating high yields. This popular reaction is finding numerous applications across a wide range of fields, including rotaxane synthesis. However, there is a prevailing deficiency in the assembly of accessible CB[7] containing rotaxanes and the difficulty of synthesizing suitable rotaxane stoppers is studied to meet this need. Therefore, one aspect of this project was to study formation of a rotaxane-like molecule composed of bulky end groups derived from the compounds synthesized in Chapter 2 and Chapter 3, and the second aspect was to determine

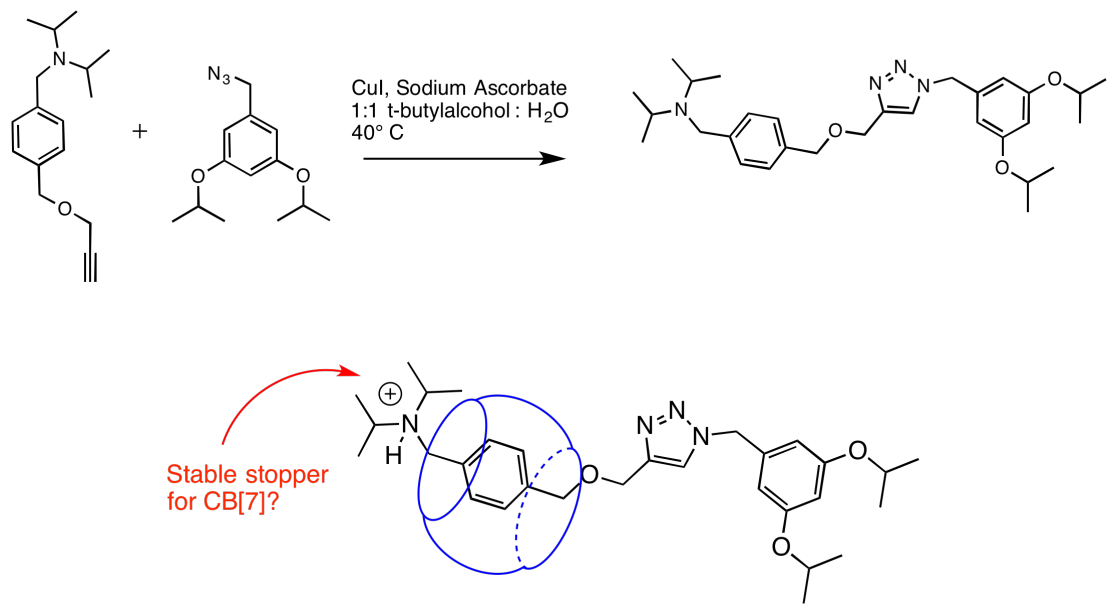

Figure 1.12 Synthesis of model rotaxane using Copper (Cu)-catalyzed Azide-Alkyne cycloaddition CuAAC "Click chemistry" (top) and investigation of ammonium stopper stability to CB[7](bottom).

stoppering efficacy against CB[7] (Figure 1.12). Additional bulky dicationic xylyl-ammonium guests were synthesized to study stoppering efficacy against CB[7]. The binding properties between the xylyl ammonium guests and the CB[7] host were studied in the presence of a competitive binder, and their binding constants were measured.

The goals of these studies is to further understanding of the host-guest binding between CB[7] and various benzyl and xylyl ammonium guest and to establish a foundation for CB[7] rotaxane stopper development.

1.4 References

1. Griffiths, K. E.; Stoddart, J. F. *Pure Appl. Chem.* **2008**, *80*, 485–506.
2. The Nobel Prize in Chemistry 2016. Nobelprize.org. Nobel Media AB 2014. Web. http://www.nobelprize.org/nobel_prizes/chemistry/laureates/2016/.
3. (a) Sauvage, J. P.; Dietrich-Buchecker, C. Molecular Catenanes, Rotaxanes, and Knots: A Journey Through the World of Molecular Topology, Wiley-VCH, Weinheim **1999**; (b) Amabilino, D. B.; Stoddart, J. F. *Chem. Rev.* **1995**, *95*, 2725-2828; (c) Cantrill, S. J.; Pease, A. R.; Stoddart. J. F. *J. Chem. Soc., Dalton Trans.*, **2000**, 21, 3715-3734; (d) Bělohradský, M.; Raymo. F. M.; Stoddart, J. F. *Collect. Czech. Chem. Commun.*, **1997**, *62*, 527-557.
4. Wasserman, E. *J. Am. Chem. Soc.* **1960**, *82*, 4433-4434.
5. Harrison, I. T.; Harrison, S. *J. Am. Chem. Soc.* **1967**, *89*, 5723-5724.
6. Schill, G.; Lüttringhaus, A. *Angew. Chem., Int. Ed. Engl.* **1964**, *3*, 546–547.
7. (a) Dietrich-Buchecker, C. O.; Sauvage J. P.; Kintzinger, J. P. *Tetrahedron Lett.*, **1983**, *24*, 5095–5098.; (b) Beves, J. E.; Blight, B. A.; Campbell, C. J., Leigh, D. A.; McBurney, R. T. *Angew. Chem. Int. Ed.* **2011**, *50*, 9260-9327.
8. (a) Ashton, P. R.; Odell, B.; Reddington, M. V.; Slawin, A. M. Z.; Stoddart, J. F.; Williams, D. J. *Angew. Chem. Int. Ed. Engl.* **1988**, *27*, 1550-1553; (b) Ashton, P. R.; Goodnow, T. T.; Kaifer, A. E.; Reddington, M. V.; Slawin, A. M. Z.; Spencer, N.; Stoddart, J. F.; Vicent, C.; Williams, D. J. *Angew. Chem. Int. Ed. Engl.* **1989**, *28*, 1396-1399; (c) Hamilton, D. G.; Davies, J. E.; Prodi, L.; Sanders, J. K. M. *Chem. Eur. J.* **1998**, *4*, 608-620; (d) Griffiths, K. E.; Stoddart, J. F. *Pure Appl. Chem.* **2008**, *80*, 485-506.

9. (a) Hunter, C. A. *J. Am. Chem. Soc.* **1992**, *114*, 5303-5311; (b) Ashton, P. R.; Campbell, P. J.; Glink, P. T.; Philp, D.; Spencer, N.; Stoddart, J. F.; Chrystal, E. J. T.; Menzer, S.; Williams, D. J.; Tasker, P. A. *Angew. Chem. Int. Ed. Engl.* **1995**, *34*, 1865-1869. (c) Johnston, A. G.; Leigh, D. A.; Pritchard, R. J.; Deegan, M. D. Facile *Angew. Chem. Int. Ed. Engl.* **1995**, *34*, 1209-1212; (d) Vögtle, F.; Dünnwald, T.; Schmidt, T. *Acc. Chem. Res.* **1996**, *29*, 451-460; (e) Guidry, E. N.; Cantrill, S. J.; Stoddart, J. F.; Grubbs, R. H. *Org. Lett.* **2005**, *7*, 2129– 2132; (f) Kay, E.; Leigh, D. *Top. Curr. Chem.* **2005**, *262*, 133-177.

10. (a) Harada, A.; Li, J.; Kamachi, M. *Nature* **1992**, *356*, 325-327; (b) Fujita, M.; Ibukuro, F.; Hagihara, H.; Ogura, K. *Nature* **1994**, *367*, 720-723.

11. (a) Faiz, J. A.; Heitz,V.; Sauvage, J. P. *Chem. Soc. Rev.*, **2009**, *38*, 422–442; (b) Forgan, R. S.; Sauvage, J. P.; Stoddart, J. F. *Chem. Rev.*, **2011**, *111*, 5434–5464; (c) Dichtel, W. R.; Miljani ́c, O. S.; Zhang, W.; Spruell, J. M.; Patel, K.; Aprahamian, I.; Heath, J. R.; Stoddart, J. F. *Acc. Chem. Res.*, **2008**, *41*, 1750–1761; (d) Stoddart, J. F. *Chem. Soc. Rev.*, **2009**, *38*, 1802–1820; (e) Klajn, R.; Stoddart, J. F.; Grzybowski, B. A. *Chem. Soc. Rev.*, **2010**, *39*, 2203–2237; (f) Coskun, A.; Spruell, J. M.; Barin, G.; Dichtel, W. R.; Flood, A. H.; Botros, Y. Y.; Stoddart, J. F. *Chem. Soc. Rev.*, **2012**, *41*, 4827–4859; (g) Harada, A.; Takashima, Y.; Yamaguchi, H. *Chem. Soc. Rev.*, **2009**, *38*, 875–882; (h) Hanni, K. D.; Leigh, D. A. *Chem. Soc. Rev.*, **2010**, *39*, 1240–1251; (i) Beves, J. E.; Blight, B.A.; Campbell, C. J.; Leigh, D. A.; McBurney, R.T. *Angew. Chem., Int. Ed.*, **2011**, *50*, 9260–9327; (j) Spence, G. T.; Beer, P. D. *Acc. Chem. Res.*, **2012**, *46*, 571–586; (k) Beer, P. D.; Sambrook, M. R.; Curiel, D. *Chem. Commun.*, **2006**, 2105–2117; (l) Vukotic, V. N.; Loeb, S. J.

Chem. Soc. Rev., **2012**, *41*, 5896–5906; (m) Neal, E. A; Goldup, S. M. *Chem. Commun.*, **2014**, *50*, 5128-5142.

12. Freeman, W. A.; Mock, W. L.; Shih, N. Y. *J. Am. Chem. Soc.*, **1981**, *103*, 7367.
13. Assaf, K. I.; Nau, W. M. *Chem. Soc. Rev.*, **2015**, *44*, 394-418.
14. Behrend, R.; Meyer, E. *Ann. Chem.* **1905**, *339*, 1-37.
15. (a) Mock, W, L.; Shih, N.-Y. *J. Org. Chem.* **1983**, *48*, 3618. (b) Mock, W, L.; Shih, N.-Y. *J. Org. Chem.* **1986**, *51*, 4440-4446.
16. (a) Mock, W. L. *Chapter 15: Cucurbituril, In Comprehensive Supramolecular Chemistry, Volume 2*, J. L. Atwood, J. E. D. Davies, D. D. MacNicol, F. Vogle, and J. M. Lehn (eds.), F. Vogtle (volume ed.), Pergamon: New York, 1996; pp. 477-493.; (b) Cintas, P. *J. Incl. Phenom. Mol. Recognit. Chem.* **1994**, *17*, 205.; (c) Oshovsky, G. V.; Reinhoudt, D. N.; Verboom, W. *Angew. Chem. Int. Ed*. **2007**, 46, 2366.
17. (a) Kim, J.; Jung, I.; Kim, S.; Lee, E.; Kang, J.; Sakamoto, S.; Yamaguchi, K.; Kim, K. *J. Am. Chem. Soc.* **2000**, *122*, 540.; (b) Day, A.; Arnold, A. P.; Blanch, R. J.; Snushall, B. *J. Org. Chem*. **2001**, *66*, 8094.
18. (a) Lagona, J.; Mukhophadhyay, P.; Chakrabarti, S.; Isaacs, L. *Angew. Chem., Int. Ed.* **2005**, *44*, 4844.; (b) Marquez, C.; Hudgins, R. R.; Nau, W. M. *J. Am. Chem. Soc.* **2004**, *126*, 5806.
19. (a) Lee, J. W.; Samal, S.; Selvapalam, N.; Kim, H.;Kim, K. *Acc. Chem. Res.* **2003**, *36*, 621. (b) Kim, K.; Selvapalam, N.; Ko, Y. H.; Park, K. M.; Kim, D.; Kim, J. *Chem. Rev.* **2007**, *36*, 267; (c) Isaacs, L. *Chem. Commun.* **2009**, 619; (d) Masson, E.; Ling, X.; Joseph, R.; Kyremeh-Mensah, L.; Lu, X. *RSC Adv.* **2012**, *2*, 1213.

20. Liu, S.; Zavalij, P. Y.; Isaacs, L. *J. Am. Chem. Soc.* **2005**, *127*, 16798.

21. (a) Mock, W, L.; Pierpont, J. *J. Chem. Soc., Chem. Commun.* **1990**, 1509.; (b) Tuncel, D.; Steinke, J. H. G. *Chem. Commun.* **1999**, 1509-1510.

22. (a)Tuncel, D.; Özsar, O.; Tiftik, H. B.; Salih, B. *Chem. Commun.* **2007**, 1369-1371.; (b) Macartney, D. H. *Isr. J. Chem.* **2011**, *51*, 600.; (c) Parvari, G.; Reany, O.; Keinan, E. *Isr. J. Chem.* **2011**, *51*, 646.

23. (a) Buschmann, H. J.; Cleve, E.; Jansen, K.; Wago, A.; Schollmeyer, E. *J. Incl. Phenom. Macrocycl. Chem.* **2001**, *40*, 117.; (b) Buschmann, H. J.; Mutihac, L.; Schollmeyer, E. *J. Incl. Phenom. Macrocycl. Chem.* **2008**, *61*, 343.; (c) Buschmann, H. J.; Mutihac, L.; Mutihac, R. C.; Schollmeyer, E. *Thermochim. Acta.* **2005**, *430*, 79.

24. Liu, S.; Ruspic, C.; Mukhopadhyay, P.; Chakrabarti, S.; Zavalij, P. Y.; Isaacs, L. *J. Am. Chem. Soc.* **2005**, *127*, 15959-15967

25. (a) Ong, W.; Gomez-Kaifer, M.; Kaifer, A. E. *Org. Lett.*, **2002,** *4*, 1791-1794.; (b) Moon, K.; Kaifer, A. E. *Org. Lett.* **2004**, *6*, 185-188.; (c) Sindelar, V.; Moon, K.; Kaifer, A. E. *Org. Lett.*, **2004**, *6*, 2665-2668.

26. (a) Sindelar, V.; Silvi, S.; Kaifer, A. E. *Chem. Commun.* **2006**, 2185-2187.; (b) Sindelar, V.; Silvi, S.; Parker, S. E.; Sobransingh, D.; Kaifer, A. E. *Adv. Funct. Mater.* **2007**, *17*, 694-701.

27. Cao, L.; Sekutor, M.; Zavalij, P. Y.; Mlinaric-Majerski, K.; Glaser, R.; Isaacs, L. *Angew. Chem., Int. Ed.* **2014**, *53*, 988−993.

28. (a) Isaacs, L. *Chem. Commun.* **2009**, 619–629 (b) Lee, J. W.; Samal, S.; Selvapalam, N.; Kim, H.-J.; Kim, K. *Acc. Chem. Res.* **2003**, *36*, 621–630. (c) Ong, W.; Kaifer, A. E. *Organometallics* **2003**, *22*, 4181–4183.

29. Singh, A.; Yip, W. T.; Halterman, R. L. *Org. Lett.* **2012**, *14*, 4046-4049.

Chapter 2: Host-Guest Binding of N-Substituted Benzyl-Ammonium Guests with Cucurbit[7]uril

2.1 Introduction to Host-Guest Chemistry and Association Constants

Supramolecular chemistry is defined as "chemistry beyond the molecule," more specifically a chemical system or molecular assembly made of two or more compounds interacting *via* various weak intermolecular interactions through non-covalent bonding. A rapidly developing interdisciplinary area of supramolecular chemistry, known as host-guest chemistry, involves the design, synthesis, and investigation of simpler organic compounds. Host-Guest chemistry is comprised of a macrocyclic host receptor that will selectively bind with a particular small guest molecule in order to produce a host-guest complex or supramolecule (Figure 2.1).

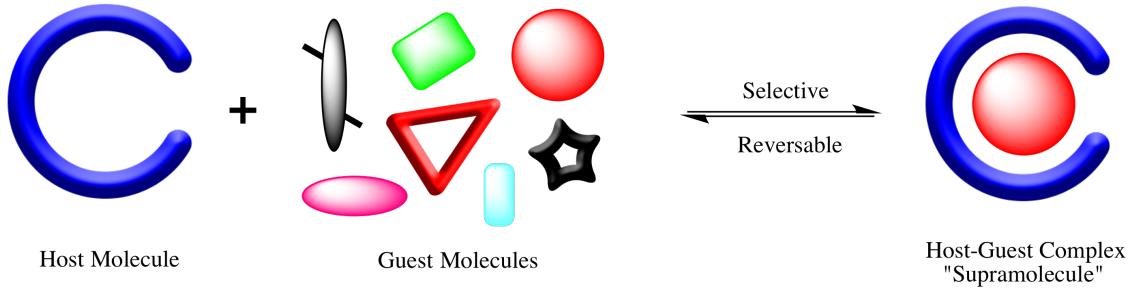

Figure 2.1 Molecular recognition between host molecule and selected complimentary guest molecule to form a host-guest supramolecular complex.

Most macrocyclic hosts have a concave interior, such as a pocket or hole similar to the hydrophobic cavity of many enzymes. This cavity allows the host to encapsulate and non-covalently bind a wide variety of cationic, neutral, and anionic guest molecules. In order for binding to occur, the host must possess binding sites with the

correct electronic character to compliment that of the guest. These binding sites must be spaced out on the host in such a way to make it possible for it to interact with the guest, in addition the size and shape of the guest must be also complimentary to the host as well as seen in Figure 2.1.

As a host binds to a guest, the product is usually a 1:1 inclusion complex as illustrated in the general equation below.

Equation 2.1

$$H_f + G_f \rightleftharpoons H{-}G$$

The equation illustrates the equilibrium that forms between the free host, free guest and host-guest complex. The equilibrium has an association constant, also recognized as binding constant and stability constant, *K*, which can be explained by the following expression.

Equation 2.2

$$K_a = \frac{[H{-}G]}{[H_f][G_f]}$$

Binding constants are frequently used to measure how strongly a guest interacts with the host in a 1:1 inclusion complex. The standard method for quantifying host-guest interactions is a titration of the guest to a solution of the host, recording the changes in some physical property through NMR spectroscopy, UV-Vis spectroscopy, fluorescence and other various techniques.[1]

Various examples of hosts have been reported, e.g. crown ethers, cyclodextrins, calixarenes, cryptands, cyclophane, cavitands, and cucurbiturils each with specific types of non-covalent interactions with guest molecules (Figure 2.2).

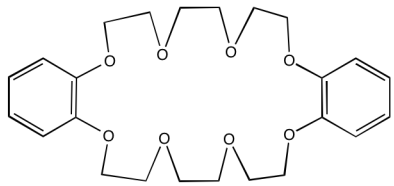

2a

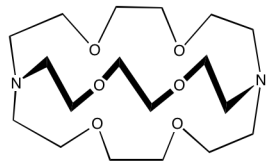

2b

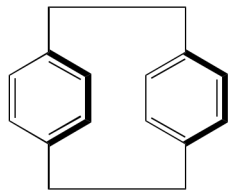

2c

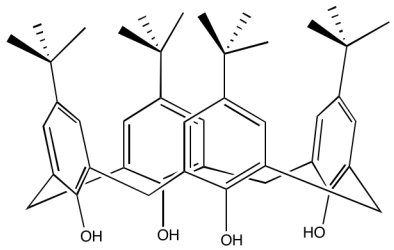

2d

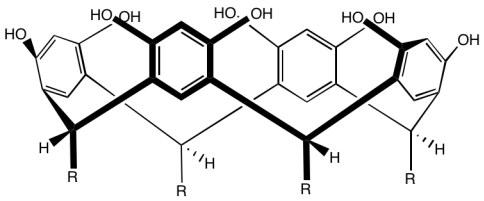

2e

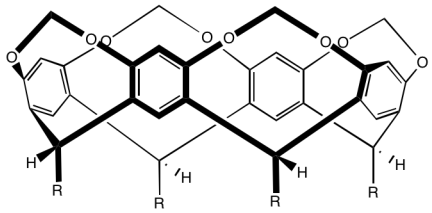

2f

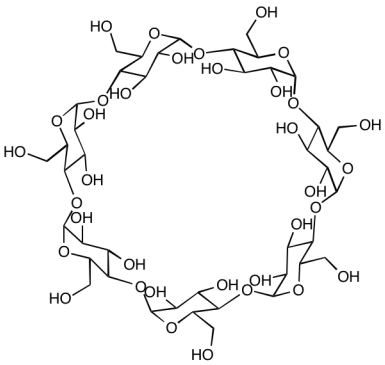

2g

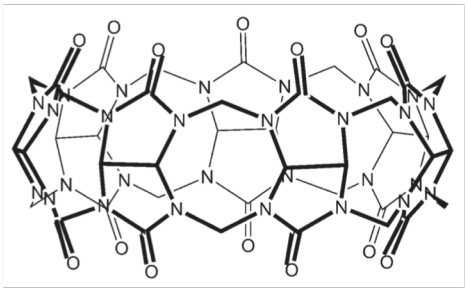

2h

Figure 2.2 Line drawing of various reported macrocyclic hosts. 2a) crown ether, 2b) cryptand, 2c) cyclophane, 2d) calix[4]arene, 2e) resorcin[4]arene, 2f) bridged resorcin[4]arene, 2g) beta-cyclodextrin, 2h) Cucurbit[7]uril

This molecular recognition and self-assembly type response seen in the Host-guest complexes typically involve interactions of hydrogen bonding, electrostatic interactions, Van der Waals forces, chelation of metal cations, pi-stacking, hydrophobic effects etc., showing inclusion, selectivity or other functionality.[2]

Within the past few decades, Cucurbit[*n*]urils have been widely investigated as macrocyclic hosts due to their binding properties.[3] As reviewed in chapter one, Cucurbit[*n*]urils are macrocyclic methylene-bridged glycoluril oligomers, synthesized by the acid-catalyzed condensation between paraformaldehyde and glycoluril (Figure 2.3). Its name is derived from the Latin word *cucurbitaceae* as it's shape resembles a pumpkin. Homologues of the CB[*n*] family include CB[5], CB[6], CB[7], CB[8], CB[10], and more recently CB[14][4] where each contain a different number of glycoluril units .

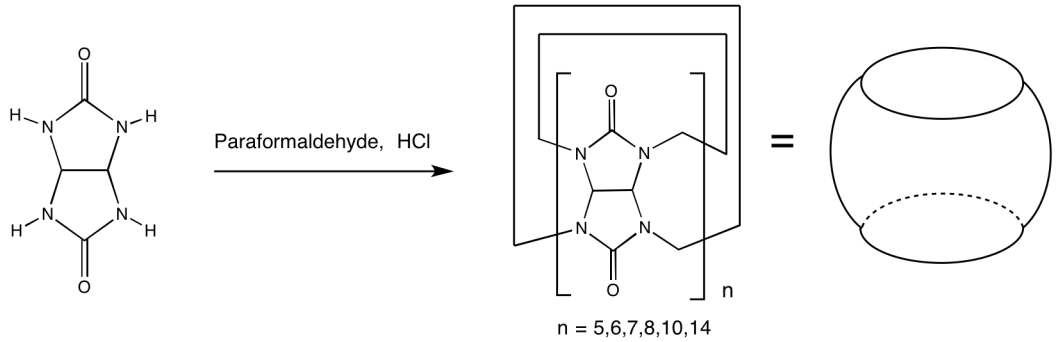

Figure 2.3 Preparation of Cucurbiturils from glycoluril and paraformaldehyde under acidic conditions.

What makes CB[n] an ideal macrocyclic host is that it bears two hydrophilic carbonylated rims and a hydrophobic cavity. This allows for binding with cationic and neutral guest molecules, where the positive charge interacts with the carbonyl rim through ion-dipole interactions, and the hydrophobic moiety sits inside the CB[n]

cavity. The Kaifer group has focused on investigated host-guest complexes with CB[7] and viologen derivatives, determining binding constants and modes of binding whether CB[7] preferred the inclusion of the bipyridal core or external binding of the end groups.[3d,5] This binding preference is important to consider when designing a shuttle rotaxane containing viologens.

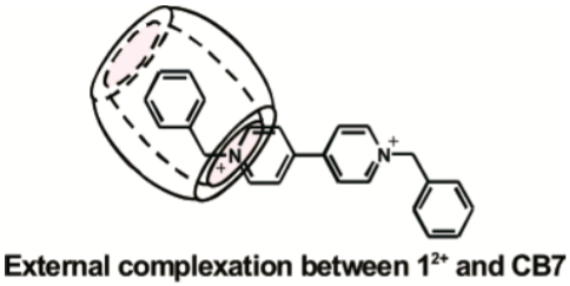

Figure 2.4 External complexation of benzylviologen $\mathbf{1}^{2+}$ and CB[7]. Adapted by Kaifer and coworkers.[5]

In 2005, the Isaacs group performed extensive binding studies with CB[7] on various selected organic guests.[3e] Among the guests examined, dimethylviologen **10** (K_a = 10^7 M^{-1}) and p-xylenediamine **20** (K_a = 10^9 M^{-1}) (Figure 2.5) contain structural characteristics that could be incorporated within a molecular shuttle rotaxane that we have proposed in Chapter one, while trimethylsilylpropanoic acid **12** (K_a = 10^7 M^{-1}) is a competitive binder we will use in our studies.

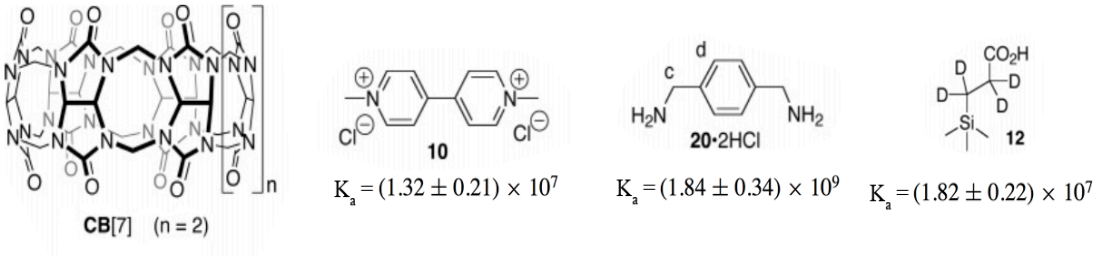

Figure 2.5 Selected guests dimethylviologen **10**, p-xylyenediamine **20**, and trimethylsilylpropanoic acid **12** used by the Isaacs group to study binding affinity with CB[7]. Adapted from Isaacs and co workers.[3e]

Therefore, we want to examine the para-substituted benzyl/xylyl ammonium scaffolds as a target for a CB[7] rotaxane binding stopper with a desired binding constant range of $K_a = 10^7 - 10^8$ M^{-1}. However, the binding strengths of both compounds (**10**, **20**) are slightly stronger than desired and should be synthetically modified to contain other functionality to assist in fine-tuning the appropriate binding strength. Our group has already established a set of viologen analogues with binding constants in the range of $K_a = 10^5 - 10^6$ M^{-1} and have been adapted for a CB[7] psuedorotaxane system.[8] These studies have been foundational to our research, giving our group insight into the design and development of a mechanically interlocked molecular shuttle rotaxane based on CB[7] host-guest complexes and their binding affinities discussed in chapter one.

Over the past decade research groups have examined a growing library of small ammonium cation guests and their binding constants with the CB[n] family.[3e,f,7] This important area of research can provide opportunities to explore various applications for chemical sensors, drug delivery systems and shuttle rotaxanes in aqueous systems.[6] However, the synthesis of these systems (chemical sensors or shuttle rotaxanes) may be difficult to accomplish due to CB[7]'s low solubility and hydrophilicity, which could hinder the total synthesis of the supramolecular system. Futhermore, there is a void in the development of benzyl/xylyl ammonium guest as rotaxane stoppers, specifically the design that must include good molecular recognition and self-assembly, synthetic strategy and utility by varying the end groups for tunable binding. Therefore, this important area of study relating to molecular devices incorporating CB[7] needs a

deeper exploration. One research focus is to design, synthesize, and measure the binding constants of benzyl amine analogues.

2.2 Specific Aims

This chapter presents the synthesis of benzyl ammonium analogs, and the measurement of binding efficiency towards Cucurbit[7]uril in aqueous solutions using competitive binding NMR spectroscopy. Given that the p-xylenediamine **20** scaffold has too strong of binding for our desired range, and the need to incorpate a binding stopper and an extendable tethering group, we focused on a benzyl amine scaffold with para-substitution.

In the fundamental design of the benzyl amine binding stopper the ammonium salt is preferred for ease of synthesis and potential pH response for binding. The amino group could hold the stoppering groups, such as a large bulky isopropyl group and the other an R-group (hexyl, cyclohexyl, benzyl, etc.) having variable recognition properties for chemical sensing in which both groups should prevent CB[7] from dethreading (Figure 2.6). The para substituent could be reactive to introduce groups, such as a tether extension or a second stopper, and therefore must contain a terminal alkyne such as a propargyl group. The propargyl group is reactive to azide-alkyne cycloaddition Cu-AAC "Click" reaction and seemed best to pursue as the reaction works well in aqueous media.

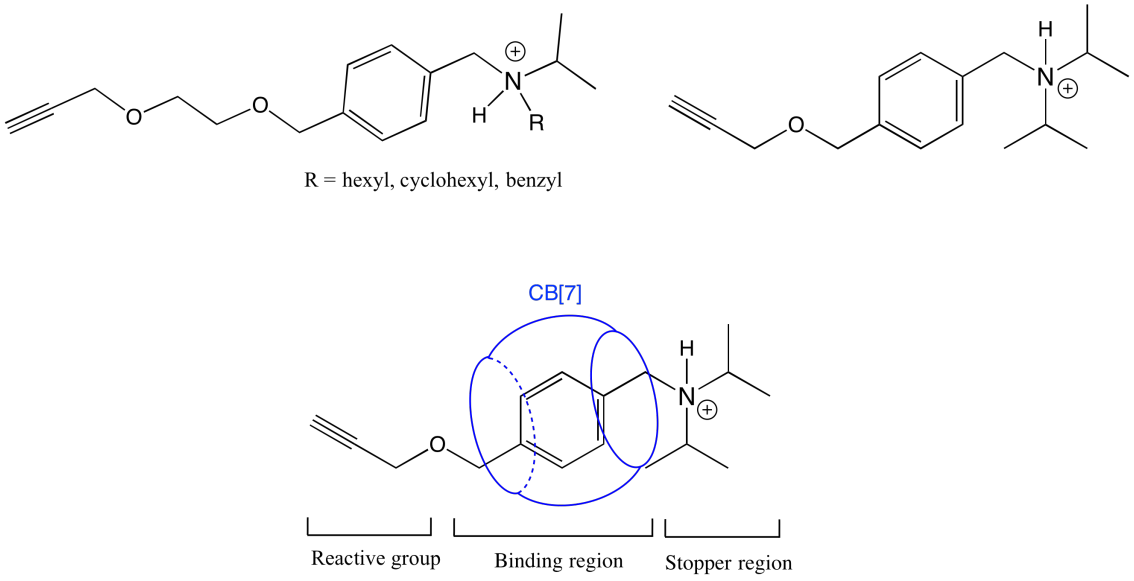

Figure 2.6 Proposed benzyl amine stoppers.

However, by establishing synthetic protocol first using diisopropyl amine (Figure 2.6) as the stopper end group and attaching it to the benzylic position through substitution will allow for quicker access of analogues to measure binding affinity with CB[7]. The diisopropyl groups were chosen for their bulkiness and could show promising results as a suitable stopper for CB[7]. Stoddart and coworkers have shown stopper effectiveness by using triisopropylsilyl groups as stoppers within their paraquat-cyclophane shuttle rotaxane system.[10] Considering the dimension of the triisopropylsilyl group is 7.5 Å wide and the paraquat-cyclophane is 6.8 Å (Figure 2.7), the triisopropylsilyl group is large enough to prevent passage of the paraquat-cyclophane.[10,11] For our system the diisopropyl amino group is 6.8 Å wide and CB[7] portal diameter is 5.4 Å(Figure 2.7).[11] Therefore, by using the same principle that the larger end groups should not allow passage of the macrocycle, we are optimistic that the diisopropyl amino group should prevent passage of CB[7]. Although stopper effectiveness will still need to be confirmed it will be discussed further in Chapter four.

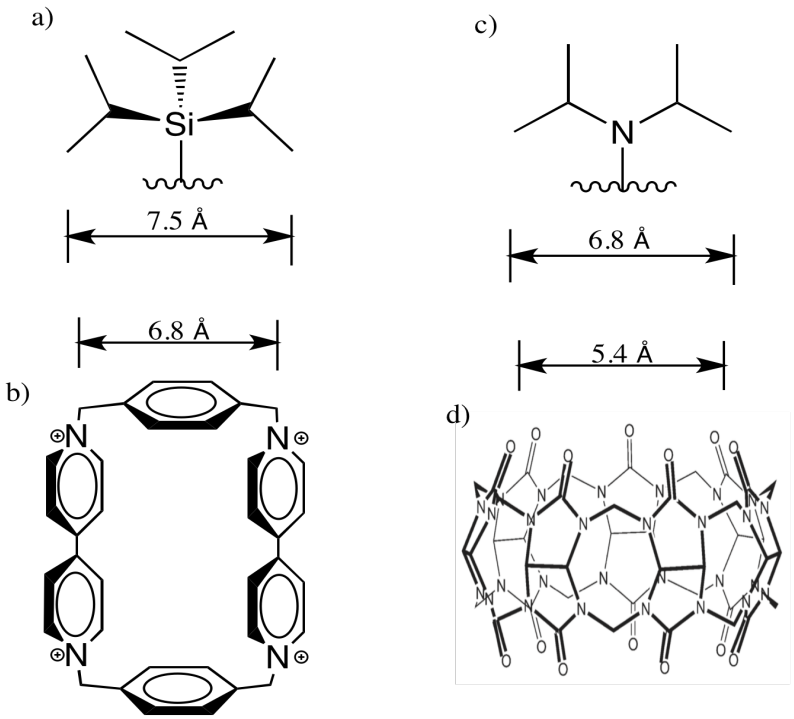

Figure 2.7 Width dimensions of a) triisopropylsilyl group, b) paraquat-cyclophane, c) diisopropyl amino group, d) CB[7].[10,11]

The estimated binding constants for the proposed benzyl ammonium analogs (blue rectangle) are in the range of $K_a = 10^7 - 10^8$ M^{-1}, 100 to 1000 fold higher (Figure 2.8) than that of Dr. Anuradha Singh's weaker binding viologen (red rectangle)-dyad of $K_a = 10^5 - 10^6$ M^{-1}.[8]

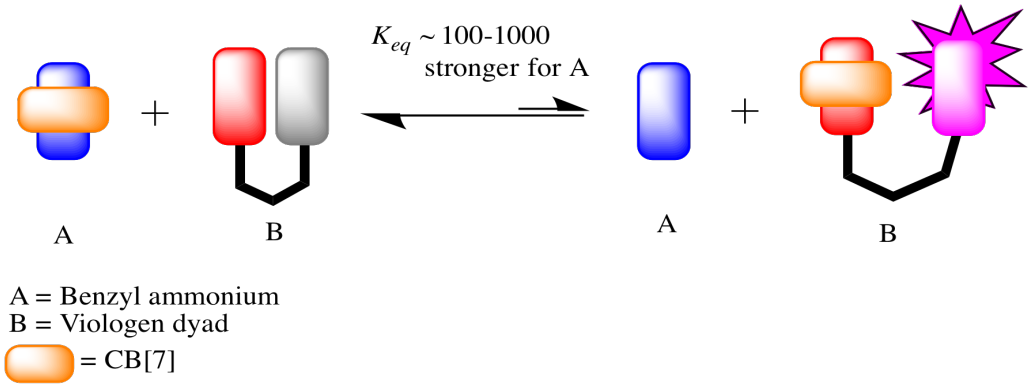

Figure 2.8 Cartoon representation of the competitive binding of CB[7](orange rectangle) between benzyl ammonium A and viologen-dyad B.

The binding constants of the proposed benzyl ammonium analogs will be measured through an indirect method using NMR spectroscopy, where a benzyl ammonium analogue and a known stronger binder will be allowed to compete for a limited amount of CB[7]. These analyses were accomplished through the use of NMR spectroscopy and HR-ESI mass spectrometry.

2.3 Synthesis

The proposed benzyl amine stopper is designed to have a reactive group to install a second stopper by azide-alkyne cycloaddition, therefore a propargyl group is used. However in order to install the propargyl group or propargyl-PEG(polyethylene glycol) ether extension, the substrate must go through an alcohol intermediate. The alcohol intermediate allows for divergence in which many different substituents can be installed. This divergence encouraged us to pursue other stopper models, in addition to the propargyl model, to solidify our understanding of how the substituent can effect binding strength with CB[7].

The three guests, 4-((diisopropylamino)methyl)benzyl alcohol, 4-((diisopropyl-amino)methyl)benzyl methyl ether, and 4-((diisopropylamino)methyl)benzyl propargyl ether, were synthesized as shown in Figure 2.9. The *para*-methyl group in methyl 4-methyl benzoate was brominated with N-bromosuccinimide followed by amination with diisopropylamine. The ester group was reduced with lithium aluminum hydride to afford the benzyl alcohol **2.1a**. Finally, the compounds methyl ether **2.2b** and propargyl ether **2.3c** can be accessed by divergent synthesis of the benzyl alcohol group by deprotonation with the strong base sodium hydride followed by alkylation with

dimethyl sulfate or propargyl bromide. Each of these ethers was purified through column chromatography with silica gel using a mixture of dichloromethane and ethyl acetate eluent. Cucurbit[7]uril (CB[7]) was synthesized following literature precedence.[9] The synthesized guests were characterized by NMR spectroscopy and mass spectrometry.

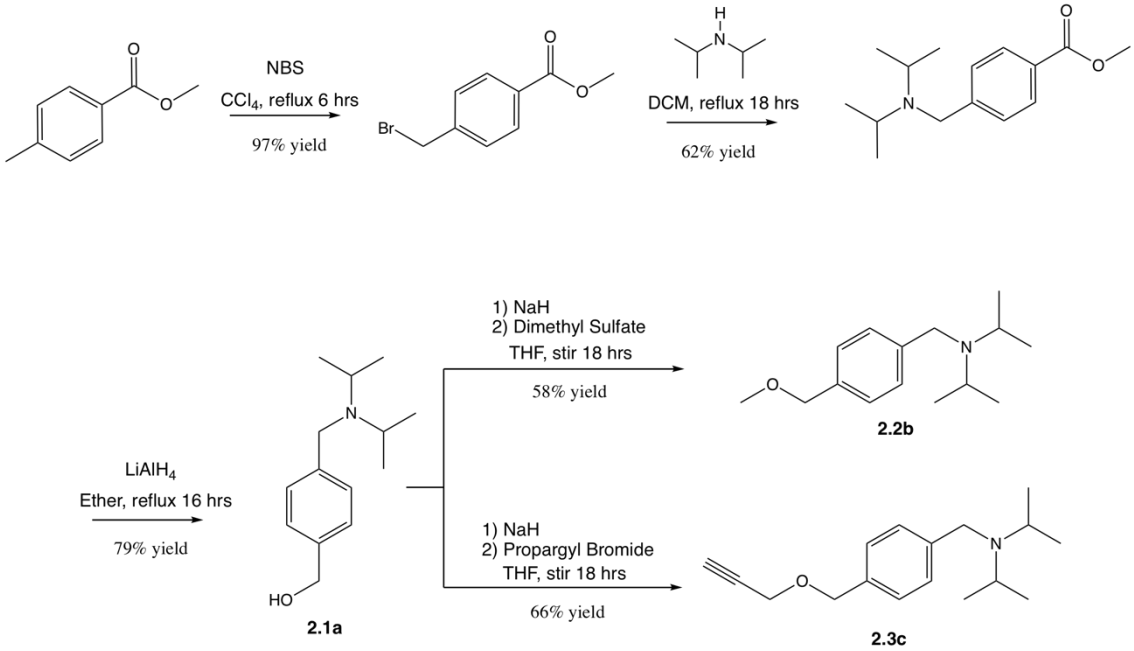

Figure 2.9 Synthetic scheme of benzyl amine stoppers 4-((diisopropylamino)methyl)benzyl alcohol (**2.1a**), 4-((diisopropyl-amino)methyl)benzyl methyl ether (**2.2b**), 4-((diisopropylamino)methyl)benzyl propargyl ether (**2.3c**).

2.4 Results and Discussion

Various well-established methods exist in the literature for determining the equilibrium binding constants of a wide range of guest molecules with a variety of hosts. It is usually impractical to determine absolute and accurate K_a values for CB[7]:guest complexes directly by NMR spectroscopy. This is because the complexes can display fast exchange on the ^{1}H-NMR timescale and can exceed the experimentally accessible range of $>10^4$ M^{-1}. However, in our study we used an indirect method based

on ^{1}H-NMR spectroscopy that was pioneered by Mock et. al. and Issacs et. al. in which they successfully used ^{1}H-NMR competition experiments referenced to an absolute K_a value.[3e] The reference compound selected for this study was 3-(trimethylsilyl)-propanoic-2,2,3,3-d4 acid **2.4d** $(Me)_3SiCD_2CD_2COOH$ (TMSP) (Figure 2.10), which has a 1:1 binding constant of $K_a = (1.82 \pm 0.22) \times 10^7\ M^{-1}$ with CB[7].

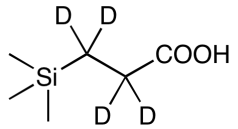 **2.4d**	$K_a = (1.82 \pm 0.22) \times 10^7\ M^{-1}$

Figure 2.10 Line drawing of 2.4d 3-(trimethylsilyl)propanoic-2,2,3,3-d4 acid $(Me)_3SiCD_2CD_2COOH$ (TMSP) and 1:1 binding constant with CB[7].

Silane **2.4d** (TMSP) has a ^{1}H-NMR shift at 0.0 ppm in its unbound state, and it has a shift at –0.7 ppm when bound to CB[7]. This compound demonstrates slow exchange on the ^{1}H-NMR timescale; therefore, both peaks can be integrated to determine an accurate ratio of bound and unbound silane **2.4d**. In our implementation of this method, the reference compound silane **2.4d** and an excess of a more weakly binding guest are allowed to compete for inclusion with a limiting quantity of CB[7].

The method of determining equilibrium binding constants was first tested on benzyl alcohol **2.1a** due to the accuracy needed in the preparation of the ^{1}H-NMR solutions and the limited quantity of methyl ether **2.2b**, and propargyl ether **2.3c** available. We first prepared a solution containing 0.125 mM CB[7], 0.300 mM silane **2.4d**, and 3.00 mM benzyl alcohol **2.1a** in 50.0 mM $Na(O_2CCD_3)$-buffered D_2O (pD = 4.45) and allowed it to reach equilibrium. Next, we determined the relative concentrations of unbound silane and bound silane by integration of the appropriate

resonances at 0.0 ppm and -0.7 ppm respectively. The integration of the bound silane was set to 1.000, and allowing the NMR software (MestReNova) to calculate the integration for the unbound silane. These determinations were done in triplicate from independently prepared stock solutions and the average ratios of the bound and unbound silane were used in the calculation of K_a for **2.1a**.

Since we know the total concentrations of all species in solution, we can use the integration ratio of unbound and bound silane to determine the concentration of unbound and bound silane in solution. The average integration of unbound silane was determined to be 2.7053, and the total integration of silane in solution is 3.7053. The bound silane integration (1.0000) was divided by the total silane integration (3.7053) and multiplied by 100 to give 26.9 % bound 73.1% unbound silane in solution. Using the relative concentrations and the mass balance expression (equation 2) allowed us to calculate $[\text{Si}]_{\text{unbound}}$ = 0.219 mM and $[\text{Si-CB[7]}]_{\text{bound}}$ = 0.0809 mM. Equation 3 is then used to calculate $[\text{CB[7]-}\mathbf{2.1a}]_{\text{bound}}$ = 0.0440 mM using the known value of $[\text{Si-CB[7]}]_{\text{bound}}$. Lastly equation 4 is used to calculate $[\mathbf{2.1a}]_{\text{unbound}}$ = 2.95 mM using the known value of [CB[7]-**2.1a**]. Substitution of the values of $[\text{CB[7]-}\mathbf{2.1a}]_{\text{bound}}$, $[\mathbf{2.1a}]_{\text{unbound}}$, $[\text{Si}]_{\text{unbound}}$, $[\text{Si }\mathbf{2.4d}\text{-CB[7]}]_{\text{bound}}$ into equation 1 gave K_{rel} = 0.0403. Finally, substitution of $K_{Si} = 1.82 \times 10^7\ \text{M}^{-1}$ and K_{rel} = 0.0403 into equation 5 gave $K_a = (7.33 \pm 2.92) \times 10^5\ \text{M}^{-1}$ for the equilibrium binding constant of **2.1a**. Error analysis was carried out according to literature.[3e]

Methodology of Binding Constant Determination

$$CB_7 + Si \underset{}{\overset{K_{Si}}{\rightleftharpoons}} CB_7 \cdot Si$$

$$CB_7 + X \overset{K_X}{\rightleftharpoons} CB_7 \cdot X$$

$$CB_7 \cdot Si + X \overset{K_{Rel}}{\rightleftharpoons} CB_7 \cdot X + Si$$

X = Competing Guest **2.1a**

Si = Known Binder (TMSP) **2.4d**

(Eq. 1) $K_{rel} = \dfrac{[CB_7 \cdot X]\,[Si]}{[CB_7 \cdot Si]\,[X]}$

(Eq. 2) $[Si]_{Total} = [Si]_{Free} + [CB_7 \cdot Si]_{Bound}$

(Eq. 3) $[CB_7]_{Total} = [CB_7 \cdot X]_{Bound} + [CB_7 \cdot Si]_{Bound}$

(Eq. 4) $[X]_{Total} = [X]_{Free} + [CB_7 \cdot X]_{Bound}$

(Eq. 5) $K_X = (K_{Si})\,(K_{rel})$

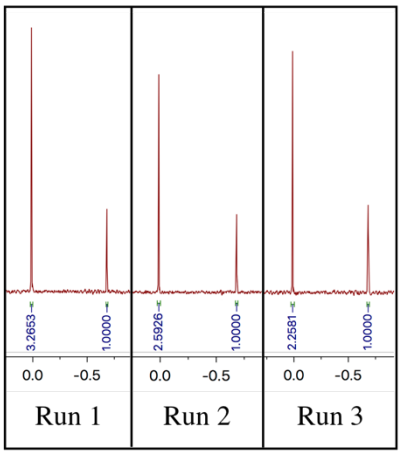

Total concentration of species in solution:
Guest [**2.1a**] = 3.00 mM
Silane [**2.4d**] = 0.300 mM
[CB[7]] = 0.125 mM

Average integration of unbound Silane = 2.7053
Integration of bound Silane = 1.0000
Total Silane Integration = 3.7053

$\dfrac{1.0000}{3.7053} = 0.269 \times 100 = 26.9$ % bound Silane

0.300 mM($[Si]_{Tot}$) x 0.269 = 0.0809 mM bound Silane

(Eq. 1) $K_{rel} = \dfrac{[CB_7 \cdot X]\,[Si]}{[CB_7 \cdot Si]\,[X]} = \dfrac{[0.0440]\,[0.219]}{[0.0809]\,[2.95]} = \mathbf{0.0403}$

(Eq. 2) $[Si]_{Total} = 0.300\text{ mM} = [0.219]_{Free} + [0.0809]_{Bound}$

(Eq. 3) $[CB_7]_{Total} = 0.125\text{ mM} = [0.0440]_{X\ Bound} + [0.0809]_{Si\ Bound}$

(Eq. 4) $[X]_{Total} = 3.00\text{ mM} = [2.95]_{Free} + [0.0440]_{Bound}$

(Eq. 5) $K_X = (K_{Si})\,(K_{rel}) = (1.82 \times 10^7) \times (0.0403) = \mathbf{(7.33 \pm 2.92) \times 10^5\ M^{-1}}$

Figure 2.11 Equations outlining concentrations of unbound and bound guests with CB[7]. Using the concentration of all species allow for calculation of K_{rel} and the absolute K_a for the competing guest.

Once the method for determining equilibrium binding constants was verified, the procedure was then replicated for compounds **2.2b** and **2.3c**. The concentration of

guests was adjusted until **2.4d** showed clear and significant peaks for bound and unbound species at 0.0 and −0.7 ppm. The binding constants for methyl ether **2.2b** and propargyl ether **2.3c** were then calculated in the same way as for compound **2.1a** (Table 2.1). All guest compounds **2.1a**, **2.2b**, **2.3c** showed remarkably similar binding constants with CB[7] in the range of 10^5 M^{-1}(Table 2.1). The highest binding constant obtained was from compound **2.1a** (K_a = (7.33 ± 2.92) × 10^5 M^{-1}), which contained both the benzyl ammonium cation and benzyl alcohol functionality. These functionalities provided two modes of binding, ion-dipole and hydrogen bonding, with both carbonyl portals of CB[7]. The binding constants for compounds **2.2b** (K_a = (5.41 ± 0.90) ×10^5 M^{-1}), and **2.3c** (K_a = (4.85 ± 0.62) × 10^5 M^{-1}) were similar due to having only one mode of binding, ion-dipole, from the benzyl ammonium cation and para-substituted electronically repulsive ether groups.

Table 2.1 1:1 Absolute binding constant values (K_a) for (Guest:CB[7])

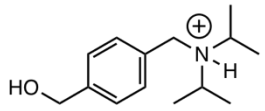 **2.1a**	K_a = (7.33 ± 2.92) x 10^5 M^{-1}
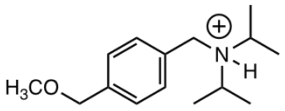 **2.2b**	K_a = (5.41 ± 0.90) x 10^5 M^{-1}
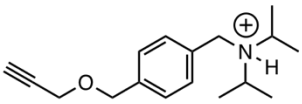 **2.3c**	K_a = (4.85 ± 0.62) x 10^5 M^{-1}

It was a concern to us that the electron rich propargyl tail of compound **2.3c** could tuck back inside the hydrophobic cavity of CB[7] when bound. If this were to occur, the binding strength would potentially increase due to the alkyne and aromatic ring pi-pi stacking and filling the internal volume of the CB[7] host. This would also reduce the rate of reaction for future Cu-AAC Click reactions for the attachment to a molecular axle, as the propargyl tail would need to be accessed from the exterior of CB[7].

However, propargyl ether **2.3c** was the most destabilizing guest and was determined to have the lowest equilibrium binding constant of $K_a = (4.85 \pm 0.62) \times 10^5$ M^{-1} with CB[7] due to only one mode of binding and a para-substituted electron-rich repulsive alkyne group. There is no clear evidence from these binding studies that the alkyne tail of compound **2.3c** is or is not concealed within the hydrophobic cavity of CB[7]. It should also be noted that these binding studies were conducted in an acidic solution to ensure that the nitrogens were in their protonated state. This is essential if these compounds were to be used as an ammonium stopper docking site for a CB[7] shuttle rotaxane.

Unfortunately, compound **2.3c** cannot be incorporated as an effective binding stopper in our proposed shuttle rotaxane. For this reason, it has a weaker binding constant ($K_a = (4.85 \pm 0.62) \times 10^5$ M^{-1}) in conjunction with Dr. Anuradha Singh's reverse benzyl azido tetraethylene glycol viologen-bodipy dyad that has a binding constant of $K_a = 2.72 \times 10^6$ M^{-1} with CB[7].[8] In this situation it is expected that CB[7] would bind to the viologen with a higher affinity than binding with the ammonium stopper. This would potentially create shuttling issues within the fluorescence-on shuttle

rotaxane discussed in chapter one causing CB[7] to spend most of its time bound to the viologen, therefore turning fluorescence on almost indefinitely.

2.5 Conclusion

In this chapter we have successfully used ^{1}H-NMR competition binding experiments to measure the relative binding constants K_{rel} for CB[7] toward para-substituted diisopropylbenzyl ammonium guests referenced to an absolute K_a. The stability constants diminish as the para-substituent increases in length and in electronic repulsion. Unfortunately, compound **2.3c** can not be used without further development in the CB[7] shuttle rotaxne design due to the lower binding constant than the viologen tethered dyad. By substituting the oxygen atom with a nitrogen atom to make a p-xylyl-ammonium species, it should give a higher binding affinity in the desired range of K_a = 10^7 – 10^9 M^{-1}. There is still a need to confirm if the diisopropyl groups are sterically bulky enough to prevent CB[7] leakage which will be discussed in Chapter 4.

2.6 Experimental

Synthesis of methyl 4-(bromomethyl)benzoate.

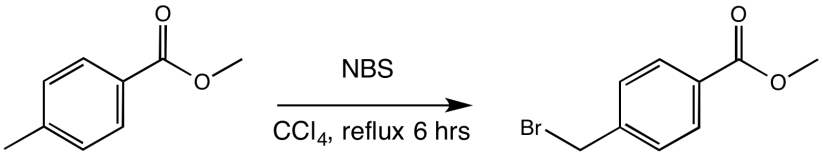

In a 250 mL reaction flask, methyl 4-methyl benzoate (2.04 g, 13.0 mmol), N-bromosuccinimide (2.74 g, 15.0 mmol) and carbon tetrachloride (60 mL) were added. The suspension was stirred at reflux for 6 h accompanied with illumination by halogen lamp. The flask was cooled to room temperature and the white succinimide residue was filtered off. The solvent was evaporated under reduced pressure to afford methyl 4-(bromomethyl)benzoate (3.03 g, 97% yield) as a tan oil. ^{1}H NMR (400 MHz, $CDCl_3$) δ 8.02 (d, J = 8.3 Hz, 2H), 7.47 (d, J = 8.2 Hz, 2H), 4.51 (s, 2H), 3.93 (s, 3H). ^{13}C NMR (101 MHz, $CDCl_3$) δ 166.5, 142.6, 130.07, 130.06, 129.0, 52.2, 32.2.

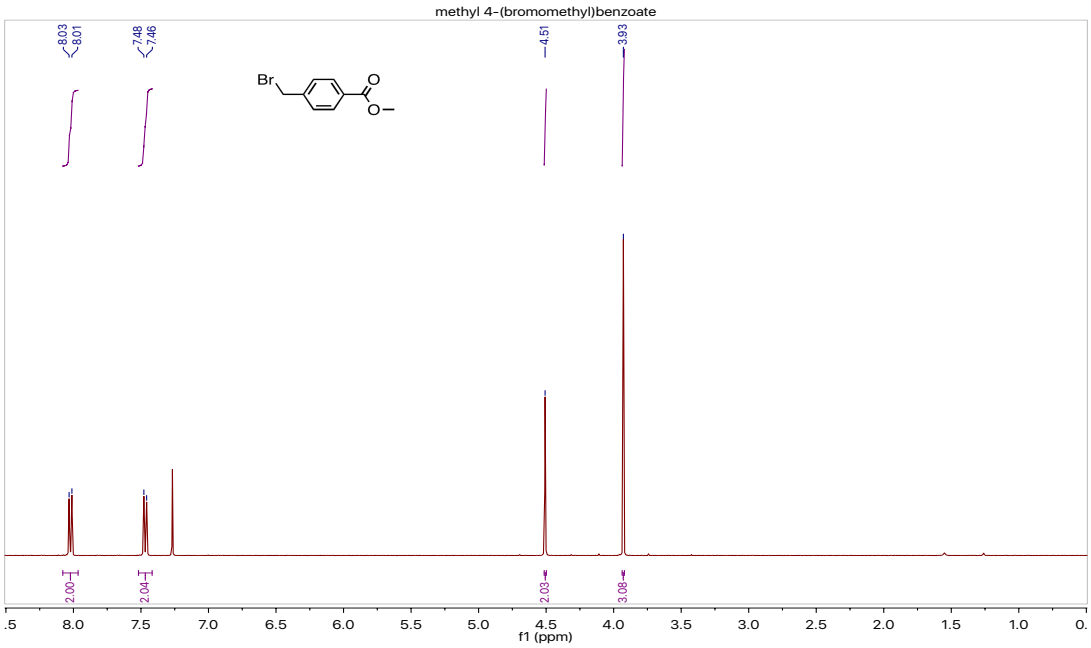

Figure 2.12 ^{1}H NMR (400 MHz, $CDCl_3$) spectrum of methyl 4-(bromomethyl)benzoate.

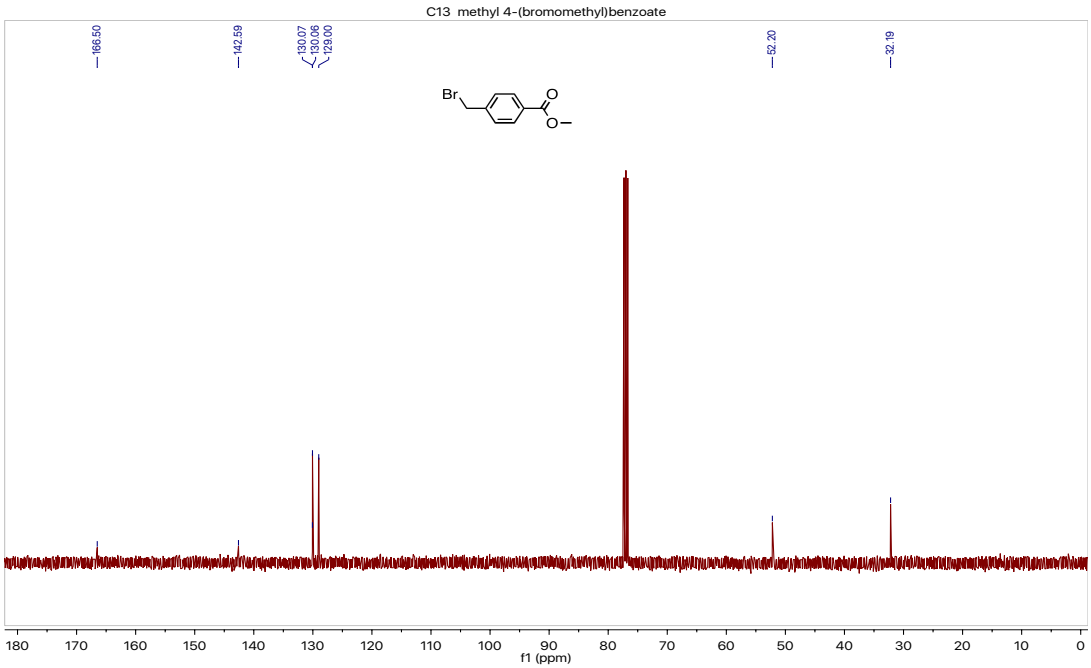

Figure 2.13 ^{13}C NMR (101 MHz, $CDCl_3$) spectrum of methyl 4-(bromomethyl)benzoate.

Synthesis of methyl 4-((diisopropylamino)methyl)benzoate.

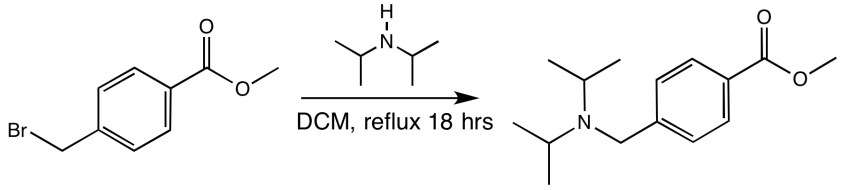

In a 250 mL reaction flask, methyl 4-(bromomethyl)benzoate (3.03 g, 13.0 mmol) was dissolved in dichloromethane (60 mL) and diisopropylamine (5.0 mL, 35 mmol) was added. The mixture was heated at reflux for 18 h. The flask was cooled to room temperature and its contents were added to a seperatory funnel. The solution was then washed with 1 M hydrochloric acid (20 mL x 3) and the layers were separated. To the acid solution, aqueous potassium hydroxide (4 M) was added there up to clearly basic, and the product was extracted with dichloromethane (25 mL x 3). The extract was washed with brine and dried over anhydrous Na_2SO_4 and filtered. The solvent was removed under reduced pressure to afford the crude methyl 4-((diisopropylamino)methyl)benzoate (2.02 g, 62 % yield) as a tan-yellow oil. Impurities are present. ^{1}H NMR (300 MHz, $CDCl_3$) δ 7.95 (d, J = 8.3 Hz, 2H), 7.45 (d, J = 8.5 Hz, 2H), 3.89 (s, 3H), 3.67 (s, 2H), 2.99 (dt, J = 13.2, 6.6 Hz, 2H), 1.01 (d, J = 6.6 Hz, 12H). ^{13}C NMR (75 MHz, $CDCl_3$) δ 167.2, 149.2, 129.3, 129.2, 127.7, 51.9, 48.9, 48.2, 20.7. HRMS-ESI: m/z calcd for [$C_{15}H_{23}NO_2$] 249.172; found 250.181 [M + H].

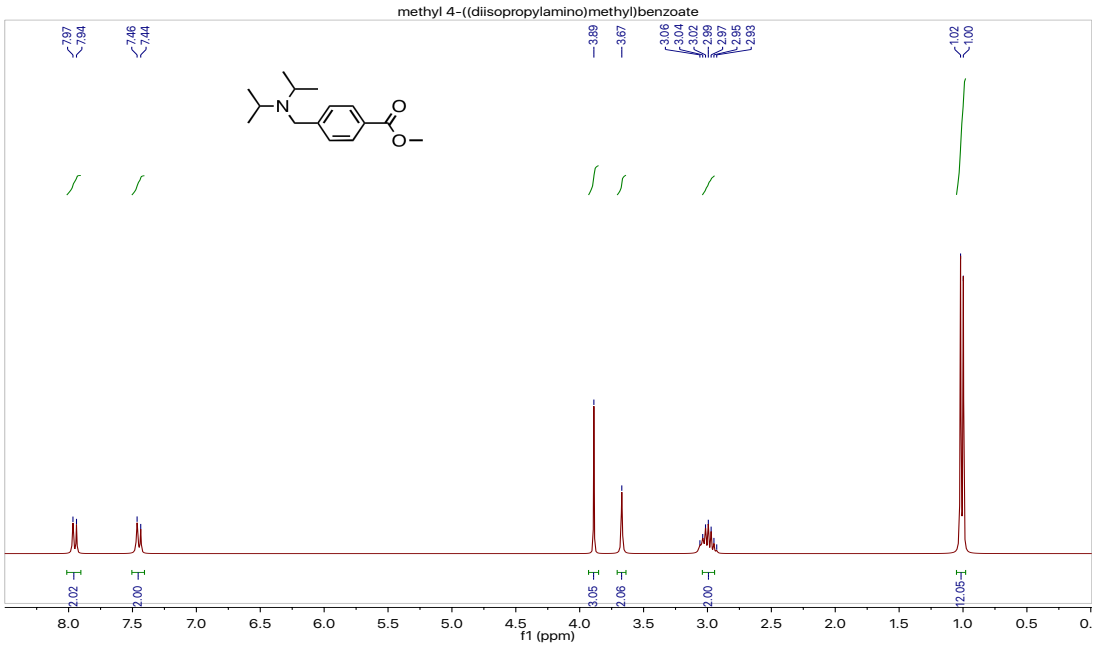

Figure 2.14 ^{1}H NMR (300 MHz, $CDCl_3$) spectrum of methyl 4-((diisopropylamino)methyl)benzoate.

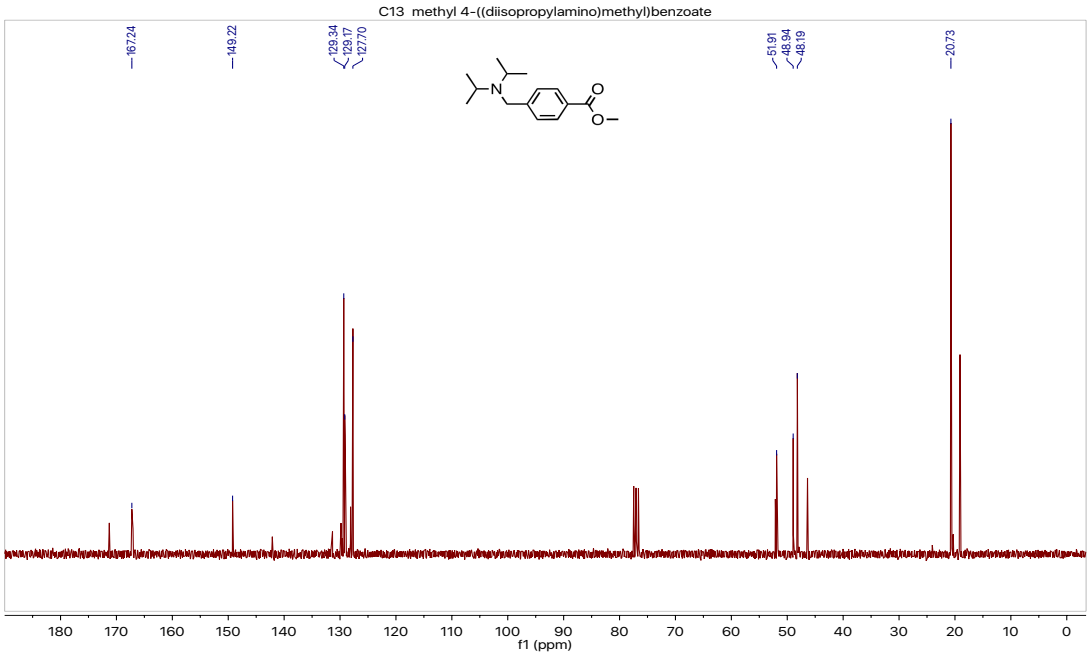

Figure 2.15 ^{13}C NMR (75 MHz, $CDCl_3$) spectrum of methyl 4-((diisopropylamino)methyl)benzoate.

Synthesis of 2.1a 4-((diisopropylamino)methyl)benzyl alcohol.

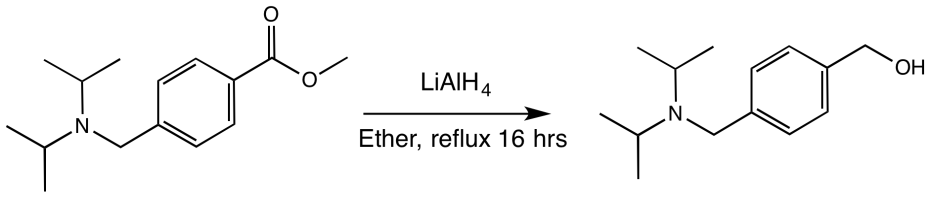

In a 250 mL reaction flask, methyl 4-((diisopropylamino)methyl)benzoate (2.02 g, 8.00 mmol) was dissolved in diethyl ether (5 mL) and set aside. Lithium aluminum hydride (924 mg, 24.0 mmol) was slowly added to diethyl ether (10 mL) at 0 °C and allowed to stir. The ester solution was added drop wise to the $LiAlH_4$ slurry with continued stirring. The mixture was allowed to warm up to r.t. and then stirred at reflux for 16 h. The reaction mixture was then cooled to r.t., then the flask was placed in an ice bath to cool to 0 °C. The solution was then slowly quenched with portions of ice water and aq. potassium hydroxide (5 M). The extract was dried over anhydrous $MgSO_4$ and filtered. The solvent was removed by reduced pressure to afford 4-((diisopropylamino)methyl)-benzyl alcohol (1.40 g, 79 % yield) as an oil.^{1}H NMR (300 MHz, $CDCl_3$) δ 7.37 (d, J = 8.1 Hz, 2H), 7.27 (d, J = 8.0 Hz, 2H), 4.64 (s, 2H), 3.62 (s, 2H), 3.00 (hept, J = 6.6 Hz, 2H), 1.75 (s, 1H), 1.01 (d, J = 6.6 Hz, 12H). ^{13}C NMR (101 MHz, $CDCl_3$) δ 142.84, 138.79, 128.08, 126.88, 65.31, 48.67, 47.83, 20.75. HRMS-ESI: m/z calcd for [$C_{14}H_{23}NO$] 221.178; found 222.185 [M + H].

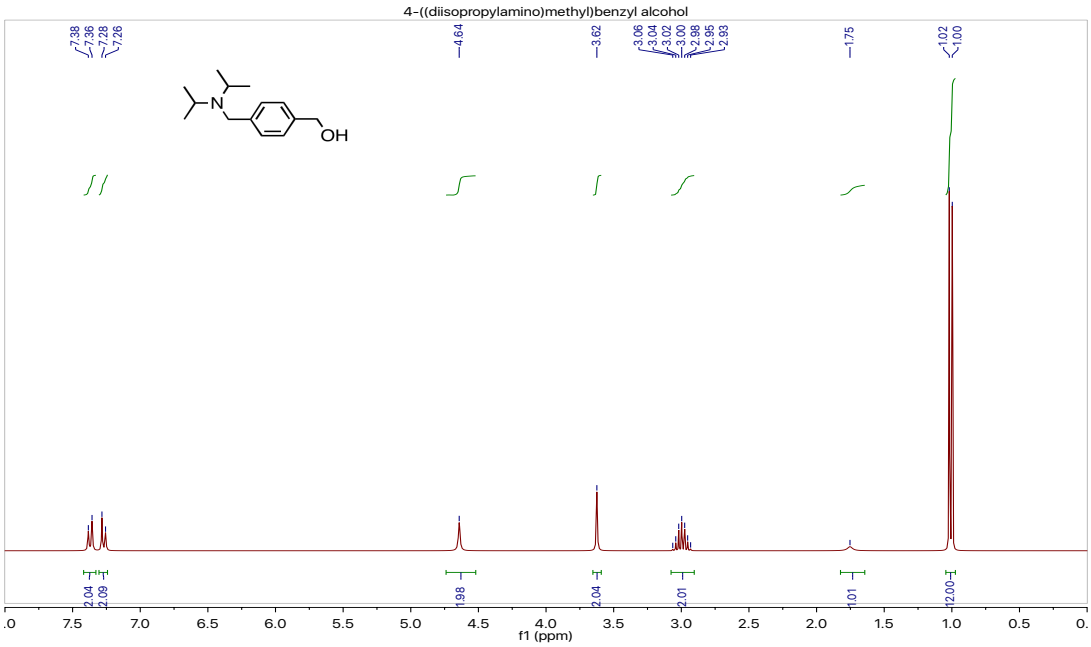

Figure 2.16 ^{1}H NMR (300 MHz, $CDCl_3$) spectrum of 2.1a 4-((diisopropylamino)methyl)benzyl alcohol.

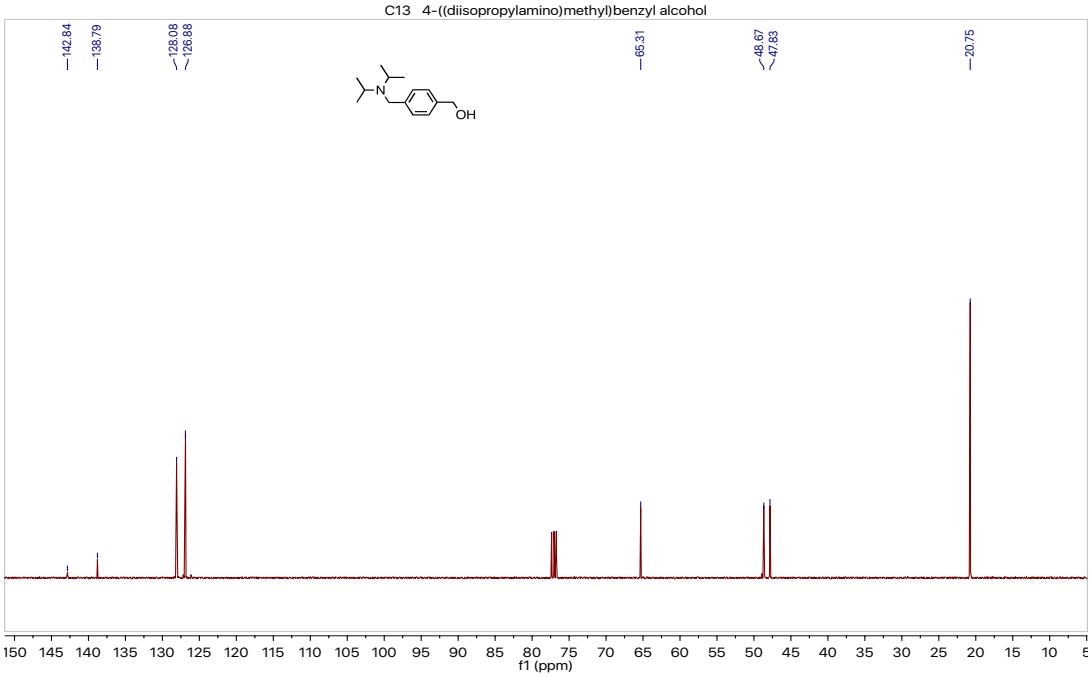

Figure 2.17 ^{13}C NMR (101 MHz, $CDCl_3$) spectrum of 2.1a 4-((diisopropylamino)methyl)benzyl alcohol.

Synthesis of 2.2b 4-((diisopropylamino)methyl)benzyl methyl ether.

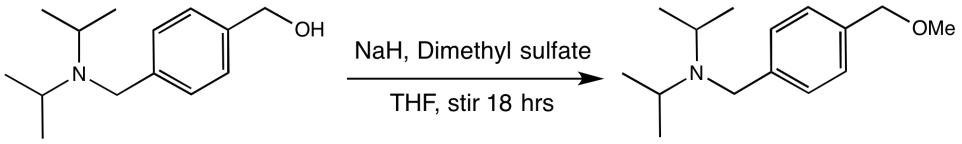

In a 2 neck 250 mL reaction flask, 4-((diisopropylamino)methyl)benzyl alcohol (497 mg, 2.25 mmol) was added dropwise to a stirred suspension of sodium hydride (125 mg, 5.20 mmol, 60% suspension in mineral oil) in dry THF (20 mL) under nitrogen. The solution was allowed to stir until no hydrogen gas bubbles evolved. Dimethyl sulfate (0.30 mL, 2.25 mmol) was then added dropwise and the solution continued to stir for 18 h. The resulting suspension was filtered (gravity filtration) and the solvent was removed under reduced pressure. The compound was purified by column chromatography (SiO_2, 5:1 dichloromethane / ethyl acetate) to provide 4-((diisopropylamino)methyl)benzyl methyl ether (307 mg, 58 % yield) as light tan oil. ^{1}H NMR (300 MHz, $CDCl_3$) δ 7.36 (d, J = 7.8 Hz, 2H), 7.25 (d, J = 7.9 Hz, 2H), 4.43 (s, 2H), 3.63 (s, 2H), 3.39 (s, 3H), 3.00 (p, J = 6.6 Hz, 2H), 1.01 (d, J = 6.6 Hz, 12H) ^{13}C NMR (75 MHz, $CDCl_3$) δ 142.8, 135.9, 127.9, 127.6, 74.7, 58.0, 48.7, 47.7, 20.7 HRMS-ESI: m/z calcd for [$C_{15}H_{25}NO$] 235.193; found 236.201 [M + H].

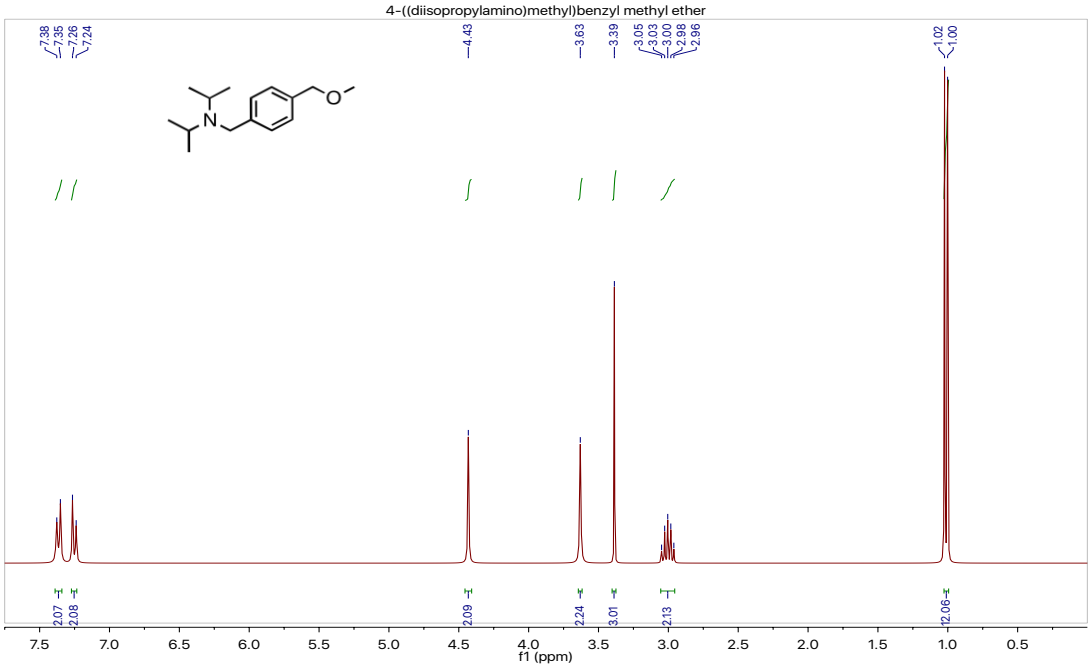

Figure 2.18 ^{1}H NMR (300 MHz, $CDCl_3$) spectrum of 4-((diisopropylamino)methyl)benzyl methyl ether.

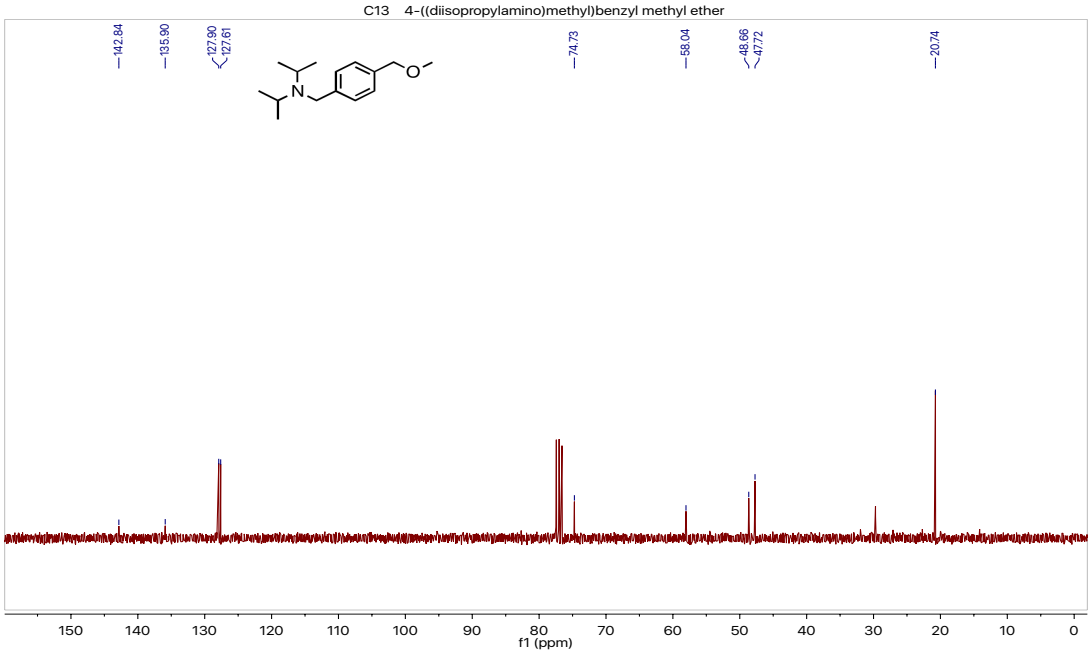

Figure 2.19 ^{13}C NMR (75 MHz, $CDCl_3$) spectrum of 4-((diisopropylamino)methyl)benzyl methyl ether.

Synthesis of 2.3c 4-((diisopropylamino)methyl)benzyl propargyl ether.

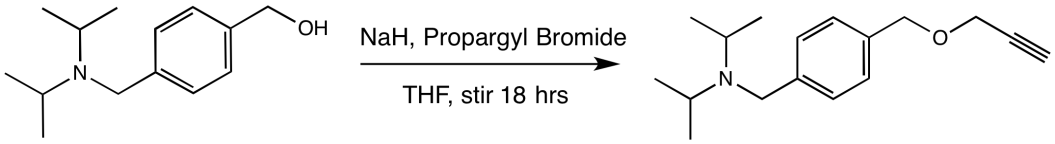

In a 2 neck 250 mL reaction flask, 4-((diisopropylamino)methyl)benzyl alcohol (1.61 g, 7.22 mmol) was added drop wise to a stirred suspension of sodium hydride (402 mg, 9.40 mmol, 60% suspension in mineral oil) in dry THF (30 mL) under nitrogen. The solution was allowed to stir until no hydrogen gas bubbles evolved. Propargyl bromide (0.55 mL, 7.2 mmol) was then added dropwise and the solution continued to stir for 18 h. The resulting suspension was filtered (gravity filtration) and the solvent was removed under reduced pressure. The compound was purified by column chromatography (SiO_2, 5:1 dichloromethane / ethyl acetate) to provide 4-((diisopropylamino)methyl)benzyl propargyl ether (1.23 g, 66 % yield) as light yellow oil. ^{1}H NMR (300 MHz, $CDCl_3$) δ 7.36 (d, J = 7.8 Hz, 2H), 7.26 (d, J = 7.8 Hz, 2H), 4.57 (s, 2H), 4.15 (d, J = 2.3 Hz, 2H), 3.62 (s, 2H), 3.00 (p, J = 6.6 Hz, 2H), 2.57 – 2.31 (m, 1H), 1.00 (d, J = 6.6 Hz, 12H). ^{13}C NMR (101 MHz, $CDCl_3$) δ 143.1, 135.0, 128.0, 127.9, 79.8, 74.5, 71.5, 56.9, 48.7, 47.8, 20.8. HRMS-ESI: m/z calcd for [$C_{17}H_{25}NO$] 259.193; found 260.201 [M + H].

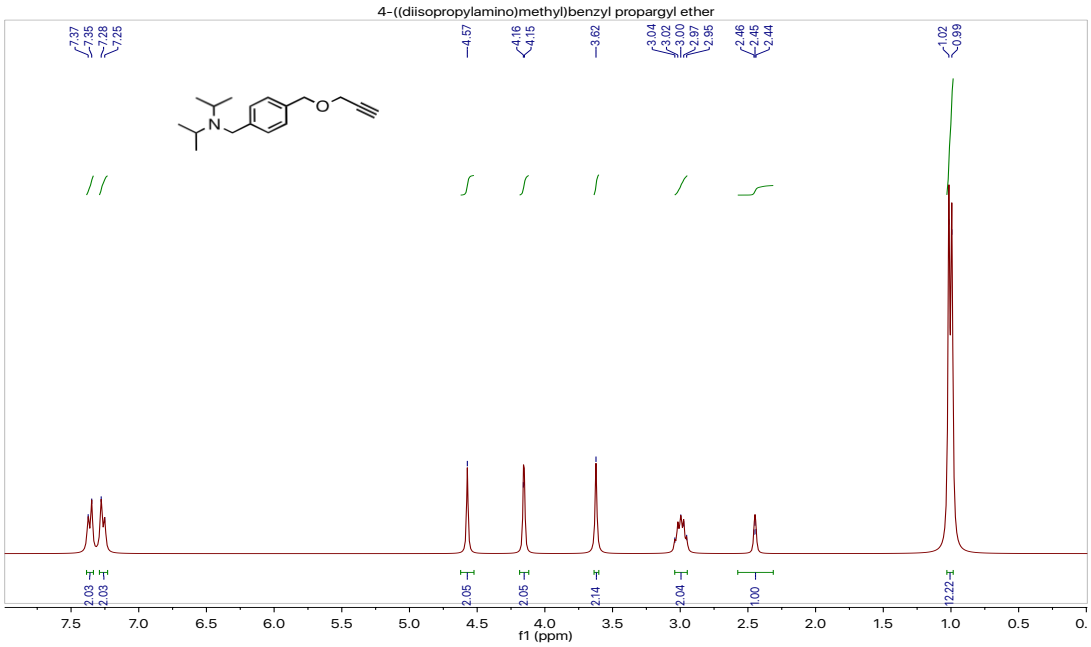

Figure 2.20 ^{1}H NMR (300 MHz, $CDCl_3$) spectrum of 4-((diisopropylamino)methyl)benzyl propargyl ether.

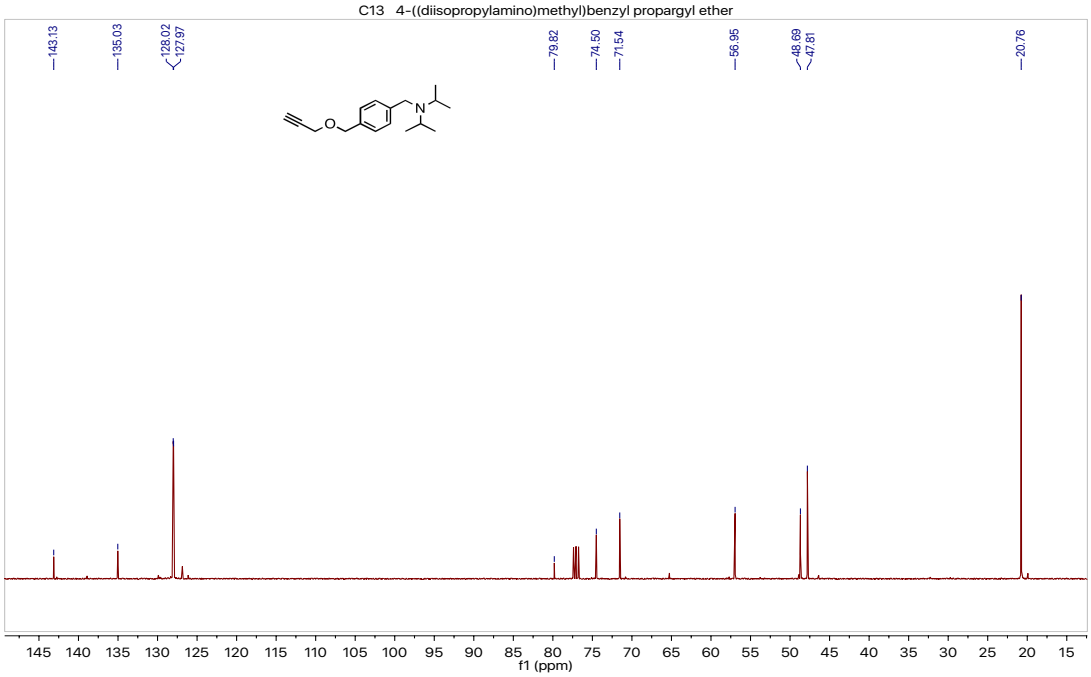

Figure 2.21 ^{13}C NMR (101 MHz, $CDCl_3$) spectrum of 4-((diisopropylamino)methyl)benzyl propargyl ether.

Synthesis of Cucurbit[7]uril.

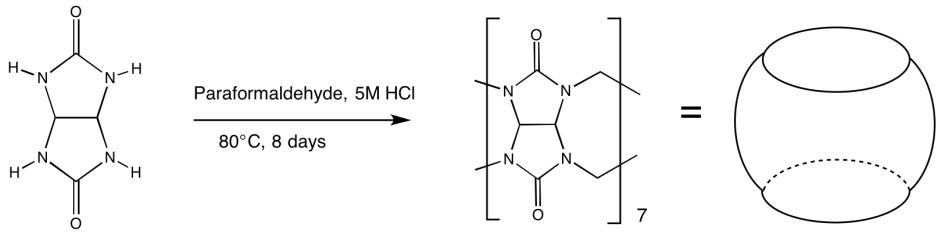

Following the procedure of Day et. al. in a 500 mL beaker, glycoluril (20.0 g, 141 mmol), paraformaldehyde (8.45 g, 282 mmol) and 5 M HCl (150 mL) were added. The mixture was heated at 80 °C for 8 d covered by a watch glass. During this period, addition of 5 M HCl was continued to keep the volume constant. The reaction mixture was cooled to room temperature and filtered. To the filtrate, methanol (400 mL) was added and settled for 1 d. The mixture was filtered and the solid was washed with methanol (2 x 100 mL). The dried solid was dissolved in 20% aq. Glycerol (500 mL v/v). The mixture was heated at 60-80 °C in open atmosphere for 3 h. The mixture was filtered. To the filtrate, methanol (400 mL) was added and the mixture was left overnight undisturbed. The mixture was filtered. The resulting solid was washed with methanol (3 x 100 mL) to obtain CB[7] (6.26 g, 27% yield) as a white solid. ^{1}H NMR (300 MHz, D_2O) δ 5.61 (d, J = 15.4 Hz, 14H), 5.36 (s, 14H), 4.06 (d, J = 15.3 Hz, 14H). ^{13}C NMR (126 MHz, D_2O) δ 156.5, 71.2, 52.5. HRMS-ESI: m/z calcd for $[(C_6H_6N_4O_2)_7Na]$ 1185.333; found 1185.333 [M+Na].

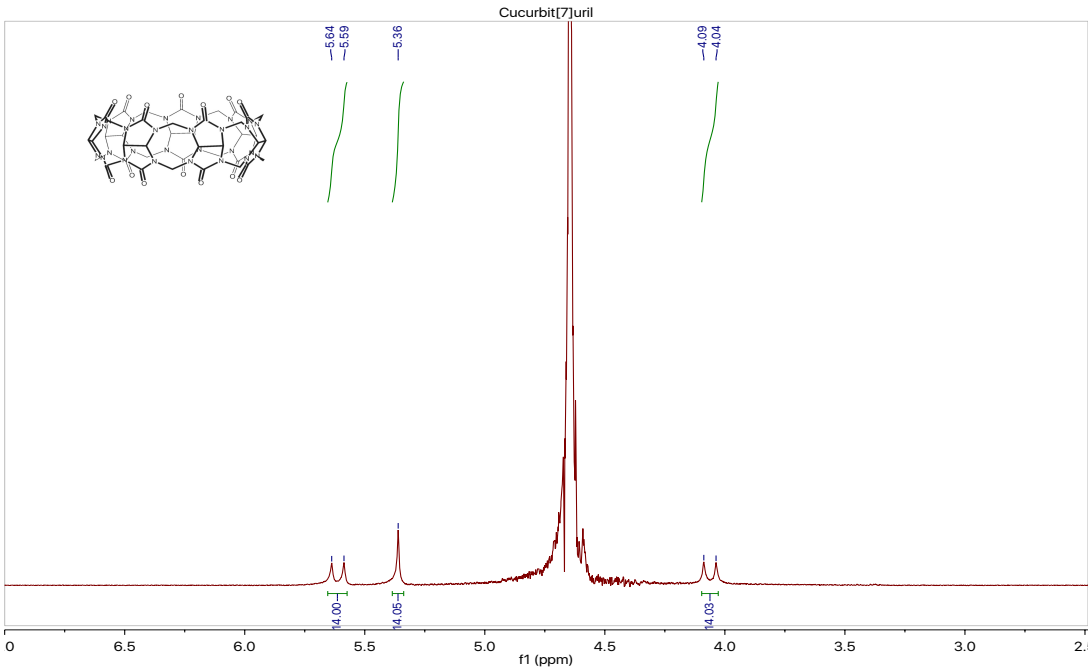

Figure 2.22 ^{1}H NMR (300 MHz, D_2O) spectrum of Cucurbit[7]uril.

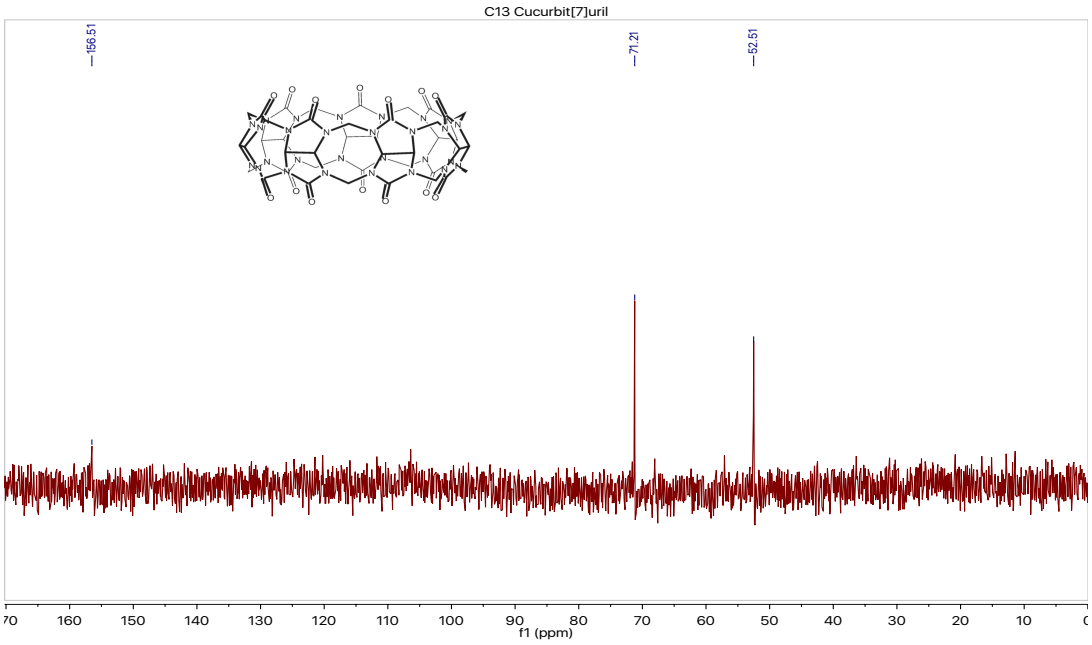

Figure 2.23 ^{13}C NMR (126 MHz, D_2O) spectrum of Cucurbit[7]uril.

^{1}H-NMR stability study of 4-((diisopropylamino)methyl)benzyl alcohol.

The equilibrium binding constant of compound alcohol **2.1a** with cucurbit[7]uril was determined by analyzing the competitive binding of **2.1a** compared to that of the reference compound $(Me)_3SiCD_2CD_2COOH$ (TMSP) **2.4d** using ^{1}H-NMR spectroscopy (500 MHz). The stability constant of the 1:1 adduct of CB[7] and silane **2.4d** is K_a = $(1.82 \pm 0.22) \times 10^7$ M^{-1}. The procedure followed was developed by Mock and Isaacs.[3e] Three solutions of 0.125 mM CB[7], 0.300 mM silane **2.4d**, and 3.00 mM alcohol **2.1a** were prepared in 50.0 mM $Na(O_2CCD_3)$-buffered D_2O (pD = 4.45). Silane **2.4d** demonstrated slow exchange kinetics on the NMR time scale resulting in clear peaks for bound and unbound silane **2.4d** at −0.7 and 0.0 ppm respectively. From the average of ratios of the bound and unbound silane **2.4d** of the three solutions (which was determined with a ±19% std. dev.), we determined the binding constant of alcohol **2.1a**: CB[7] (1:1) to be $K_a = (7.33 \pm 2.92) \times 10^5$ M^{-1}. Error analysis was carried out according to literature.[3e]

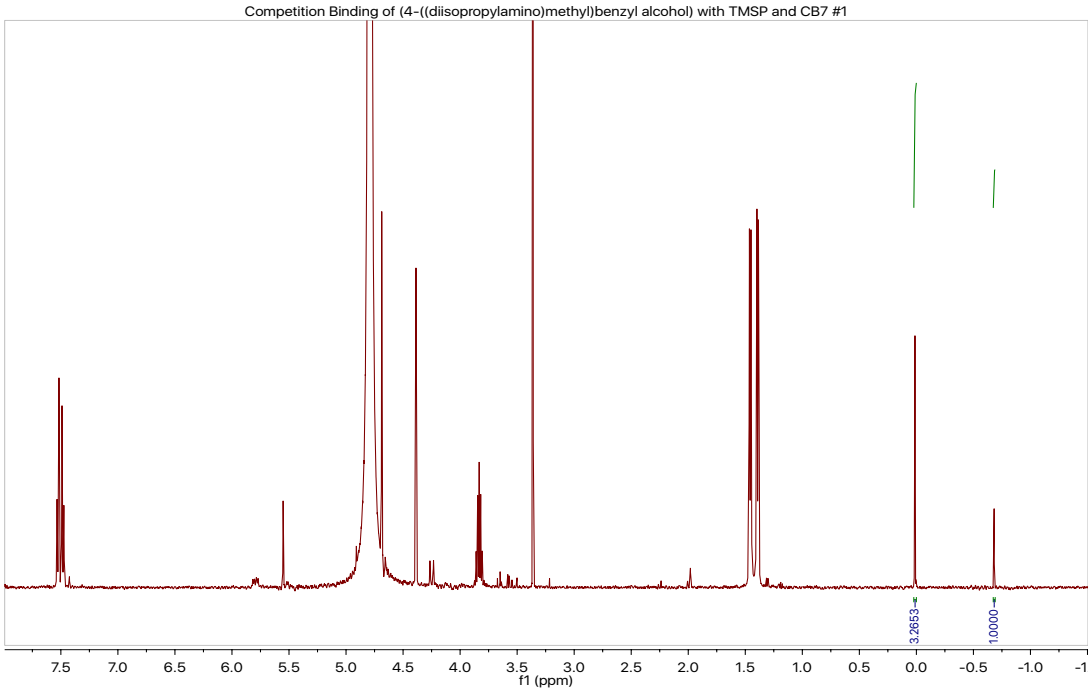

Figure 2.24 ^{1}H-NMR (500 MHz, Na(O_2CCD_3)-buffered D_2O (pD = 4.45)) spectrum 1 of competitive binding of **2.1a**, **2.4d**, and CB[7].

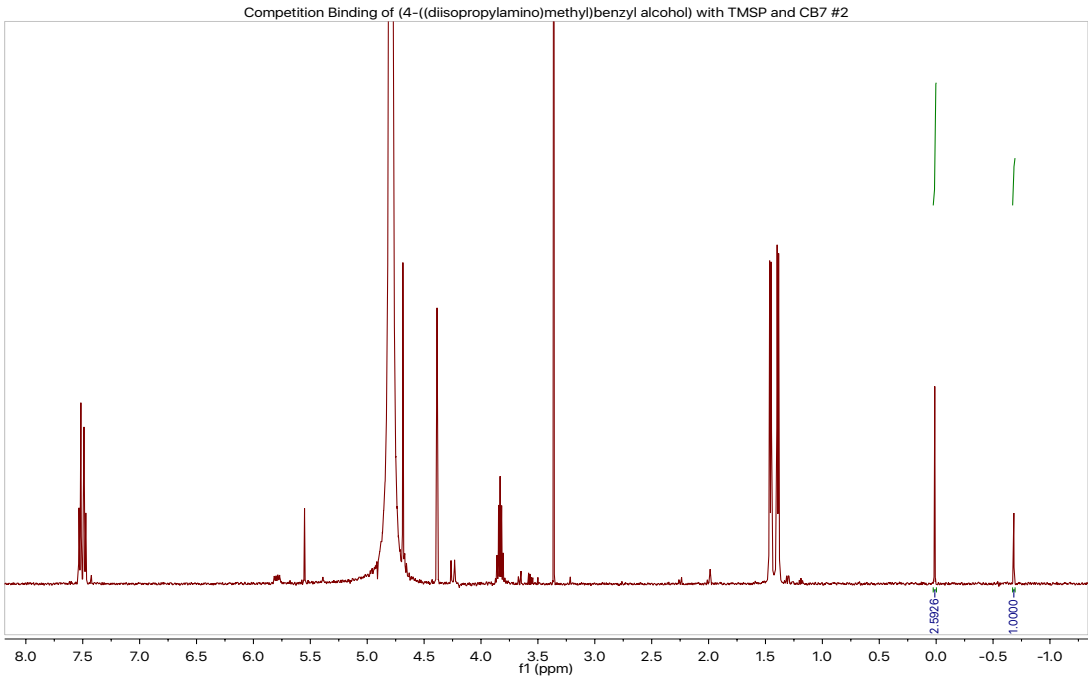

Figure 2.25 ^{1}H-NMR (500 MHz, Na(O_2CCD_3)-buffered D_2O (pD = 4.45)) spectrum 2 of competitive binding of **2.1a**, **2.4d**, and CB[7].

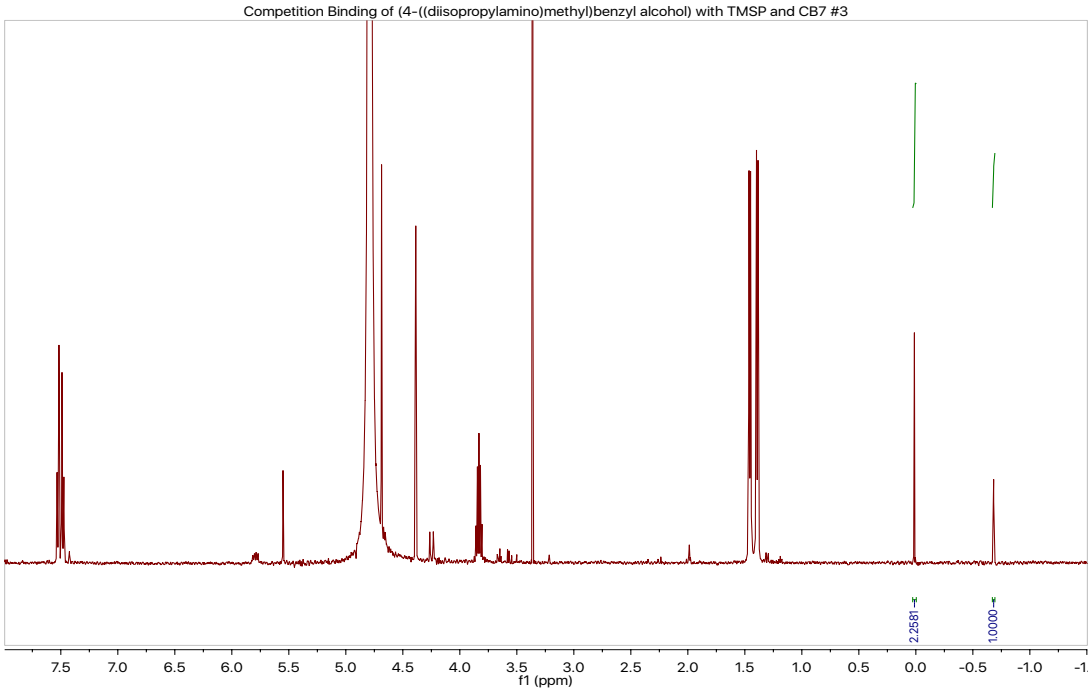

Figure 2.26 ^{1}H-NMR (500 MHz, Na(O_2CCD_3)-buffered D_2O (pD = 4.45)) spectrum 3 of competitive binding of **2.1a**, **2.4d**, and CB[7].

^{1}H-NMR stability study of 4-((diisopropylamino)methyl)benzyl methyl ether.

The equilibrium binding constant of compound methyl ether **2.2b** with cucurbit[7]uril was determined by analyzing the competitive binding of methyl ether **2.2b** compared to that of the reference compound $(Me)_3SiCD_2CD_2COOH$ (TMSP) **2.4d** using ^{1}H-NMR spectroscopy (500 MHz). The stability constant of the 1:1 adduct of CB[7] and silane **2.4d** is $K_a = (1.82 \pm 0.22) \times 10^7$ M^{-1}. The procedure followed was developed by Mock and Isaacs.[3e] Three solutions of 0.125 mM CB[7], 0.300 mM silane **2.4d**, and 3.50 mM methyl ether **2.2b** were prepared in 50.0 mM Na(O_2CCD_3)-buffered D_2O (pD = 4.45). Silane **2.4d** demonstrated slow exchange kinetics on the NMR time scale resulting in clear peaks for bound and unbound silane **2.4d** at –0.7 and 0.0 ppm

respectively. From the average of ratios of the bound and unbound silane **2.4d** of the three solutions (which was determined with a ±5.6% std. dev.), we determined the binding constant of methyl ether **2.2b**:CB[7] (1:1) to be K_a = (5.41 ± 0.90) ×10^5 M^{-1}. Error analysis was carried out according to literature.[3e]

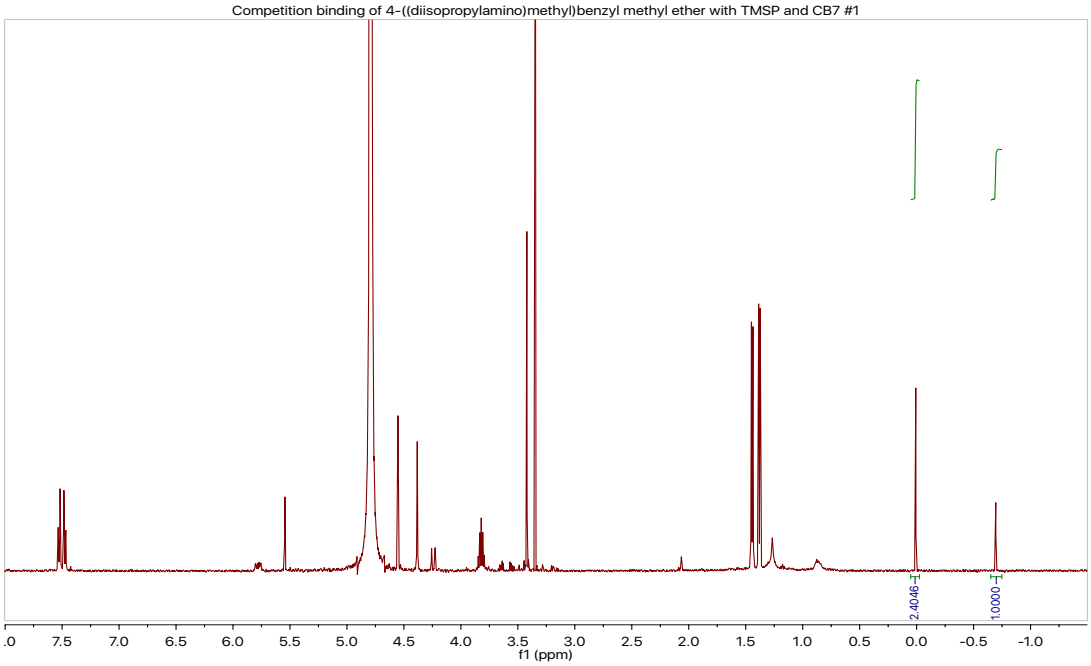

Figure 2.27 ^{1}H-NMR (500 MHz, Na(O_2CCD_3)-buffered D_2O (pD = 4.45)) spectrum 1 of competitive binding of **2.2b**, **2.4d**, and CB[7].

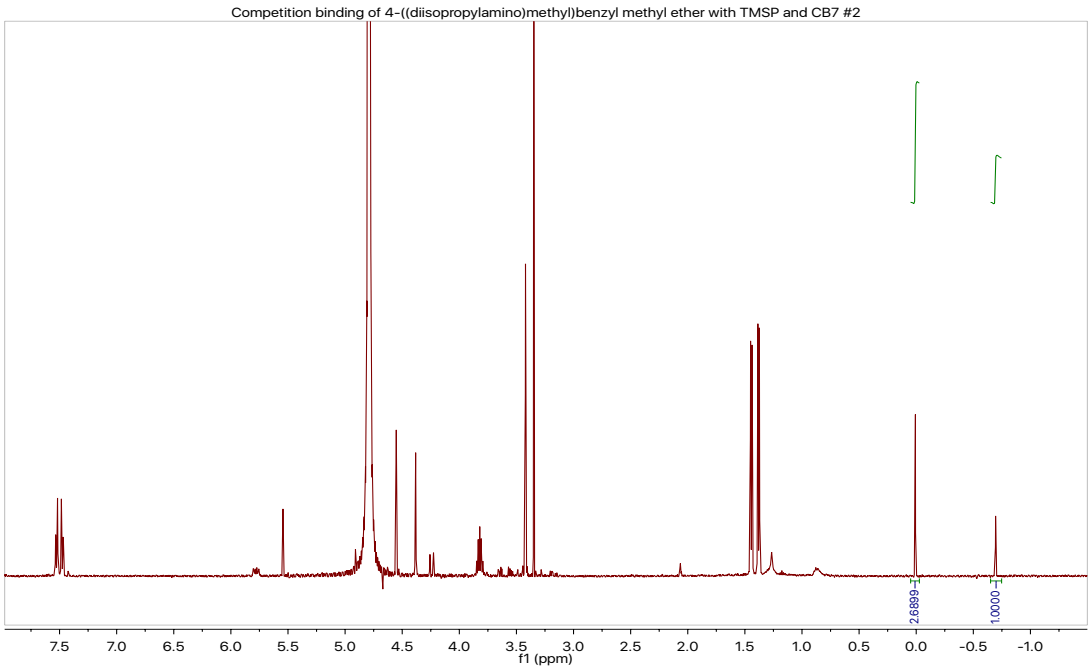

Figure 2.28 ^{1}H-NMR (500 MHz, Na(O_2CCD_3)-buffered D_2O (pD = 4.45)) spectrum 2 of competitive binding of **2.2b**, **2.4d**, and CB[7].

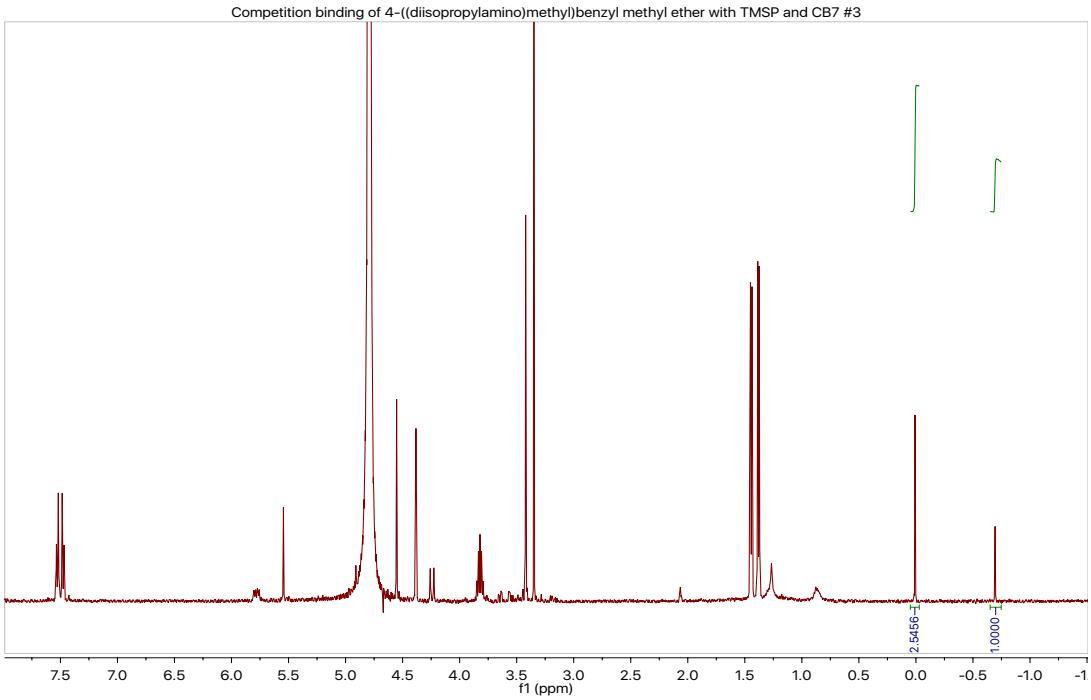

Figure 2.29 ^{1}H-NMR (500 MHz, Na(O_2CCD_3)-buffered D_2O (pD = 4.45)) spectrum 3 of competitive binding of **2.2b**, **2.4d**, and CB[7].

^{1}H-NMR stability study of 4-((diisopropylamino)methyl)benzyl propargyl ether.

The equilibrium constant of compound propargyl ether **2.3c** with cucurbit[7]uril was determined by analyzing the competitive binding of propargyl ether **2.3c** compared to that of the reference compound $(Me)_3SiCD_2CD_2COOH$ (TMSP) silane **2.4d** using ^{1}H-NMR spectroscopy (500 MHz). The stability constant of the 1:1 adduct of CB[7] and silane **2.4d** is $K_a = (1.82 \pm 0.22) \times 10^7\ M^{-1}$. The procedure followed was developed by Mock and Isaacs.[3e] Three solutions of 0.125 mM CB[7], 0.300 mM silane **2.4d**, and 4.00 mM propargyl ether **2.3c** were prepared in 50.0 mM $Na(O_2CCD_3)$-buffered D_2O (pD = 4.45). Silane **2.4d** demonstrated slow exchange kinetics on the NMR time scale resulting in clear peaks for bound and unbound silane **2.4d** at −0.7 and 0.0 ppm respectively. From the average of ratios of the bound and unbound silane **2.4d** of the three solutions (which was determined with a ±1.6% std. dev.), we determined the binding constant of propargyl ether **2.3c**:CB[7] (1:1) to be $K_a = (4.85 \pm 0.62) \times 10^5\ M^{-1}$. Error analysis was carried out according to literature.[3e]

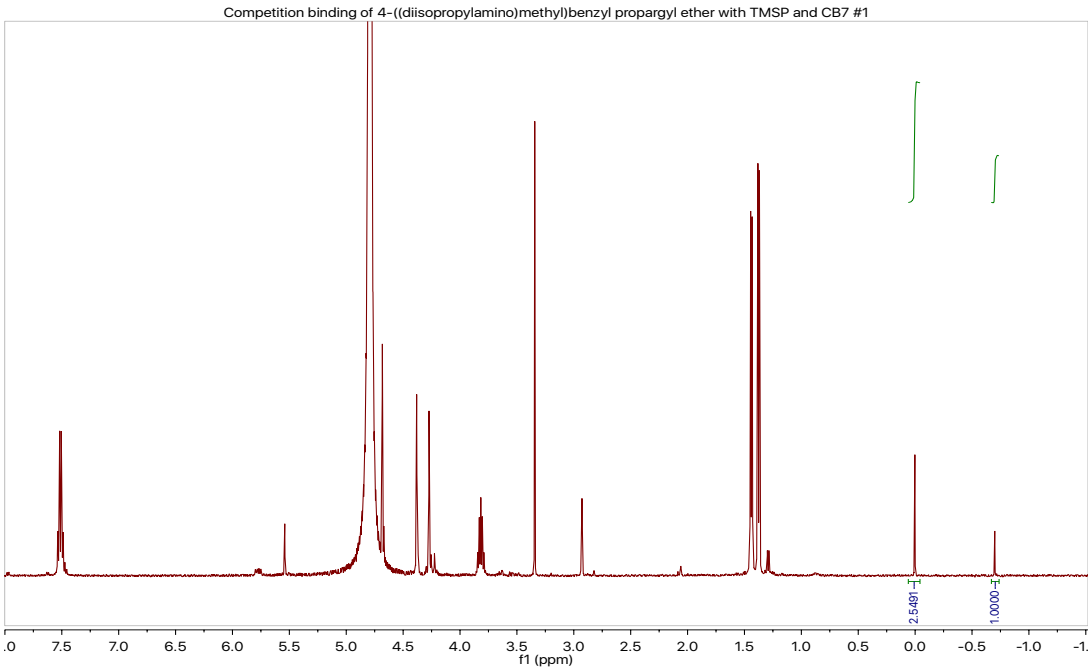

Figure 2.30 ^{1}H-NMR (500 MHz, Na(O_2CCD_3)-buffered D_2O (pD = 4.45)) spectrum 1 of competitive binding of **2.3c**, **2.4d**, and CB[7].

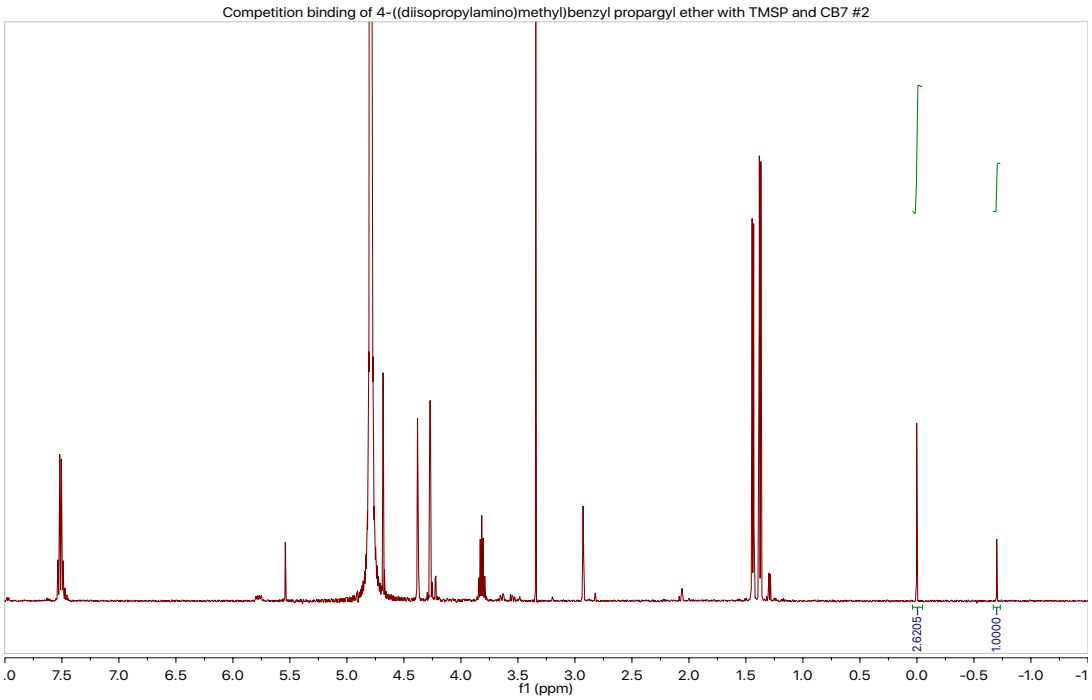

Figure 2.31 ^{1}H-NMR (500 MHz, Na(O_2CCD_3)-buffered D_2O (pD = 4.45)) spectrum 2 of competitive binding of **2.3c**, **2.4d**, and CB[7].

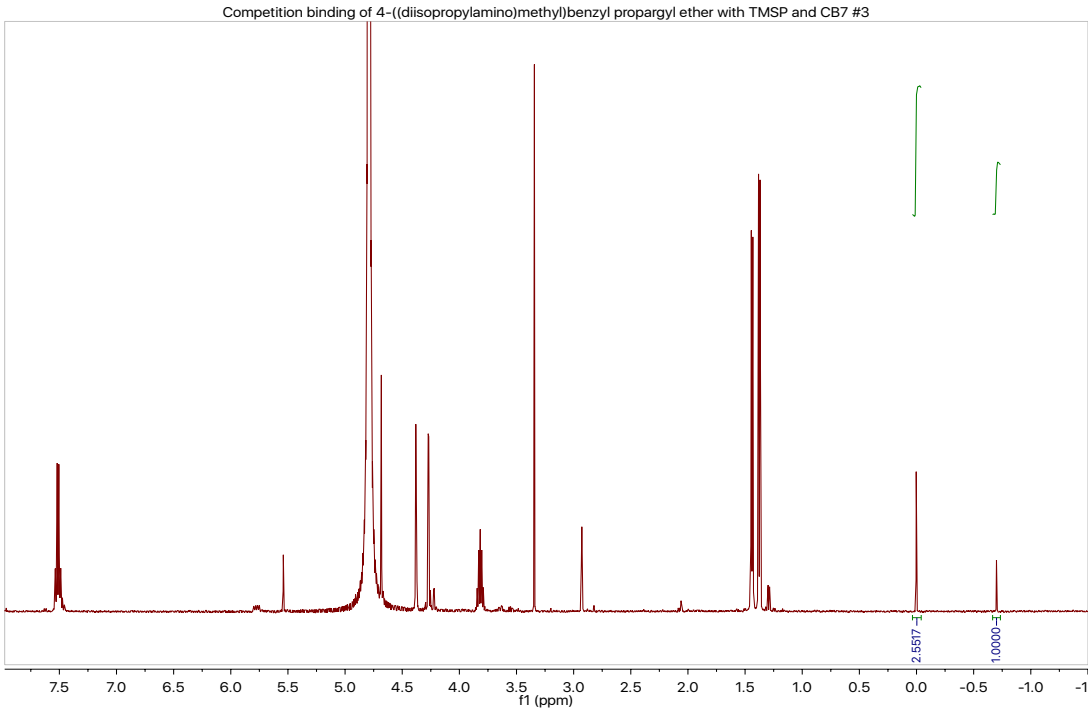

Figure 2.32 ^{1}H-NMR (500 MHz, Na(O_2CCD_3)-buffered D_2O (pD = 4.45)) spectrum 3 of competitive binding of **2.3c**, **2.4d**, and CB[7].

2.7 References

1. Thordarson, P. *Chem. Soc. Rev.* **2011**, *40*, 1305-1323.
2. (a) Dodziuk, H. *Introduction to Supramolecular Chemistry*, Kluwer Academic Publishers: New York, 2002. (b) Beer, P. D.; Gale, P. A.; Smith, D. K. *Supramolecular Chemistry*, Oxford Chemistry Primers, 74, Oxford University Press: Oxford, 2003. (c) Steed, J. W.; Turner, D. R.; Wallace, K. J. *Core Concepts in Supramolecular Chemistry and Nanochemistry*, John Wiley & Sons, Ltd.: Chichester, 2007. (d) Steed, J. W.; Atwood, J. L.; *Supramolecular Chemistry*, John Wiley and Sons, Ltd.: Chichester, 2000. (e) Schalley, C. A. *Analytical Methods in Supramolecular Chemistry*, Wiley-VCH Verlag GmbH & Co. KGaA: Weinheim, 2007.
3. (a) Mock, W. L.; Shih, N. Y. *J. Org. Chem.* **1986**, *51*, 4440-4446; (b) Mock, W. L.; Pierpont, J. *J. Chem. Soc., Chem Comm* **1990**, 1509-1511.; (c) Ong, W.; Gomez-Kaifer, M.; Kaifer, A. E. *Org. Lett.* **2002**, *4*, 1791-1794.; (d) Moon, K.; Kaifer, A. E. *Org. Lett.* **2004**, *6*, 185-188.; (e) Liu, S.; Ruspic, C.; Mukhopadhyay, P.; Chakrabarti, S.; Zavalij, P. Y.; Isaacs, L. *J. Am. Chem. Soc.* **2005**, *127*, 15959-15967; (f) Barrow, S. J.; Kasera, S.; Rowland, M. J.; Barrio, J.; Scherman, O. R. *Chem. Rev.* **2015**, *115*, 12320-12406.; (g) Assaf, K. I.; Nau, W. M. *Chem. Soc. Rev.* **2015**, *44*, 394-418.
4. Cheng, X.-J.; Liang, L.-L.; Chen, K.; Ji, N.-N.; Xiao, X.; Zhang, J.-X.; Zhang, Y.-Q.; Xue, S.-F.; Zhu, Q.-J.; Ni, X.-L.; Tao, Z. *Angew. Chem, Int. Ed.* **2013**, *52*, 7252-7255
5. Sindelar, V.; Moon, K.; Kaifer, A. E. *Org. Lett.*, **2004**, *6*, 2665-2668.

6. (a) Parvari, G.; Reany, O.; Keinan, E. *Isr. J. Chem.* **2011**, *51*, 646.; (b) Urbach, A. R.; Ramalingam, V. *Isr. J. Chem.* **2011**, *51*, 664-678.; (c) Logsdon, L. A.; Schardon, C. L.; Ramalingam, V.; Kwee, S. K.; Urbach, A. R. *J. Am. Chem. Soc.* **2011**, *133*, 17087-17092.; (d) Angelos, S.; Yang, Y.-W.; Patel, K.; Stoddart, J. F.; Zink, J. I. *Angew. Chem., Int. Ed.* **2008**, *47*, 2222.; (e) Angelos, S.; Khashab, N. M.; Yang, Y.-W.; Trabolsi, A.; Khatib, H. A.; Stoddart, J. F.; Zink, J. I. *J. Am. Chem. Soc.* **2009**, *131*, 12912.; (f) Sun, Y.-L.; Yang, B.-J.; Zhang, S. X.-A.; Yang, Y.-W. *Chem. Eur. J.* **2012**, *18*, 9212.; (g) Macartney, D. H. *Isr. J. Chem.* **2011**, *51*, 600.; (h) Walker, S.; Oun, R.; McInnes, F.J.; Wheate, N.J. *Isr. J. Chem.* **2011**, *51*, 616.; (i) Jeon, Y. J.; Kim, S.Y.; Ko, Y.H.; Sakamoto, S.; Yamaguchi, K.; Kim, K. *Org. Biomol. Chem.* **2005**, *3*, 2122. (j) Tuncel, D.; Özsar, O.; Tiftik, H. B.; Salih, B. *Chem. Commun.* **2007**, 1369-1371.; (k) Xue, M.; Yang, Y.; Chi, X.; Yan, X.; Huang, F. *Chem. Rev.,* **2015**, *115*, 7398-7501.

7. Huang, Z.; Qin, K.; Deng, G.; Wu, G.; Bai, Y.; Xu, J.-F.; Wang, Z.; Yu, Z.; Scherman, O. A.; Zhang, X. *Langmuir* **2016,** *32 (47)*, 12352-12360.

8. Singh, A.; Yip, W. T.; Halterman, R. L. *Org. Lett.* **2012**, *14*, 4046-4049. Singh, A. Cucurbit[7]uril mediated viologen-fluorophore dyad for fluorescence off/on switch. Ph.D. dissertation. University of Oklahoma, 2012.

9. Day, A. I.; Arnold, A. P.; Blanch, R. J. Snushall, B. *J. Org. Chem.* **2001**, *66*, 8094-8100.

10. (a) Odell, B.; Redington, M. V.; Slawin, A. M. Z., Spencer, N.; Stoddart, J. F.; Williams, D. J. *Angew. Chem. Int. Ed. Engl.* **1988**, *27*, 1547-1550.; (b) Spencer, N.;

Stoddart, J. F. *J. Am. Chem. Soc.* **1991**, *113*, 5131-5133.; (c) Sobransingh, D.; Kaifer, A. E. *Org. Lett.* **2006**, *8*, 3247.

11. Molecules were drawn and dimensions were measured at the widest point using Spartan '14 molecular modeling.

Chapter 3: Development and Analysis of Stoppering Groups for Viologen Rotaxanes

3.1 Introduction to Rotaxanes

The study of rotaxanes has been an area of particular interest within the vastly growing field of mechanically interlocked molecules (MIMs). Since their first development in the late 1960's, much of the research being done on rotaxanes and their architecture has been focused on their efficient synthesis and applications as artificial nanomachines. The word "rotaxane" originates from the Latin words for wheel (rota) and axle (axis). Rotaxanes are dumbbell shaped molecules that consist of a linear rod shaped guest species and a cyclic species that acts as a beadlike host in which they are bound together through non-covalent bonds in a threadlike structure (Figure 3.1).[1] Rotaxanes are particulary interesting for nanomachines in that they will have a stable assembly that can be characterized and used.

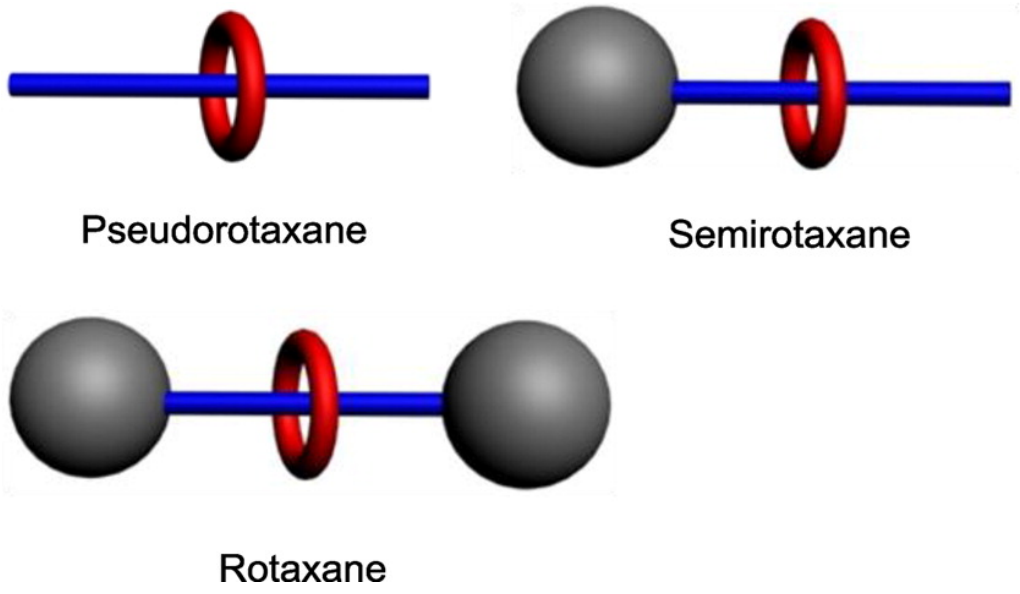

Figure 3.1 Cartoon representation of rotaxane, pseudorotaxane, semirotaxane. Adapted from Huang et. at.[1]

Pseudorotaxanes are a subcategory of rotaxanes in which "pseudo" means false. Therefore "pseudorotaxanes" are false rotaxanes or rather they do not consist of having bulky stopper groups at the ends of the axle, however if a pseudorotaxane contains one bulky stopper it is called a semirotaxane. The pseudorotaxane and semirotaxane are less stable and in both cases the cyclic host can "de-thread" off of the axle when in the presence of a stronger binding guest. Therefore, in order to be considered a full rotaxane the cyclic host must be sterically blocked from de-threading by bulky stoppers at both ends of the axle.

The earliest strategies for developing rotaxanes began with statistical threading, introduced by Harrison et. al.,[2] was based on purely statistical progress without any evident attractive forces between linear guest and cyclic host. In the last 30 years, rotaxanes have been synthesized easily by direct template methods,[3] stemming from hydrogen bonding,[4] hydrophobic interactions,[5] metal ion coordination,[6] and pi-pi stacking.[7] Currently, there are five typical methods (Figure 3.2) used when constructing rotaxanes through template directed methodologies. Figure 3.2 displays the capping method where the macrocyclic host "pre-threads" the axle to form a pseudorotaxane and then a [2]rotaxane is formed by capping the ends of the axle with bulky groups preventing the macrocycle from de-threading. A similar pathway is snapping in which a semirotaxane is formed first, then another bulky end group is added. This is an excellent method to prepare unsymmetrical rotaxanes where the end groups bear different functionality. The clipping method is used when forming the macrocycle around the preformed dumbbell-like axle. However, in the slipping method the macrocycle can thread over a blocking group of a preformed axle at elevated temperatures. The active

metal template method is when the metal serves two roles in bringing together and positioning ligands in addition to catalyzing the covalent bond formation of the threaded structure.[1]

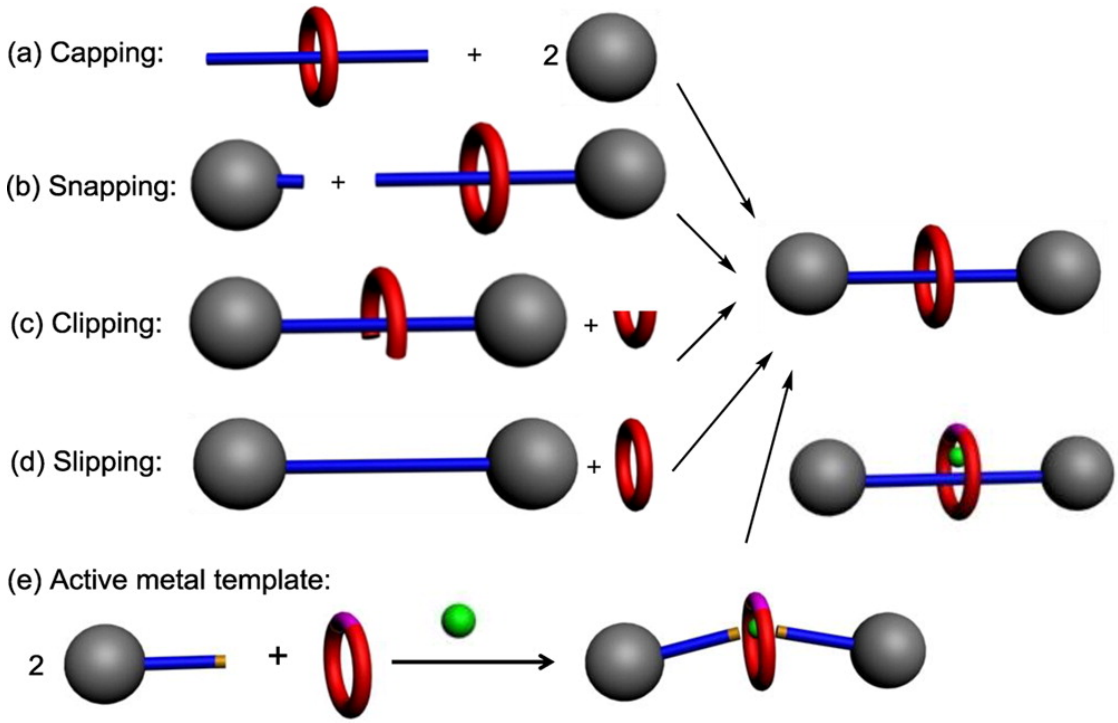

Figure 3.2 Cartoon representation of the construction of rotaxanes. Adapted from Haung et. al.[1]

The use of rotaxanes as molecular machines has gained popularity as a result of their ability to undergo translational isomerisation between two or more molecules.[8] This isomerisation is a result of the translational molecular motion of the macrocyclic bead moving along the linear axle. This characteristic allows rotaxanes to be applied in the construction of various molecular devices such as shuttles,[9] switches,[10] sensors,[11] muscles,[12] elevators,[13] and nanovalves[14] just to name a few. The typical motion of the macrocycle is rotation and shuttling across the axle.

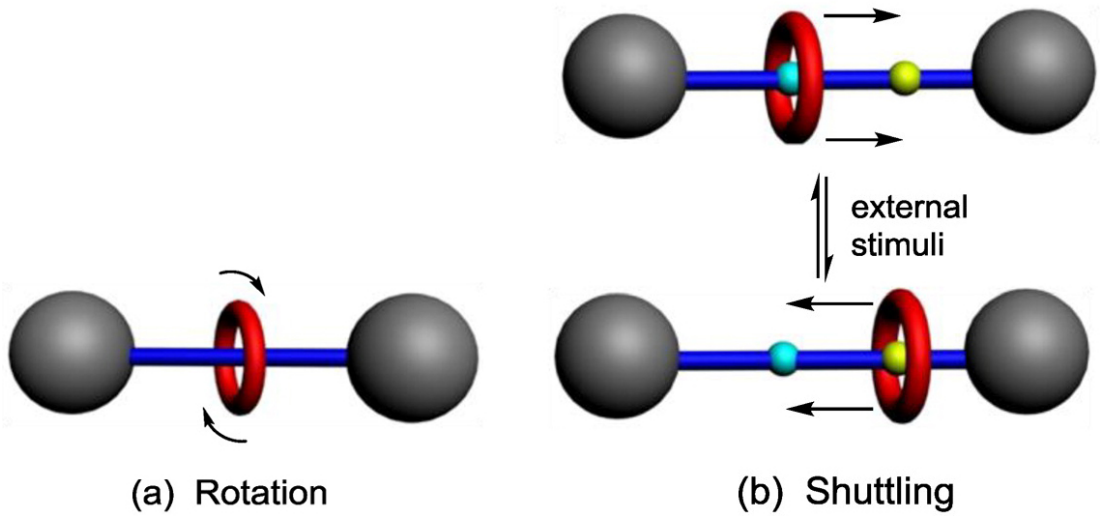

Figure 3.3 Cartoon representation of the types of molecular mobility of rotaxanes. Adapted from Huang et. al.[1]

Stoddart and co-workers initially observed this shuttling effect in 1991 with their [2]rotaxane consisting of a paraquat-cyclophane bead and a polyether axle.[9a] The axle contained two hydroquinol binding units or "stations" for the paraquat-cyclophane bead to bind to when shuttling back and forth, in addition to the triisopropylsilyl stoppers which prevent de-threading. The mode of binding is through pi-pi stacking between the pi-electron deficient paraquat-cyclophane and the pi-electron rich hydroquinol units. The shuttling effect was observed through temperature dependence in the H-NMR spectrum. At room temperature, the aromatic proton shifts for the hydroquinol units were merged with the base line indicating fast exchange with the bead as it was shuttling between the stations. When cooling the same sample to -50°C two independent signals were observed for the hydroquinol units, indicating that the bead had "docked" with one station.

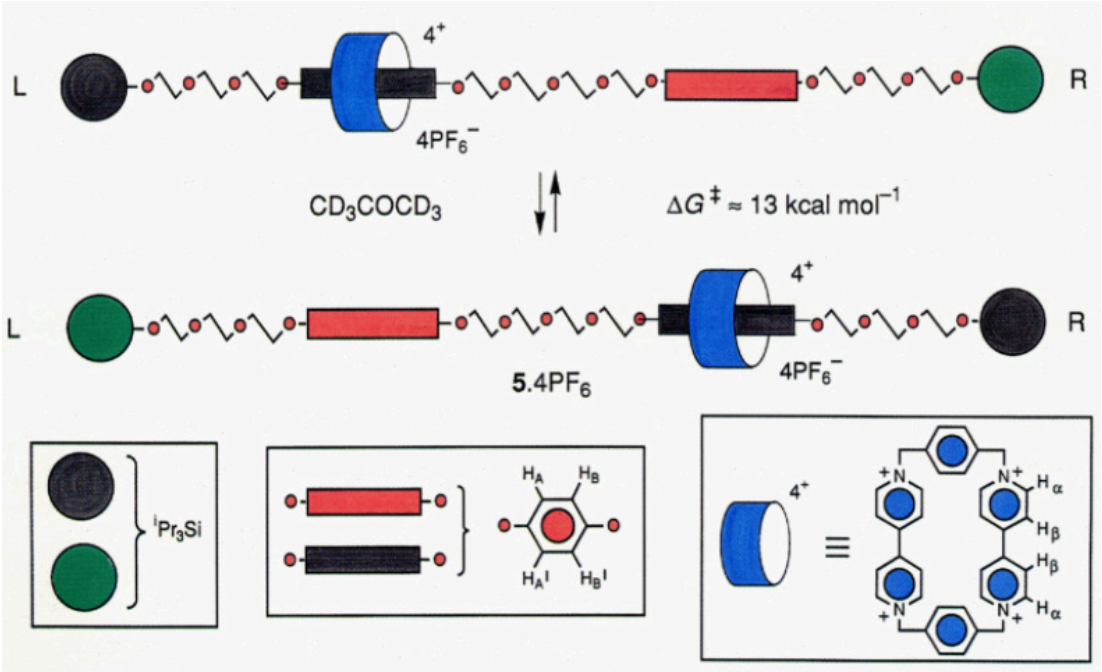

Figure 3.4 Paraquat-cyclophane rotaxane from Stoddart et. al.[9a]

Due to the observed mobility of early rotaxanes and pseudorotaxanes, rigorous investigations from controlling the mobile rate,[15] or even stopping its behavior,[16] to manipulating its motion *via* external stimuli[17] such as pH, light, temperature and electric current have been devoted to this field.

Kaifer and coworkers had collaborated with Stoddart to expand upon this foundational shuttle [2]rotaxane. They developed a new polyether rotaxane axle with two different pi-electron stations consisting of biphenol and benzidine units (as pi-electron donors) with bulky triisopropylsilyl stoppers that prevent the paraquat-cyclophane (pi-electron acceptor) bead from de-threading (Figure 3.5). At room temperature, the bead shuttles between stations with no preference indicated by broadening of signals in the ^{1}H-NMR spectrum, however when cooled to –44 °C the H-NMR spectrum showed two translational isomers where the paraquat-cyclophane

showed preference to the benzidine station at 84% occupation and the biphenol at 16% occupation. However, the position of the bead can be switched to the biphenol unit by protonation of the nitrogens in the benzidine unit and reversal by neutralization, or by electrochemical oxidation to produce the corresponding dication.[18]

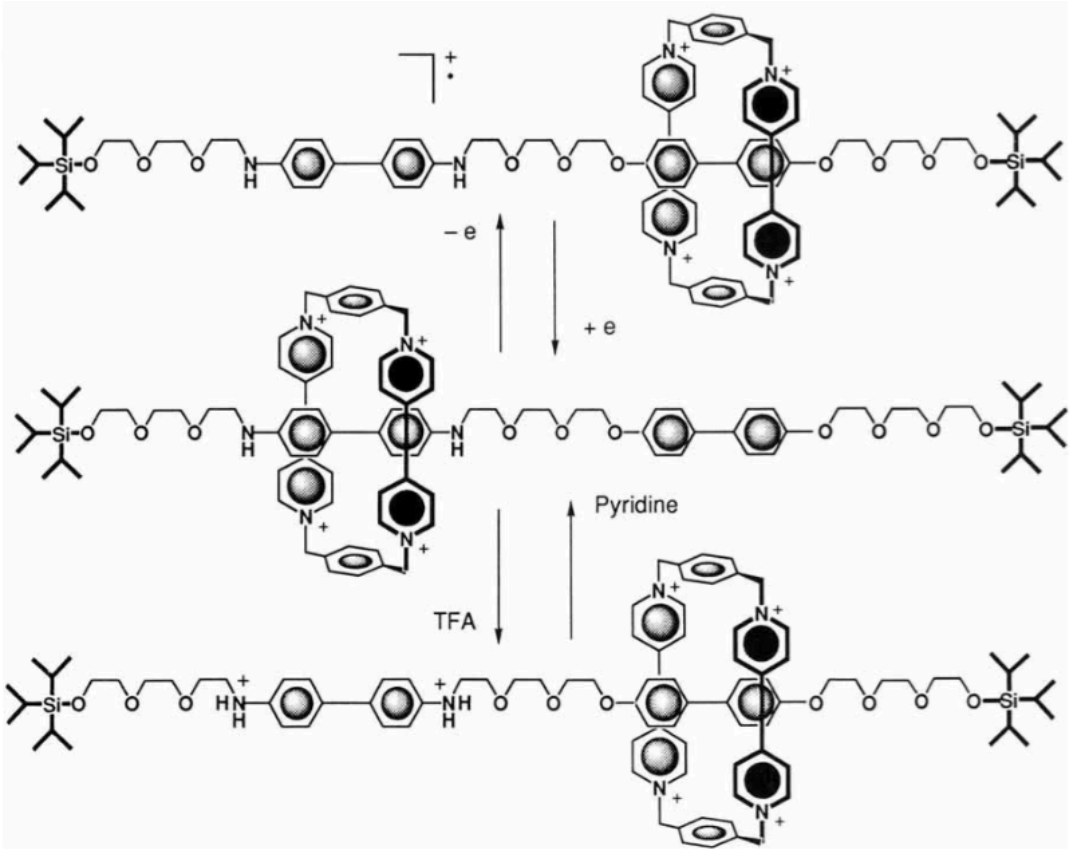

Figure 3.5 Paraquat-cyclophane shuttles mediated by pH and electrochemical oxidation from Stoddart and Kaifer et. al.[18]

Later in 2006 Tuncel et. al. had developed a [3]rotaxane switch using pH and temperature for shuttling of cucurbit[6]urils. This [3]rotaxane was the first of its kind, and consists of a dodecyl axle with terminal propargyl amino groups (Figure 3.6).[19] The terminal alkyne groups allow for attachment of variable sizes of the stoppers containing an azide group through 1,3 dipolar cycloadditions. The CB[6] units are prethreaded onto

the axle first, followed by CB[6] catalyzing the 1,3 dipolar cycloadditions between the azide and alkyne to yield a 1,4 triaizole, without the need of a copper(I) metal catalyst. The axle has two binding sites for the CB[6]s to shuttle between, the diaminotriazole and the dodecamethylene alkyl chain. As previously mentioned in Chapter one cucurbiturils bind extremely well with cations, specifically protonated amines, through ion-dipole interactions. The movement of the CB[6]s is controlled by the addition of base, acid and heat. Under acidic conditions the CB[6]s will encapsulate the triazoles between the ammonium groups, when the pH is brought up with 5 equivalents of NaOH the CB[6]s shuttled over the dodecyl chain. Subsequent addition of excess HCl had protonated the amine groups, however, the CB[6]s still remained over the dodecyl spacers. It wasn't until the sample was heated to 60 °C which allowed for the CB[6]s to overcome the activation energy and shuttle over the triazole units.

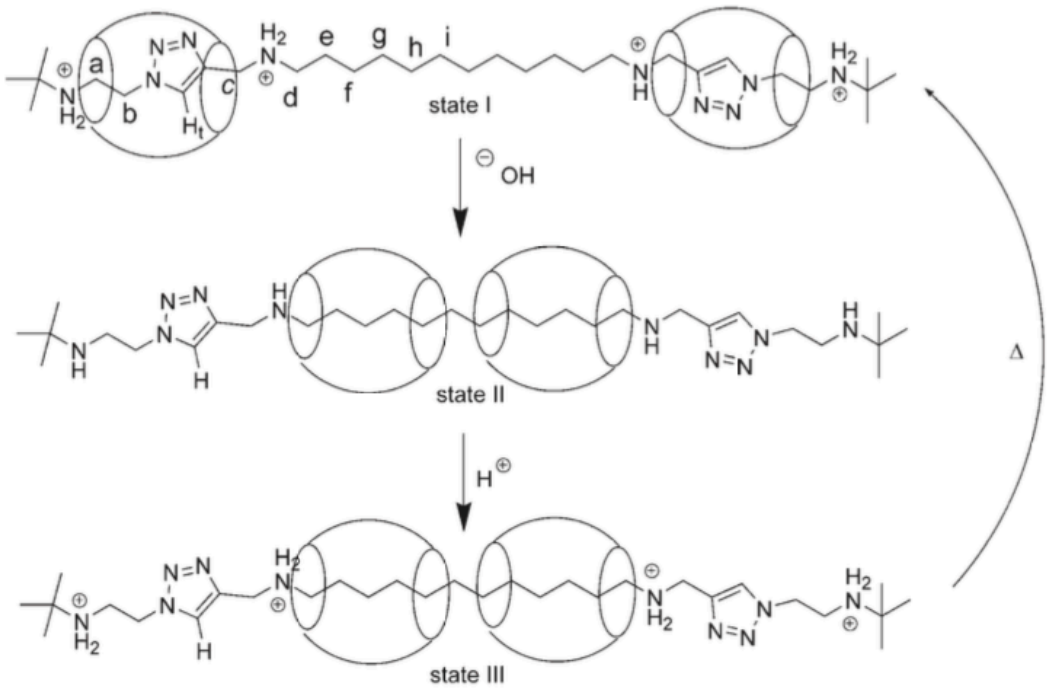

Figure 3.6 Molecular switch based cucurbit[6]uril rotaxane by Tuncel and co-workers.[19]

Recently our group has developed an important example of a molecular switch that uses cucurbit[7]uril to facilitate a fluorescence-on response in a viologen tethered BODIPY-dyad pseudorotaxane.[20] Knowing that CB[7] associates strongly with viologens[21], our group was confident that CB[7] would bind more effectively with the viologen instead of the neutral BODIPY dye. In the absence of CB[7], the viologen-dyad aggregates through pi-pi stacking turning fluorescence off. Upon the addition of CB[7], the macrocycle disrupts the pi-pi stacking by association of the viologen moiety, thus turning fluorescence on. This type of pseudorotaxane could be further developed into a full rotaxane by pre-threading CB[7] and then capping with a bulkier end group. These results gave our group a first look as to its potential in biosensor applications.

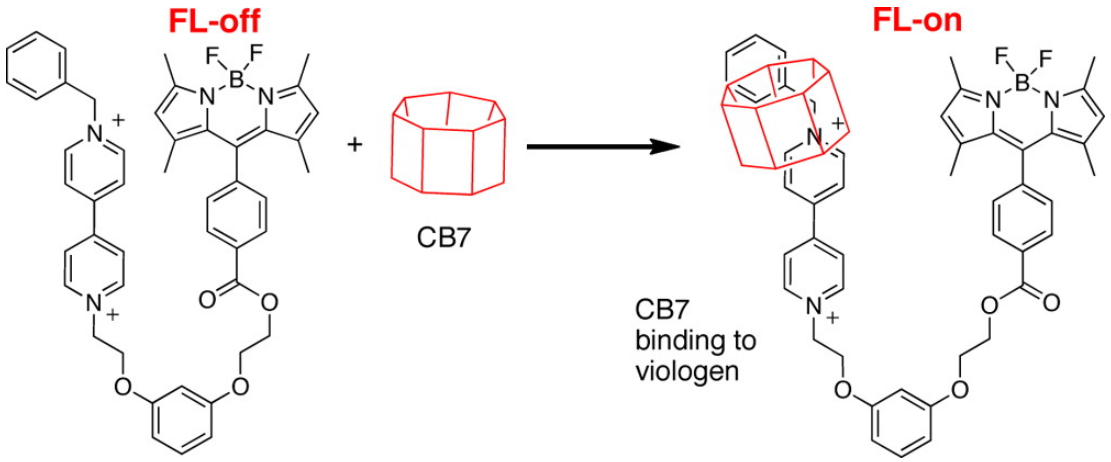

Figure 3.7 Fluorescence-On CB[7] viologen-dyad pseudorotaxane from Singh and Halterman.[20]

Our group is interested in the shuttling capabilities of cucurbiturils, specifically CB[7], and to date there are only a few full rotaxanes containing CB[7].[22] This interesting macrocycle can bind to a variety of guests with a wide range of binding affinities that include benzyl ammoniums (K_a = 10^5 M^{-1}), xylyl ammoniums (K_a = 10^8

M^{-1}), and viologens (K_a = 10^7 M^{-1}).[21] This is an important feature to consider when designing a shuttle rotaxane that will include variable binding units. However, due to the limited amount of full rotaxanes containing CB[7], for our purpose we are more interested in the size of and synthetic accessibility of stoppering end groups that will inhibit CB[7] from dethreading off of a rotaxane. Given the docking units discussed in chapter two, we need to develop stoppering efficiency for these potential rotaxanes. Therefore, this chapter explores the design and synthesis of bulky stoppers and its stability to sterically block CB[7] from "slipping" to form a rotaxane.

3.2 Specific Aims

This chapter presents the synthesis, theoretical and spectroscopic analysis of two rotaxane stoppers as to their ability to sterically block CB[7] from "slipping" over the stoppers and binding with a viologen core to form a rotaxane. This feature is important for the construction of the model rotaxane outlined in chapter one. Based on their synthetic utility the two stoppers to be investigated are bis(3,5-dimethoxybenzyl)-4,4'-bipyridinium dibromide **3.1A** and bis(3,5-diisopropoxybenzyl)-4,4'-bipyridinium dibromide **3.2B**. The first stopper had been previously investigated by our group to determine if it is suitable as an effective stopper against CB[7] due to steric hindrance and electronics, however the results were inconclusive at the time. Therefore this stopper needed to be reexamined for efficacy. The second proposed stopper has much more steric bulk in comparison to the first and should have enough bulk to prevent CB[7] from threading. If the second stopper is determined to be effective against CB[7] threading, it will be used again in attempts to form a permanent full rotaxane which is

further discussed in Chapter four. These analyses were accomplished through the use of NMR spectroscopy and semi-emperical calculations in Spartan ’14.

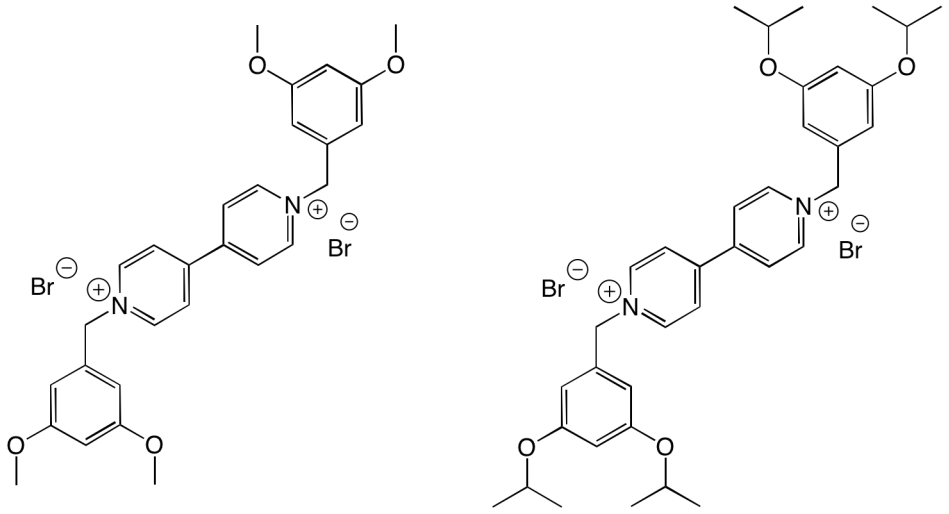

3.1A **3.2B**

Figure 3.8 Figure of proposed viologen rotaxane stoppers, (left) bis(3,5-dimethoxybenzyl)-4,4'-bipyridinium dibromide **3.1A**, (right) bis(3,5-diisopropoxybenzyl)-4,4'-bipyridinium dibromide **3.2B**.

3.3 Synthesis

The bis(3,5-dimethoxybenzyl)-4,4'-bipyridinium dibromide (Figure 3.7) and bis(3,5-diisopropoxybenzyl)-4,4'-bipyridinium dibromide (Figure 3.7) was synthesized by following schemes Figure 3.8 and 3.9 respectively. The viologen **3.1A** was synthesized by dialkylation of 4,4’-bipyridine with an excess of 3,5-dimethoxybenzyl bromide to provide bis(3,5-dimethoxybenzyl)-4,4'-bipyridinium dibromide **3.1A**.

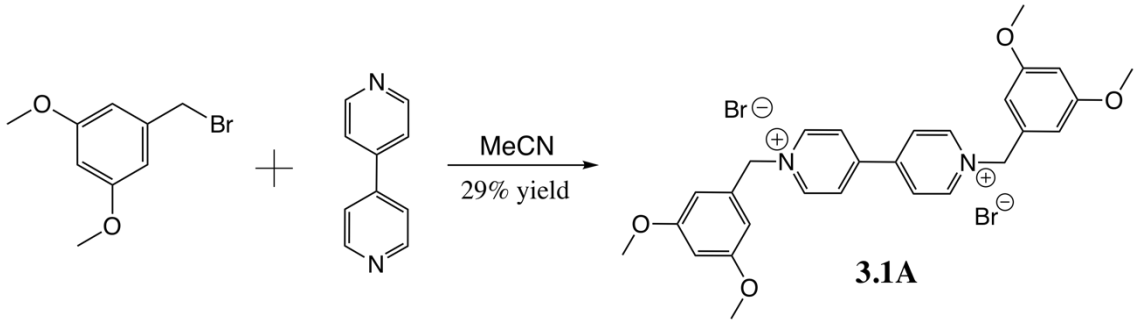

Figure 3.9 Synthetic scheme for the syntheisis of **3.1A** bis(3,5-dimethoxybenzyl)-4,4'-bipyridinium dibromide

The bulkier bis(3,5-diisopropoxybenzyl)-4,4'-bipyridinium dibromide **3.2B** was synthesized by following scheme (Figure 3.9). For the bulkier stopper, each hydroxyl groups and the carboxylic acid group were deprotonated with an excess of potassium carbonate to give the corresponding oxyanions and then subsequent alkylation with an excess of isopropyl bromide to give the corresponding ester and phenyl ethers. The ester was then reduced with lithium aluminum hydride to give the resulting alcohol. The alcohol was then brominated with PBr_3 to give the 3,5-diisopropoxybenzyl bromide as shown in (Figure 3.9). Viologen **3.2B** was then synthesized by dialkylation of 4,4'-bipyridine with an excess of 3,5-diisopropoxybenzyl bromide to provide bis(3,5-diisopropoxybenzyl)-4,4'-bipyridinium dibromide **3.2B.** CB[7] was synthesized following literature precedence.[23] The synthesized viologens were characterized by NMR spectroscopy and mass spectrometry.

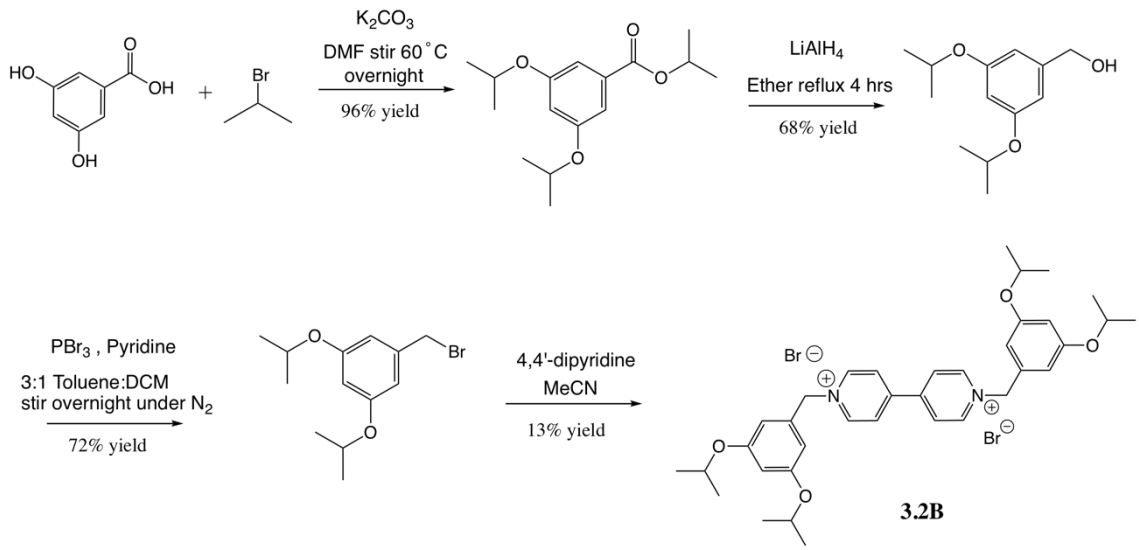

Figure 3.10 Synthetic scheme for the syntheisis of **3.2B** bis(3,5-diisopropoxybenzyl)-4,4'-bipyridinium dibromide.

3.4 Results and Discussion

Our group has previously used bis(3,5-dimethoxybenzyl)-4,4'-bipyridinium dibromide **3.1A** to determine if the end groups were sterically bulky enough to prevent threading of CB[7]. This data was inconclusive at the time and the system needed to be reexamined. As we began to reexamine and synthesize bis(3,5-dimethoxybenzyl)-4,4'-bipyridinium dibromide, Kaifer and co-workers had reported that mixing CB[7] and viologen **3.1A** lead to rapid formation of CB[7]-viologen complex at room temperature.[24] This report inspired us to continue our efforts towards the confirmation of these findings, and then towards the pursuit and development of a viologen-containing guest with larger end groups with the aim of establishing to its synthetic utility in forming a rotaxane. The larger stopper we have proposed is bis(3,5-diisopropoxybenzyl)-4,4'-bipyridinium dibromide **3.2B** (Figure 3.7). A bulkier viologen stopper based on this approach would potentially prevent threading of CB[7].

3.4.1 Theoretical Investigations of Bis(3,5-diisopropoxybenzyl)-4,4'-bipyridinium Dibromide with Cucurbit[7]uril

The potential surface plot of compound **3.2B** with 1 equivalent of CB[7] were calculated at a semi-empirical level using Spartan ’14 molecular modeling software to study the complexation of the host:guest system. The CB[7] host and viologen guest were allowed to complex using energy minimization and then PM3 semi-empirical calculations were run to give a local energy minimum (-513.3 kJ/mol, -122.9 kcal/mol), with the host:guest system having an incomplete or peripheral complex where the CB[7] host partially threaded on to bulky end groups on viologen **3.2B** as shown in (Figure 3.11). The lack of full complexation suggests that the end groups on the viologen guest could be large enough to prevent CB[7] from threading.

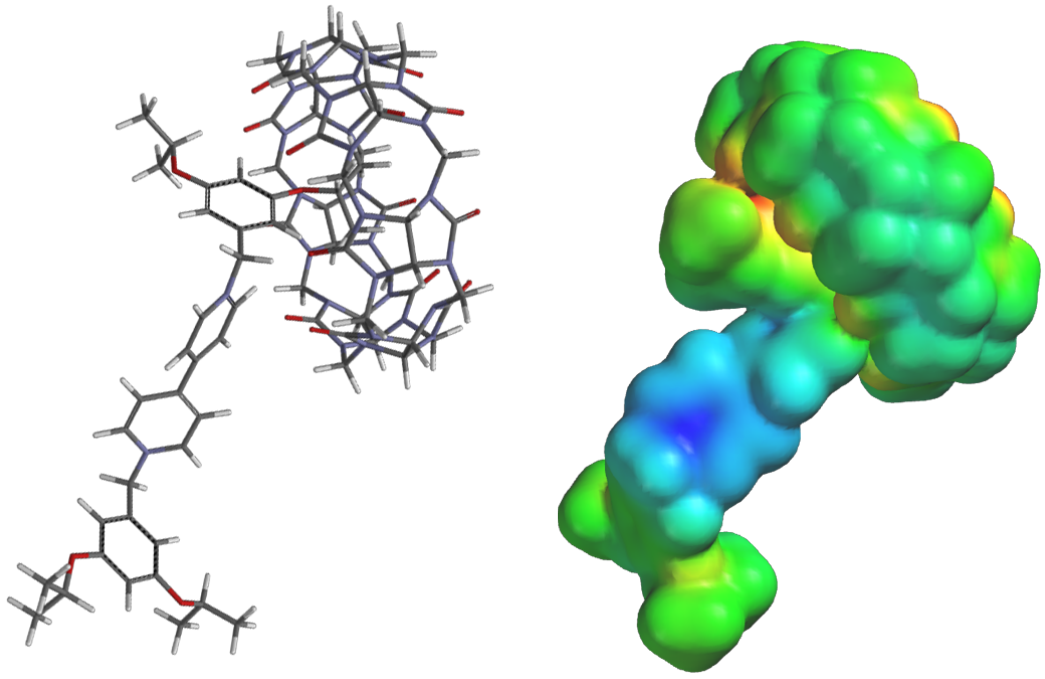

Figure 3.11 External complexation of **3.2B** with CB[7].

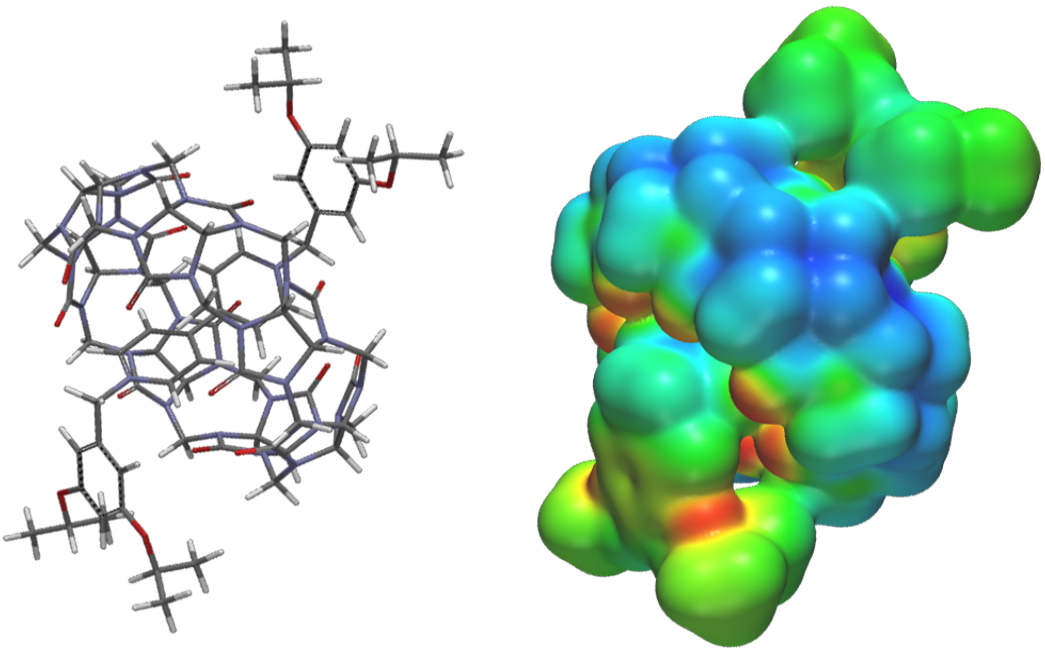

Figure 3.12 Internal Complexation of **3.2B** with CB[7].

CB[7] was purposefully moved along the viologen to the internal binding site to force full complexation (Figure 3.12) and a local energy minimum of the complex (-732.9 kJ/mol, -175.2 kcal/mol) was found by PM3 semi-empirical calculations. The rotaxane when complexed peripherally was -513.3 kJ/mol in energy, and when complexed internally was -732.9 kJ/mol in energy showed an overall decrease of -219.6 kJ/mol (-52.3 kcal/mol) in energy from external association to internal binding. Based on semi-empirical calculations it was not fully concluded that CB[7] is able to thread over the bulky stopper of compound **3.2B**, therefore further synthetic study and complexation analysis by NMR spectroscopy was necessary.

3.4.2 Spectroscopic Investigations of Bis(3,5-dimethoxybenzyl)-4,4'-bipyridinium Dibromide with Cucurbit[7]uril

In order to gain experimental evidence regarding threading CB[7] over the bulky stoppers, we adopted Kaifer's complexation methodology for our systems. Initially, we replicated his procedure for the complexation of compound **3.1A** and CB[7]. Compound **3.1A** and CB[7] was combined in a 1:1 concentration in neutral D_2O at room temperature and analyzed by NMR spectroscopy. According to the NMR spectra (Figure 3.13) compound **3.1A** and CB[7] formed a full complex within minutes of mixing.

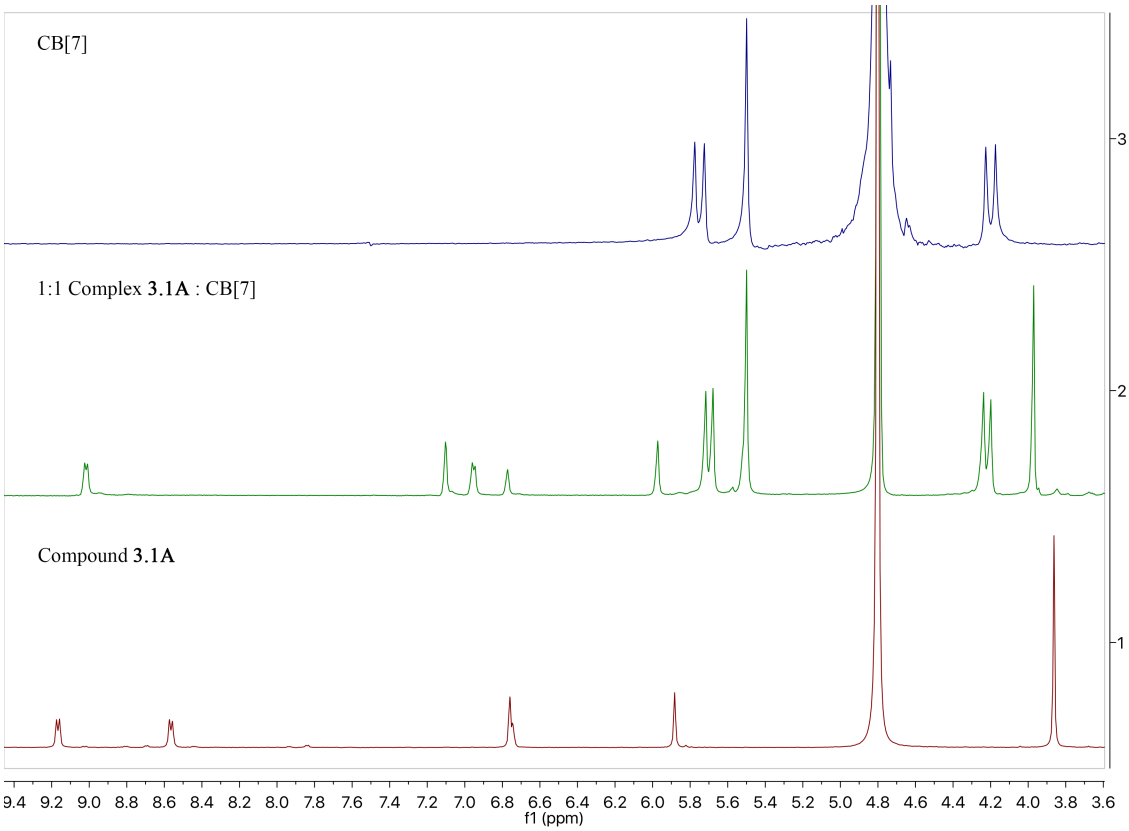

Figure 3.13 ^{1}H NMR spectra (400 MHz, D_2O) of CB[7] (top), bis(3,5-dimethoxybenzyl)-4,4'-bipyridinium dibromide **3.1A** in the presence of 1:1 (middle) and absence of CB[7] (bottom).

The beta protons on the bipyridyl moiety had a substantial upfield shift from 8.56 ppm to 7.10 ppm. This upfield shift indicates that the viologen core is encapsulated within the CB[7] host cavity, and that the 3,5-dimethoxybenzyl end groups are not bulky enough to prevent threading of the macrocyclic host. This data was consistent with Kaifer's literature results.[24]

Follow up studies were conducted with the 1:1 CB[7]:**3.1A** complex with a titration of adamantylammonium in D_2O at 0, 0.5, and 1 eq to determine the rate of dissociation. We knew that complexation was fast, but we wanted to establish whether decomplexation or dissociation occurred on a minute or hour time scale when we added the stronger binding unit adamantylammonium. According to the spectra taken within two minutes, after mixing in 0.5 eq of adamantylammonium with the already formed CB[7]-viologen complex, the viologen already showed two sets of signals for unbound and bound, 9.15–8.53 ppm and 9.0–7.09 ppm respectively. Upon mixing the addition of 1 eq of adamantylamine to the complex, the initial spectra already showed full dissociation of CB[7] and compound **3.1A** and instead complexation of CB[7] with adamantylammonium, this is seen by the apparent downfield shift of the viologen core protons and an upfield shift signals of the adamantyl group. It can be concluded that CB[7] has fast association with compound **3.1A** and fast dissociation when a more competitive binder is added, indicating that compound **3.1A** is a pseudorotaxane on the time frame of devices. The rate of dissociation was too fast to measure by standard NMR spectroscopy.

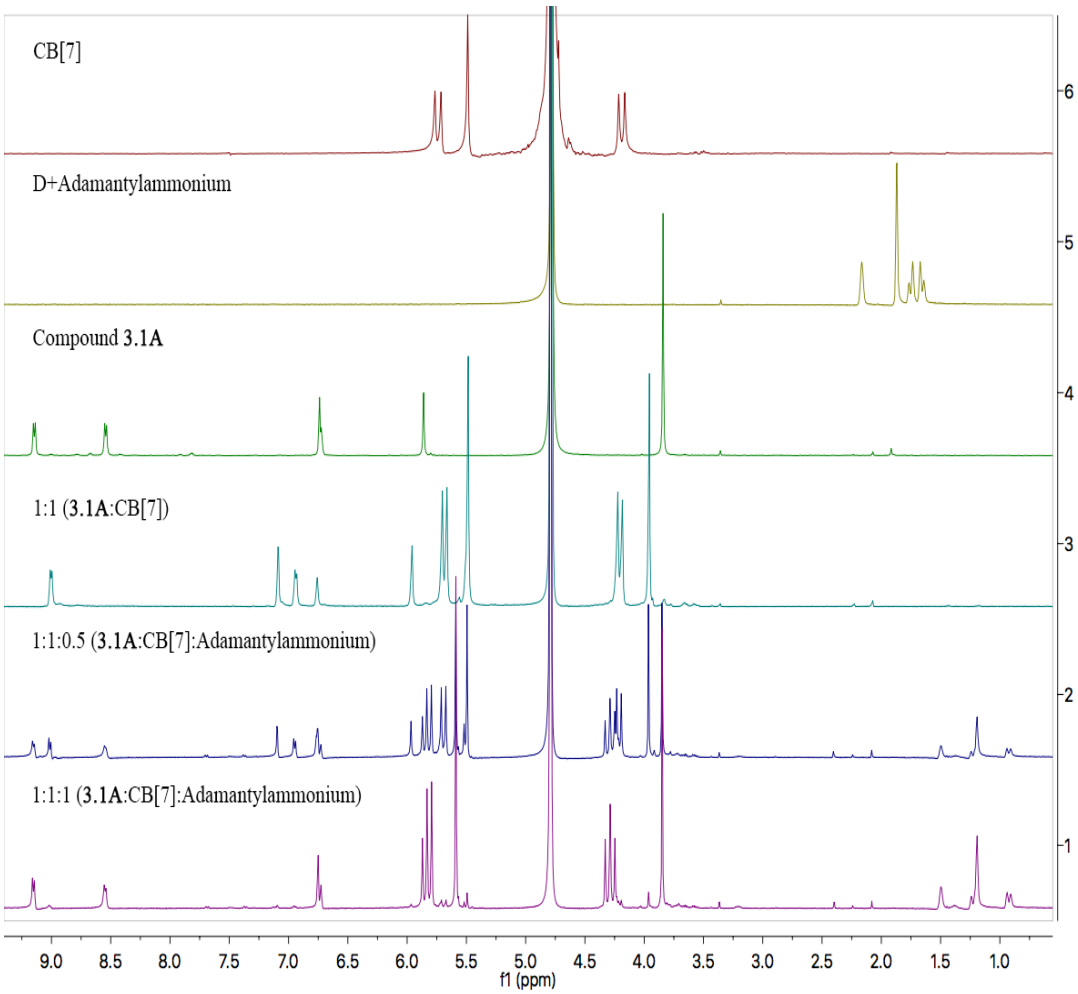

Figure 3.14 ^{1}H NMR spectra of (400 MHz, D_2O) of bis(3,5-dimethoxybenzyl)-4,4'-bipyridinium dibromide **3.1A** with CB[7] and adamantylammonium (0 to 1 equivalent).

3.4.3 Spectroscopic Investigations of bis(3,5-diisopropoxybenzyl)-4,4'-bipyridinium dibromide with Cucurbit[7]uril

In order to confirm the efficacy of the bulky stopper, CB[7] was combined with compound **3.2B** in a 1:1 concentration in neutral D_2O at room temperature and analyzed by NMR spectroscopy at time = 1 min, 12 h, 72 h, and 8 d. If CB[7] were to fully thread onto compound **3.2B** there should be an evident chemical shift change of the aromatic protons of the bipyridyl moiety. However, if CB[7] did not thread onto compound **3.2B** there would be no apparent change in the aromatic protons of the

bipyridyl moiety. In the absence of CB[7], the NMR shifts representing the protons alpha and beta to the nitrogen cations of the bipyridyl moiety of compound **3.2B** are 9.10 ppm and 8.52 ppm respectively. The peaks associated with CB[7] in the 1:1 complex are found at 4.35 ppm, 5.64 ppm, and 5.92 ppm, which correspond to the 14 outer methylene protons, the 14 methine protons, and the 14 inner methylene protons respectively. In the 1:1 complex, bis(3,5-diisopropoxybenzyl)-4,4'-bipyridinium dibromide did not show a significant change in chemical shifts, even after 8 d, of the protons alpha and beta to the nitrogen cations of the bipyridyl moiety. The alpha protons shifted downfield from 9.10 ppm to 9.24 ppm, and the beta protons shifted slightly upfield from 8.52 ppm to 8.49 ppm. These data suggest that CB[7] did not thread onto the bulkier viologen since there was not a significant chemical shift, as was observed with compound **3.1A**. However, the protons on aromatic ring of the benzyl group, and of the isopropyl groups did show substantial changes. The NMR shifts representing the benzyl aromatic protons split from a tight cluster at 6.85 ppm to 6.75 ppm and 6.96 ppm, which correspond to the protons at the 2,6-positions and 4-position respectively. The NMR shifts of the benzylic methylene protons had a downshift from 5.97 ppm to 6.11 ppm. The NMR shifts of the methine, and methyl groups of the isopropyl moiety were broadened and shifted upfield from 4.82 ppm to 4.69 ppm, and 1.45 ppm to 1.30 ppm respectively. This upfield shifting is due to typical shielding by encapsulation of CB[7].[25] The broadening indicates fast exchange on the NMR timescale between either bound and unbound CB[7] with compound **3.2B**. When these observations and individual shift changes are considered together, they suggest an

external complexation of CB[7] with compound **3.2B**, in which the macrocycle only encapsulates a branched isopropoxy region and partial aromatic ring (Figure 3.14).

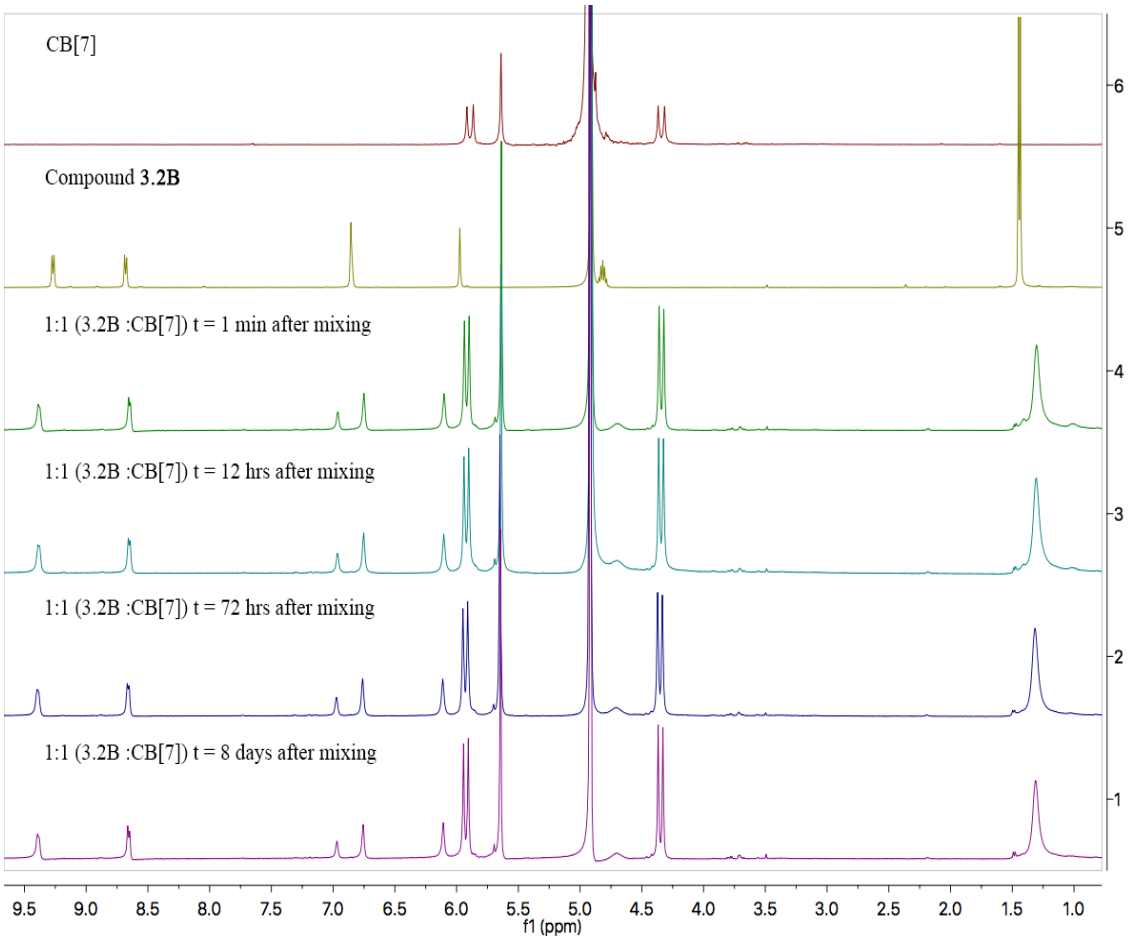

Figure 3.15 ^{1}H NMR spectra of (400 MHz, D_2O) of bis(3,5-diisopropoxybenzyl)-4,4'-bipyridinium dibromide **3.2B** with CB[7] (0 to 1 equivalent at times 1 min to 8 d).

A follow up study was done to the same 1:1 complex of CB[7] and compound **3.2B**. The NMR tube containing the 1:1 complex was heated to 80 °C for 24 h then allowed to cool to room temp and then studied by NMR spectroscopy. The spectra (Figure 3.15) shows no significant change in the chemical shifts of the viologen/CB[7]

complex when comparing to the spectra of t = 1 min and t = 8 d. This confirms that compound **3.2B** is stable at higher temperatures and should prevent CB[7] from threading over the bulkier end groups of the viologen indicating that compound **3.2B** should be a true rotaxane.

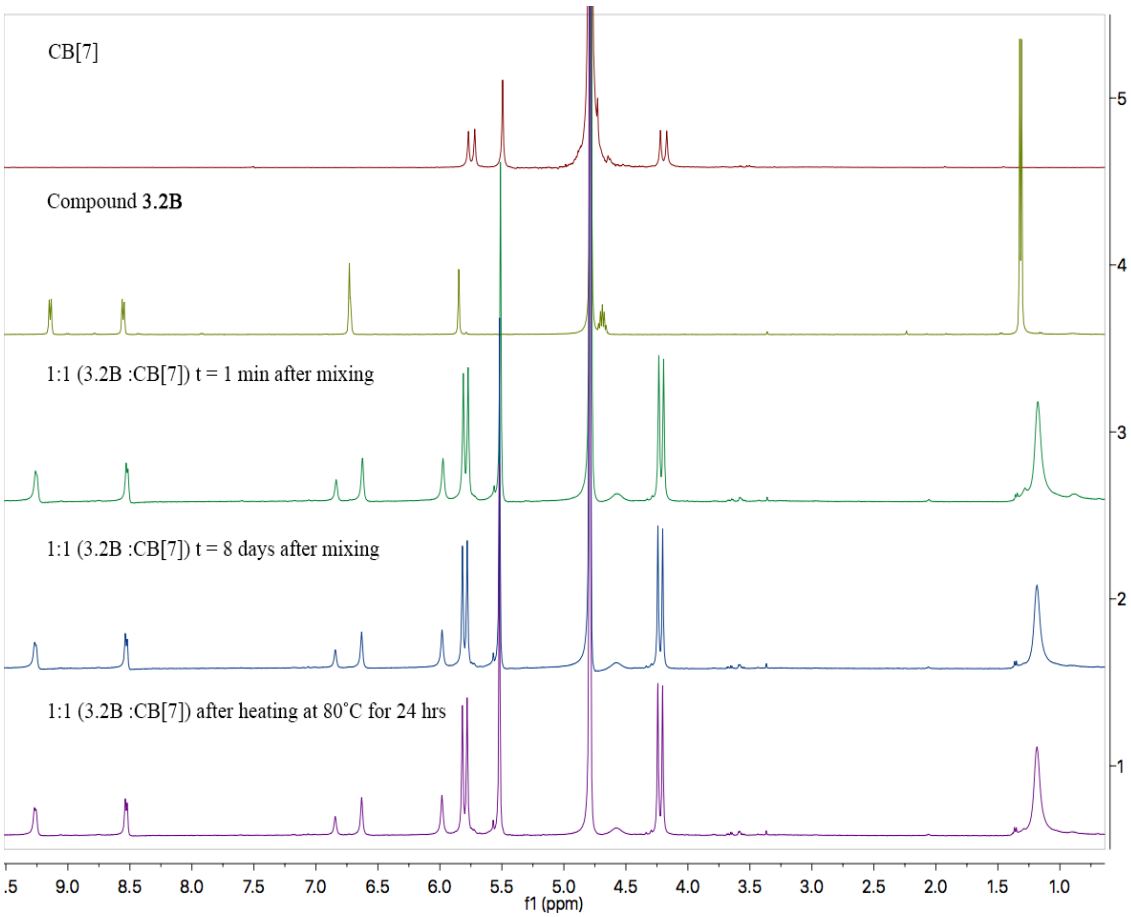

Figure 3.16 ^{1}H NMR spectra of (400 MHz, D_2O) of bis(3,5-diisopropoxybenzyl)-4,4'-bipyridinium dibromide **3.2B** with CB[7] (0 to 1 equivalent at times 1 min to 8 d and after heating at 80 °C for 24 h).

3.5 Conclusion

This chapter details our efforts to develop a suitable rotaxane stopper to prevent cucurbit[7]uril from passing over and encapsulating the viologen core. Two bulky viologen compounds were successfully synthesized and characterized by performing NMR spectroscopy and mass spectrometry experiments. The stopper efficacy of viologen rotaxanes upon the addition of CB[7] was studied. Theoretical calculations and NMR spectroscopy experiments were conducted to examine the behavioral effects of CB[7] complexation with the viologen compounds.

According to our findings, bis(3,5-dimethoxybenzyl)-4,4'-bipyridinium dibromide showed evidence of a 1:1 full inclusion complex with CB[7], in addition to trapping any dethreaded or unbound CB[7] with adamantylammonium from NMR spectroscopy. In comparison, bis(3,5-diisopropoxybenzyl)-4,4'-bipyridinium dibromide did not show evidence of a 1:1 full inclusion complex with CB[7], and the results obtained from the ^{1}H-NMR experiments did not provide evidence for the expected upfield shifts typically associated with inclusion binding. Instead, the results suggested complexation at the peripheral or external to the viologen. This conclusion supports our hypothesis that the bulkier end groups on the viologen prevented CB[7] from threading into bis(3,5-diisopropoxybenzyl)-4,4'-bipyridinium dibromide giving only external complexation and not full inclusion. This effort was crucial for the development of a rotaxane stopper that will be further explored to produce a model rotaxane in Chapter 4.

3.6 Experimental

Synthesis of isopropyl 3,5-diisopropoxybenzoate

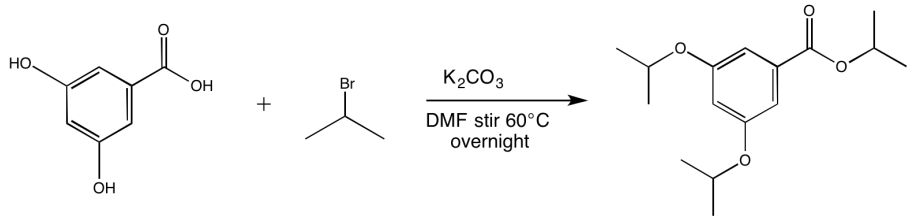

In a 250 mL reaction flask, 3,5-dihydroxybenzoic acid (5.08g 0.033 mol) and K_2CO_3 (18.2 g, 0.0115 mol) and DMF (60 mL) was added. The suspension was allowed to stir for 1 h and isopropyl bromide (10.8 mL, 0.115 mol) was added drop wise. The solution was heated to 60 °C and stirred for 36 h. The mixture was diluted with water and the product was extracted with ethyl acetate. The organic layer was separated and washed with brine. The extract was dried over anhydrous $MgSO_4$ and filtered. The solvent was removed by reduced pressure to afford isopropyl 3,5-diisopropoxybenzoate (8.95 g, 96 % yield) as a dark brown oil.^{1}H NMR (400 MHz, $CDCl_3$) δ 7.15 (d, *J* = 2.3 Hz, 2H), 6.61 (t, *J* = 2.4 Hz, 1H), 5.25 – 5.19 (m, 1H), 4.57 (p, *J* = 6.2 Hz, 2H), 1.35 (t, *J* = 6.5 Hz, 18H). ^{13}C NMR (101 MHz, $CDCl_3$) δ 166.1, 158.9, 132.7, 108.9, 108.5, 70.2, 68.6, 21.98, 21.90. HRMS-ESI: m/z calculated for [$C_{16}H_{24}O_4Na$] 303.157; found 303.157 [M + Na].

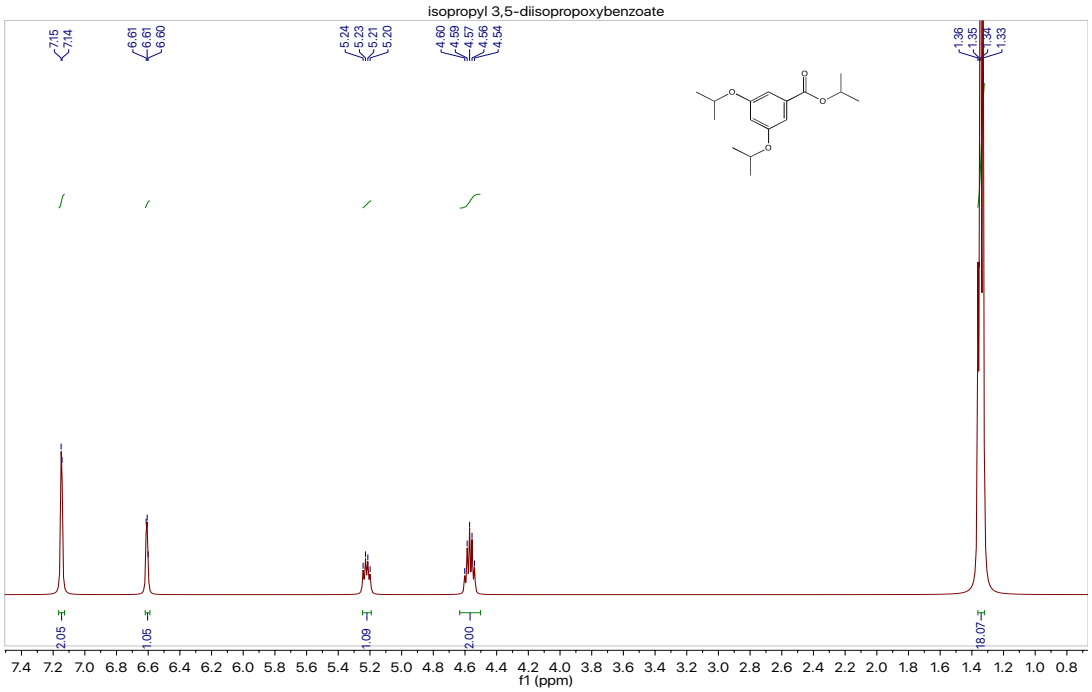

Figure 3.17 ^{1}H NMR (400 MHz, $CDCl_3$) spectrum of isopropyl 3,5-diisopropoxybenzoate

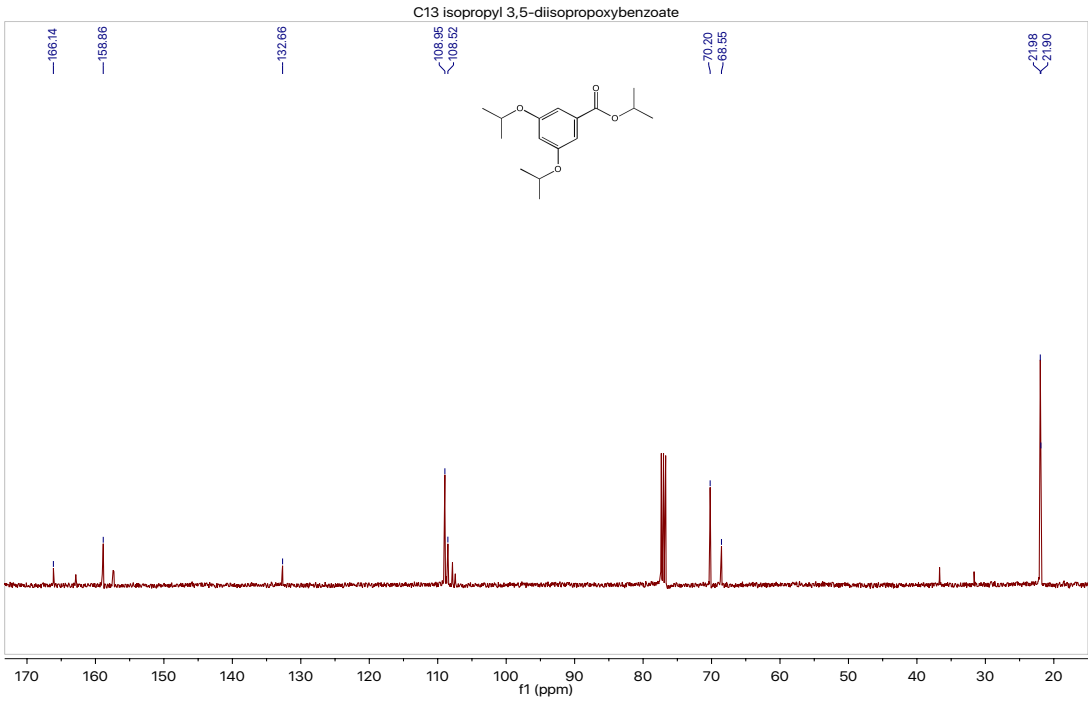

Figure 3.18 ^{13}C NMR (101 MHz, $CDCl_3$)) spectrum of isopropyl 3,5-diisopropoxybenzoate

Synthesis of 3,5-diisopropoxybenzyl alcohol

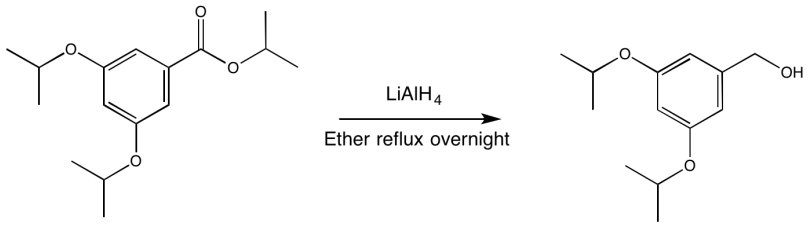

In a 250 mL reaction flask, isopropyl 3,5-diisopropoxybenzoate (2.81 g, 10.0 mmol) was dissolved in diethyl ether (5 mL) and set aside. Lithium aluminum hydride (1.16 g, 30.0 mmol) was slowly added to diethyl ether (50 mL) at 0 °C and allowed to stir. The ester solution was added drop wise to the $LiAlH_4$ slurry with continued stirring. The mixture was allowed to warm up to room temp and then stirred at reflux overnight. The reaction mixture was then cooled to r.t., then to 0 °C and slowly quenched with portions of water and aq. potassium hydroxide (5 M). The extract was dried over anhydrous $MgSO_4$ and filtered. The solvent was removed by reduced pressure to afford the crude 3,5-diisopropoxybenzyl alcohol (1.53 g, 68 % yield) as a light-yellow oil. Impurities are present. ^{1}H NMR (500 MHz, $CDCl_3$) δ 6.48 (d, J = 2.2 Hz, 2H), 6.36 (t, J = 2.3 Hz, 1H), 4.59 (s, 2H), 4.53 – 4.48 (m, 2H), 2.00 (d, J = 4.6 Hz, 1H), 1.32 (d, J = 6.1 Hz, 12H). ^{13}C NMR (126 MHz, $CDCl_3$) δ 159.3, 143.2, 106.5, 103.1, 69.9, 65.4, 22.1. HRMS-ESI: m/z calculated for [$C_{13}H_{20}O_3Na$] 247.131; found 247.131 [M + Na].

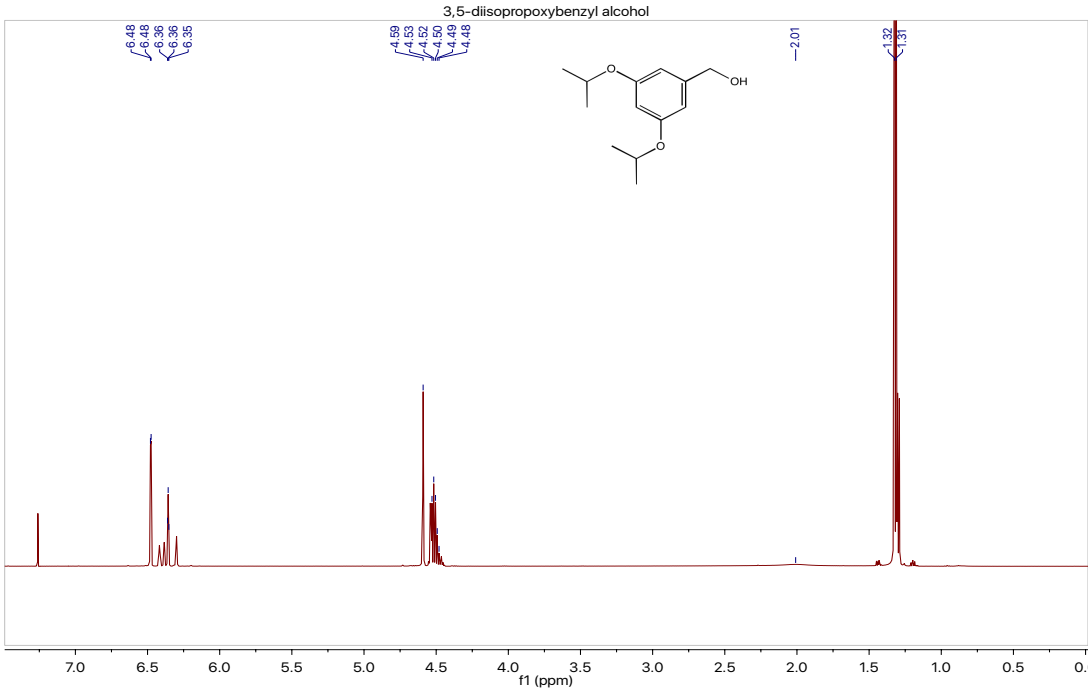

Figure 3.19 ^{1}H NMR (500 MHz, $CDCl_3$) spectrum of 3,5-diisopropoxybenzyl alcohol

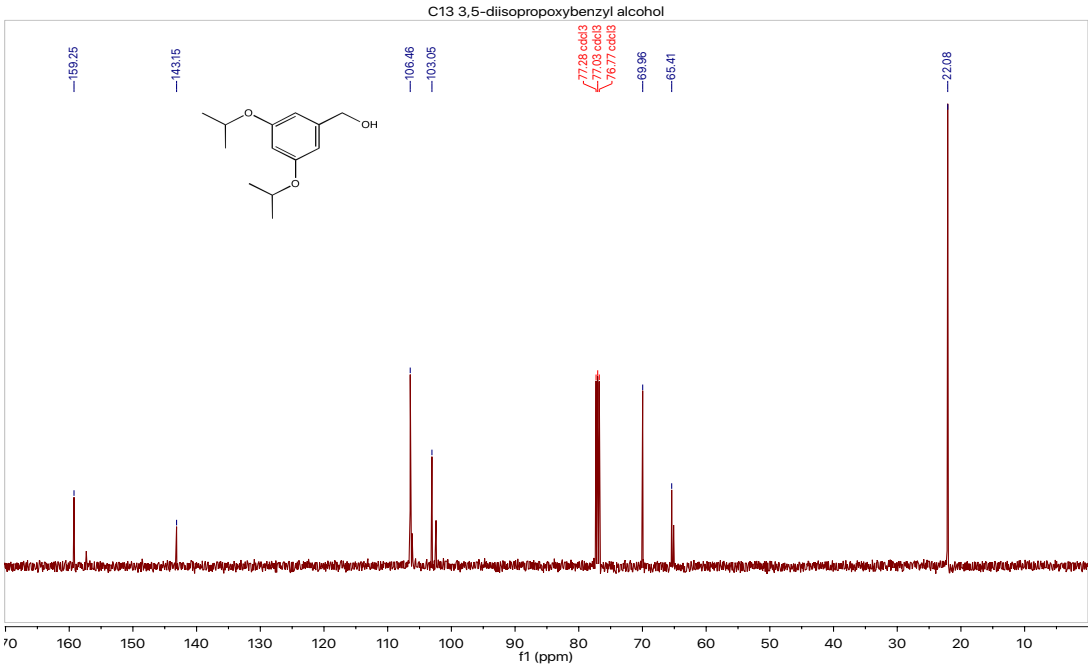

Figure 3.20 ^{13}C NMR (126 MHz, $CDCl_3$) spectrum of 3,5-diisopropoxybenzyl alcohol

Synthesis of 3,5-diisopropoxybenzyl bromide

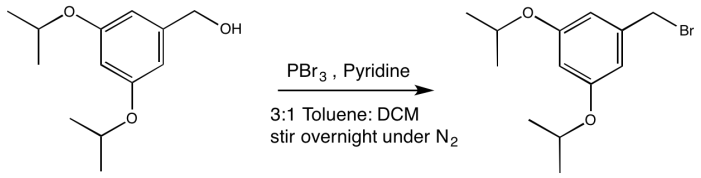

In a 250 mL reaction flask, 3,5-diisopropoxybenzyl alcohol (1.18 g, 5.25 mmol) was added to a 3:1 toluene / dichloromethane (20 mL) solution. PBr_3 (0.50 mL, 5.3 mmol) was added drop wise by syringe and stirred overnight at r.t. under nitrogen. The reaction was quenched with water and extracted with ether. The ether layer was washed with sat. $NaHCO_3$ and then again with brine, dried over anhydrous Na_2SO_4 and filtered. The solvent was removed by reduced pressure to afford 3,5-diisopropoxybenzyl bromide (1.08 g, 71.8 % yield) as an oil. ^{1}H NMR (500 MHz, $CDCl_3$) δ 6.51 (s, 2H), 6.37 (s, 1H), 4.53 (s, 2H), 4.41 (s, 2H), 1.34 (d, J = 5.9 Hz, 12H). ^{13}C NMR (126 MHz, $CDCl_3$) δ 159.2, 139.6, 108.6, 103.7, 69.9, 33.8, 22.0, 30.0(Acetone). HRMS-ESI: m/z calculated for [$C_{13}H_{19}BrO_2$] 286.056; found 207.137 [M - Br].

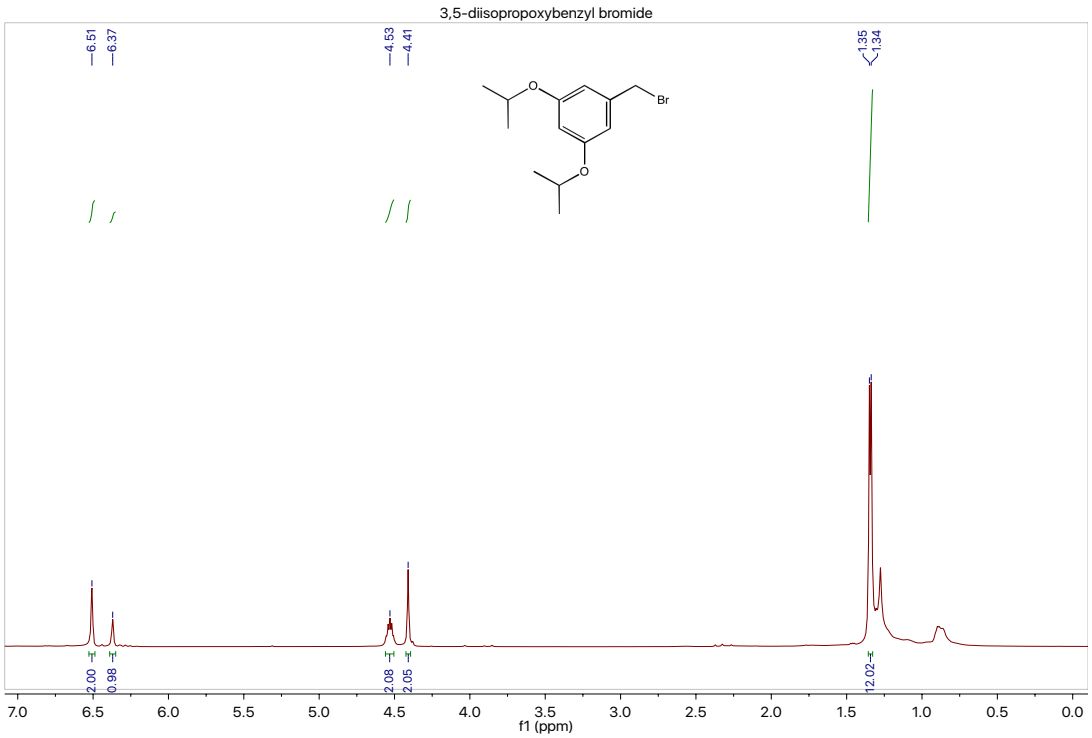

Figure 3.21 ^{1}H NMR (500 MHz, $CDCl_3$) spectrum of 3,5-diisopropoxybenzyl bromide

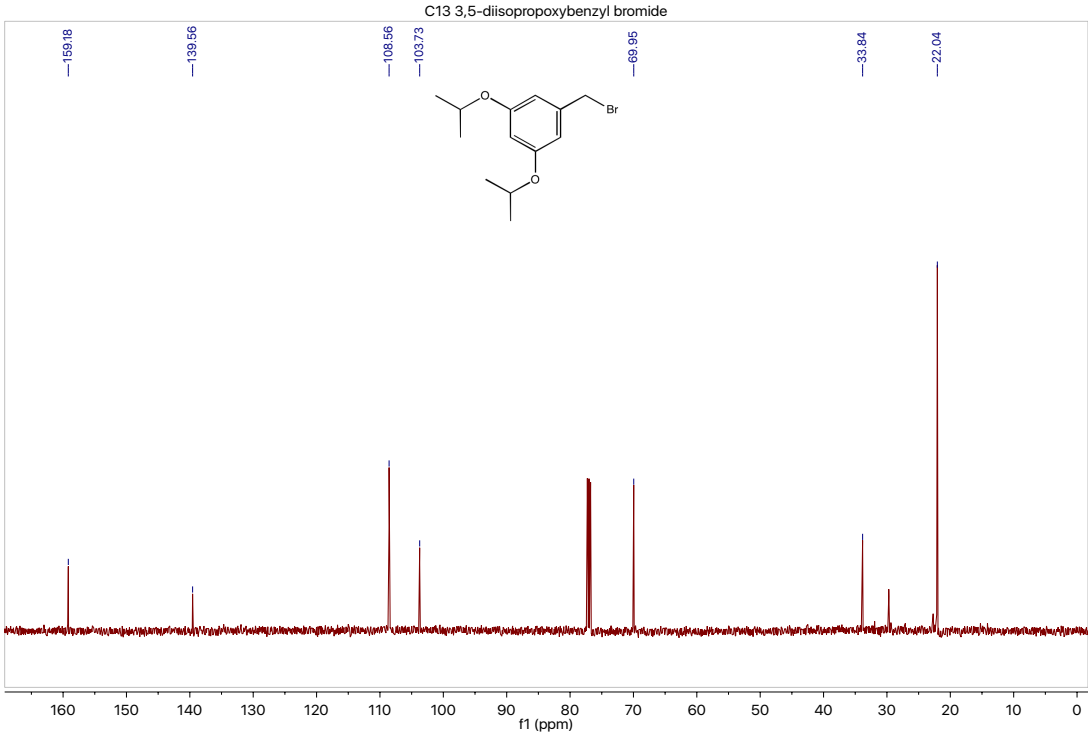

Figure 3.22 ^{13}C NMR (126 MHz, $CDCl_3$) spectrum of 3,5-diisopropoxybenzyl bromide

Synthesis of bis(3,5-dimethoxybenzyl)-4,4'-bipyridinium dibromide

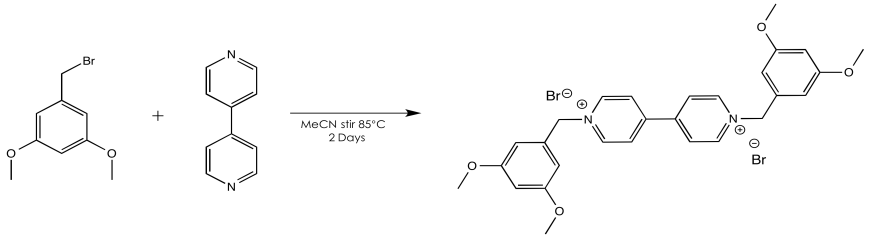

In a 50 mL reaction flask, 4,4'-bipyridine (150 mg, 0.96 mmol) and 3,5-dimethoxybenzyl bromide (540 mg, 2.4 mmol) and acetonitrile (15 mL) was added. The solution was heated to 85 °C and allowed to stir for 2 d. The precipitate was collected by filtration to afford bis(3,5-dimethoxybenzyl)-4,4'-bipyridinium dibromide (430 mg, 28.9 %yield) as a dark yellow solid. ^{1}H NMR (400 MHz, D_2O) δ 9.13 (d, J = 7.0 Hz, 4H), 8.53 (d, J = 6.9 Hz, 4H), 6.72 (s, 4H), 6.71 (d, J = 2.1 Hz, 2H), 5.85 (s, 4H), 3.83 (s, 12H).

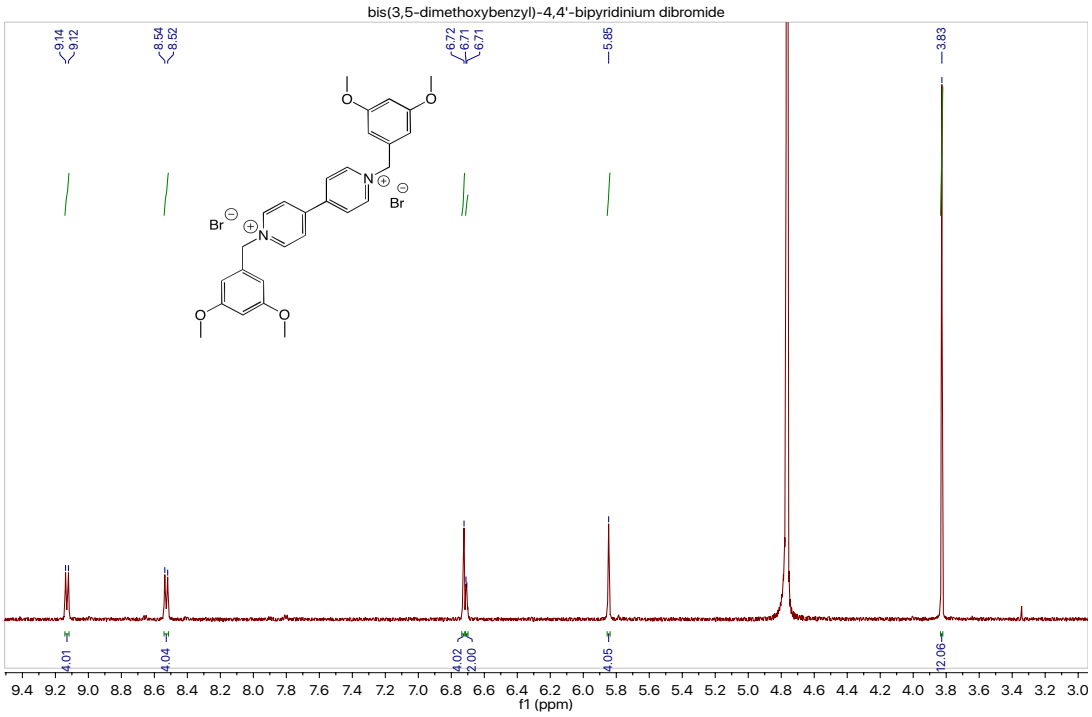

Figure 3.23 ^{1}H NMR (400 MHz, D_2O) spectrum of bis(3,5-dimethoxybenzyl)-4,4'-bipyridinium dibromide

Synthesis of bis(3,5-diisopropoxybenzyl)-4,4'-bipyridinium dibromide

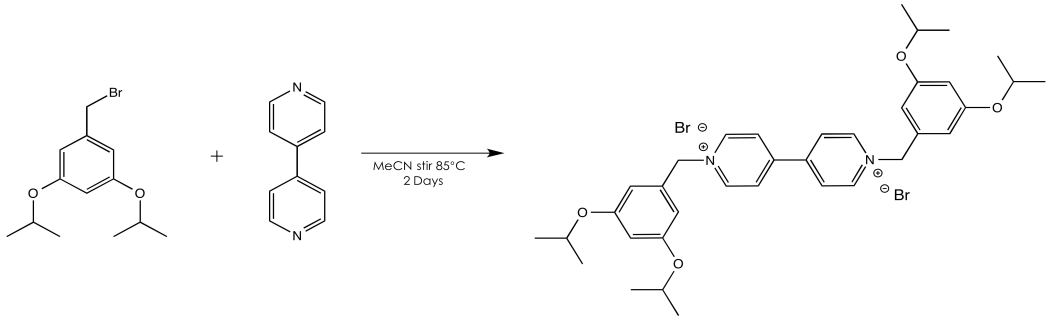

In a 50 mL reaction flask, 4,4'-bipyridine (150 mg, 0.96 mmol) and 3,5-diisopropoxybenzyl bromide (690 mg, 2.4 mmol) and acetonitrile (15 mL) was added. The solution was heated to 85 °C and allowed to stir for 2 d. The precipitate was collected by filtration to afford bis(3,5-diisopropoxybenzyl)-4,4'-bipyridinium dibromide (71 mg, 13 %yield) as a bright yellow solid. ^{1}H NMR (400 MHz, D_2O) δ 9.15 (d, *J* = 6.4 Hz, 4H), 8.56 (d, *J* = 6.4 Hz, 4H), 6.74 (s, 4H), 6.73 (s, 2H), 5.85 (s, 4H), 4.70 (p, *J* = 6.1 Hz, 4H), 1.32 (d, *J* = 6.0 Hz, 24H). HRMS-ESI: m/z calculated for [$C_{36}H_{46}Br_2N_2O_4$] 728.182; found 727.173 [M - H].

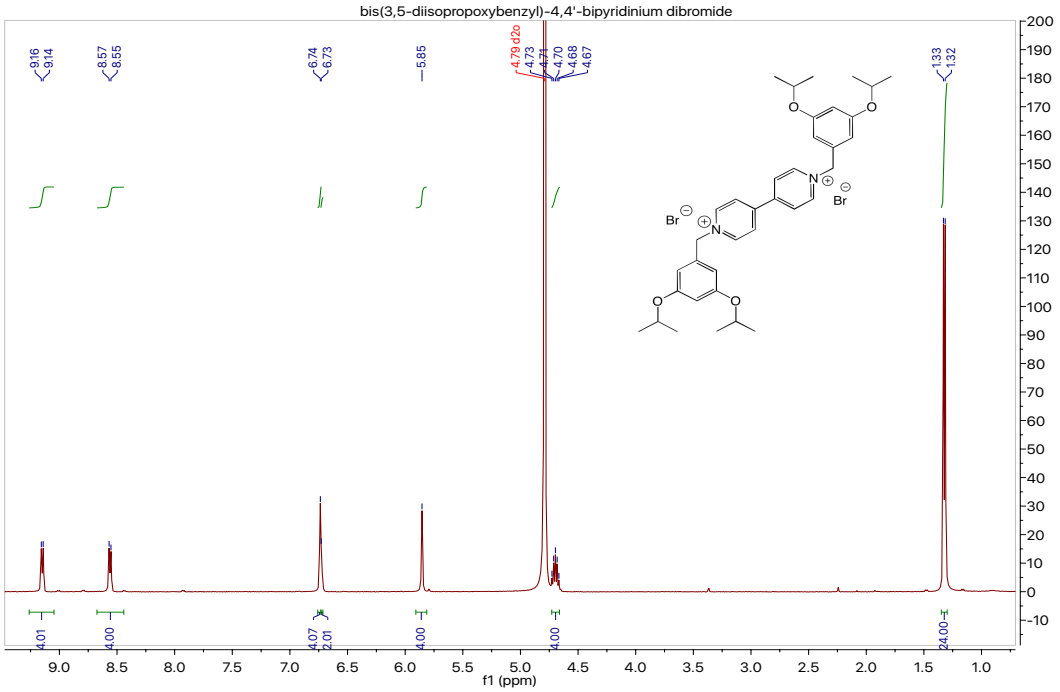

Figure 3.24 ^{1}H NMR (400 MHz, D_2O) spectrum of bis(3,5-diisopropoxybenzyl)-4,4'-bipyridinium dibromide

Procedure for ^{1}H NMR docking studies.

Synthesis of CB[7]. CB[7] was synthesized using the same procedure from chapter two.

Stock solution of CB[7]. A CB[7] stock solution (4.0 mM) was prepared by dissolving CB[7] (23 mg, 0.02 mmol) in D_2O (5 mL).

Stock solution of bis(3,5-dimethoxybenzyl)-4,4'-bipyridinium dibromide. A bis(3,5-dimethoxybenzyl)-4,4'-bipyridinium dibromide stock solution (4.0 mM) was prepared by dissolving bis(3,5-dimethoxybenzyl)-4,4'-bipyridinium dibromide (12 mg, 0.020 mmol) in D_2O (5 mL).

Stock solution of bis(3,5-diisopropoxybenzyl)-4,4'-bipyridinium dibromide. A bis(3,5-diisopropoxybenzyl)-4,4'-bipyridinium dibromide stock solution (4.0 mM) was prepared by dissolving bis(3,5-diisopropoxybenzyll)-4,4'-bipyridinium dibromide (14 mg, 0.020 mmol) in D_2O (5 mL).

Stock solution of adamantylammonium An adamantylammonium stock solution (16 mM) was prepared by dissolving 1-adamantylamine (12 mg, 0.080 mmol) in D_2O (5 mL) and DCl was added until pD = 2. A portion of the stock solution (50 μL) was taken in a 5 mL volumetric flask and diluted up to 5 mL with D_2O to prepare 4.0 mM solution.

Inclusion measurement of bis(3,5-dimethoxybenzyl)-4,4'-bipyridinium dibromide with CB[7]. To an NMR tube, portions of bis(3,5-dimethoxybenzyl)-4,4'-bipyridinium dibromide stock solution (4.0 mM, 250 μL) and of CB[7] stock solution (4.0 mM, 250

μL) were added respectively and mixed well. For the measurement of NMR spectroscopy, after the solutions were added to the NMR tube, measurements were carried out on a 400 MHz NMR instrument at r.t. (Figure 3.13).

Decomplexation measurement of bis(3,5-dimethoxybenzyl)-4,4'-bipyridinium dibromide and CB[7] with adamantlyammonium. To a vial, portions of bis(3,5-dimethoxybenzyl)-4,4'-bipyridinium dibromide stock solution (4.0 mM, 250 μL) and of CB[7] stock solution (4.0 mM, 250 μL) were added respectively and mixed well to allow for complexation. The CB[7] complexed solution (500 μL) was added to an NMR tube and 0.5 eq of adamantyl ammonium was (125 μL) added. A second NMR tube was prepared using the same method with the CB[7] complexed solution and 1 eq adamantylammonium. For the measurement of NMR spectroscopy, after the solutions were added to the NMR tube, measurements were carried out on a 400 MHz NMR instrument at r.t. (Figure 3.14).

Inclusion measurements of bis(3,5-diisopropoxybenzyl)-4,4'-bipyridinium dibromide with CB[7]. To an NMR tube, portions of bis(3,5-diisopropoxybenzyl)-4,4'-bipyridinium dibromide stock solution (250 μL) and of CB[7] stock solution (250 μL) were added respectively and mixed well. For the measurement of NMR spectroscopy, after the solutions were added to the NMR tube, measurements were carried out on a 400 MHz NMR instrument at r.t. at times 1 min to 8 d. (Figure 3.15). Follow up analysis of the same solution was conducted by first heating the NMR tube to 80 °C for 24 h in a water bath, next allowed to cool to room temperature and analyzed by NMR (Figure 3.16).

3.7 References

1. Xue, M.; Yang, Y.; Chi, X.; Yan, X.; Huang, F. *Chem. Rev.,* **2015**, *115*, 7398-7501.
2. Harrison, I.; Harrison, S. *J. Am. Chem. Soc.,* **1967**, *89*, 5723-4.
3. Amabilino, D. B.; Stoddart, J. F. *Chem. Rev.* **1995**, *95*, 2725.
4. Schalley, C. A.; Weilandt, T.; Brüggemann, J.; Vögtle, F. Top. *Curr. Chem*. **2004**, *248*, 141.
5. Nepogodiev, S. A.; Stoddart, J. F. *Chem. Rev.* **1998**, *98*, 1959.
6. Chambron, J.-C.; Heitz, V.; Sauvage, J.-P. *J. Am. Chem. Soc.* **1993**, *115*, 12378.
7. Asakawa, M.; Ashton, P. R.; Ballardini, R.; Balzani, V.; Belohradsky, M.; Gandolfi, M. T.; Kocian, O.; Prodi, L.; Raymo, F. M.; Stoddart, J. F.; Venturi, M. *J. Am. Chem. Soc.* **1997**, *119*, 302.
8. Konstas, K.; Langford, S. J.; Latter, M. J. *Int. J. Mol. Sci.* **2010**, *11*, 2453-2472.
9. (a) Spencer, N.; Stoddart, J. F. *J. Am. Chem. Soc.* **1991**, *113*, 5131-5133.; (b) Sobransingh, D.; Kaifer, A. E. *Org. Lett.* **2006**, *8*, 3247.; (c) Ma, X.; Tian, H. *Chem Soc. Rev.* **2010**, *39*, 70-80.
10. (a) Liu, Y.; Saha, S.; Vignon, S. A.; Flood, A. H.; Stoddart, J. F. *Synthesis* **2005**, 3437.; (b) Share, A. I.; Parimal, K.; Flood, A. H. *J. Am. Chem. Soc.* **2010**, *132*, 1665.
11. Yamauchi, A.; Sakashita, Y.; Hirose, K.; Hayashita, T.; Suzuki, I. *Chem. Commun.* **2006**, 4312.
12. (a) Jimenez, M.C.; Dietrich-Buchecker, C.; Sauvage, J.-P. *Angew. Chem. Int. Ed.* **2000**, *39*, 3284-3287.; (b) Collin, J.-P.; Dietrich-Buchecker, C.; Gavina, P.;

Sauvage, J.-P. *Acc. Chem. Res.* **2001**, *43*, 477-487.; (c) Bruns, C. J.; Stoddart J. F. *Acc. Chem. Res.* **2014**, *47*, 2186-2199.

13. Badjić, J. D.; Balzani, V.; Credi, A.; Silvi, S.; Stoddart, J. F. *Science* **2004**, *303*, 1845.
14. (a) Saha, S.; Leung, K. C.-F.; Nguyen, T. D.; Stoddart, J. F.; Zink, J. I. *Adv. Funct. Mater.* **2007**, *17*, 685.; (b) Angelos, S.; Yang, Y.-W.; Patel, K.; Stoddart, J. F.; Zink, J. I. *Angew. Chem., Int. Ed.* **2008**, *47*, 2222.
15. Benniston, A. C.; Harriman, A.; Lynch, V. M. *J. Am. Chem. Soc.* **1995**, *117*, 5275.
16. Leigh, D. A.; Lusby, P. J.; Slawin, A. M. Z.; Walker, D. B. *Angew. Chem., Int. Ed.* **2005**, *44*, 4557.
17. Kay, E. R.; Leigh, D. A.; Zerbetto, F. *Angew. Chem., Int. Ed.* **2007**, *46*, 72.
18. Bissell, R. A.; Córdova, E.; Kaifer, A. E.; Stoddart, J. F. *Nature* **1994**, *369*, 133-137.
19. Tuncel, D.; Özsar, O.; Tiftik, H. B.; Salih, B. *Chem. Commun.* **2007**, 1369-1371.
20. Singh, A.; Yip, W. T.; Halterman, R. L. *Org. Lett.* **2012**, *14*, 4046-4049.
21. (a) Ong, W.; Kaifer, A. E. *J. Org. Chem.* **2004**, *69*, 1383-1385.; (b) Lui, S.; Ruspic, C.; Mukhopadhyay, P.; Chakrabarti, S.; Zavalij, P.Y.; Isaacs, L. *J. Am. Chem. Soc.* **2005**, *127*, 15959-15967.
22. (a) Sindelar, V.; Moon, K.; Kaifer, A. E. *Org. Lett.* **2004**, *16*, 2665-2668.; (b) Eelkema, R.; Maeda, K.; Odell, B.; Anderson, H. L. *J. Am. Chem. Soc.* **2007**, *129*, 12384-12385.; (c) Huang, X.; Huang, S.; Zhai, B.; Zhang, Y.; Xu, Y.; Wang, Q. *Tet. Lett.* **2012**, *53*, 6414-6417.; (d) Qian, Z.; Huang, X.; Wang, Q. *Dyes Pigm.* **2017**, *145*, 365-370.

23. Day, A. I.; Arnold, A. P.; Blanch, R. J. Snushall, B. *J. Org. Chem.* **2001**, *66*, 8094-8100.

24. Senler, S.; Cheng, B.; Kaifer, A. E. *Org. Lett.* **2014**, *16*, 5834-5837.

25. (a)Lagona, J.; Mukhopadhyay, P.; Chakrabarti, S.; Isaacs, L. *Angew. Chem., Int. Ed.* **2005**, *44*, 4844-4870. (b) Wheate, N. J.; Kumar, P. G. A.; Torres, A. M.; Aldrich-Wright, J. R.; Prince, W. *J. Phys. Chem. B* **2008**, *112*, 2311-2314.

Chapter 4: Investigation of Stopper Effectiveness of Cucurbit[7]uril Shuttle Rotaxanes

4.1 Introduction

The unique design and operation of mechanically interlocked molecules (MIMs), such as rotaxanes and catenanes, has piqued an increasing interest in recent chemical research. Having the ablilty to control the active function of these systems is an essential first step goal of their development into molecular machines. The potential for these structures to be used in molecular recognition and sensing has yet to be fully utilized. A molecular sensor or biosensor consists of two main components, a receptor unit that interacts with an analyte and a reporting unit that converts the response into a measurable signal such as fluorescence and chemiluminescence. Molecular sensors have limitless opportunities in biological and medical applications, such as monitoring cellular processes and early screening of diseases such as cancer.[1] One approach to cancer diagnostics is to use "chemical nose" array sensors, where differential interactions between the sensors and analytes create distinguishable patterns, very similar to our own sense of smell. Chemical nose sensors do not require a previous knowledge of the analytes but are instead trained to recognize the analytes themselves (Figure 4.1).[2,3,5] Chemical nose array sensors have been employed for the detection of a wide variety of analytes such as metal ions, aromatic amines, volatile organic compounds, amino acids, carbohydrates and proteins.[4-9] Extending shuttle rotaxanes with a fluorescent reporter into chemical nose sensors would be a novel approach for the improved screenings.

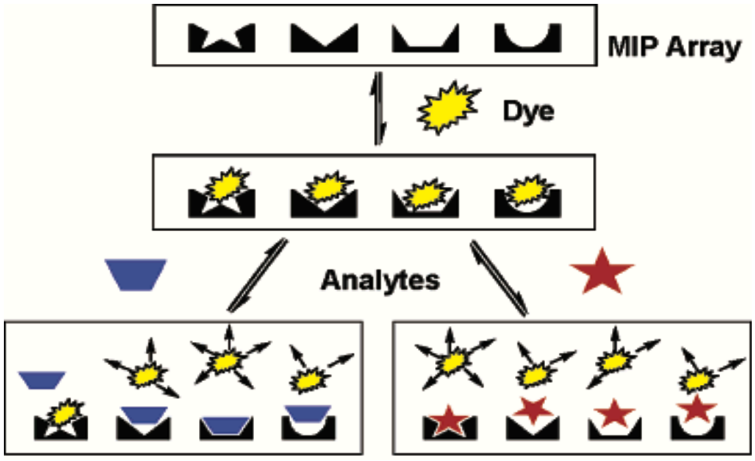

Figure 4.1 Schematic depiction of differential "chemical nose" based sensing array using imprinted polymers. Adapted from Shimizu.[5]

Our group is engaged in the design and synthesis of a molecular sensing rotaxane that uses cucurbit[7]uril as a shuttle to communicate between the receptor unit and fluorescent reporter (Figure 4.2). The receptor unit serves as a molecular sensing component as well as a binding stopper. The binding stopper is designed based on previously reported benzyl- and xylyl-ammonium guests that bind strongly with CB[7] ideally in the range of 10^7–10^8 M^{-1}.[10,11]

However, to be incorporated as a rotaxane stopper to prevent CB[7] from dethreading, sterically bulky groups need to be installed with one group being a variable R group. The variable R group can be modified with aliphatic, aromatic, ammonium, and alcohol substituents or a combination thereof based on the sensing needs of a certain biomolecule or cell receptor containing different functionality types. The binding stopper must also have a high binding affinity with CB[7] that is ideally 100-1000 fold stronger than any other docking site on the rotaxane sensor or with the biomolecule itself.

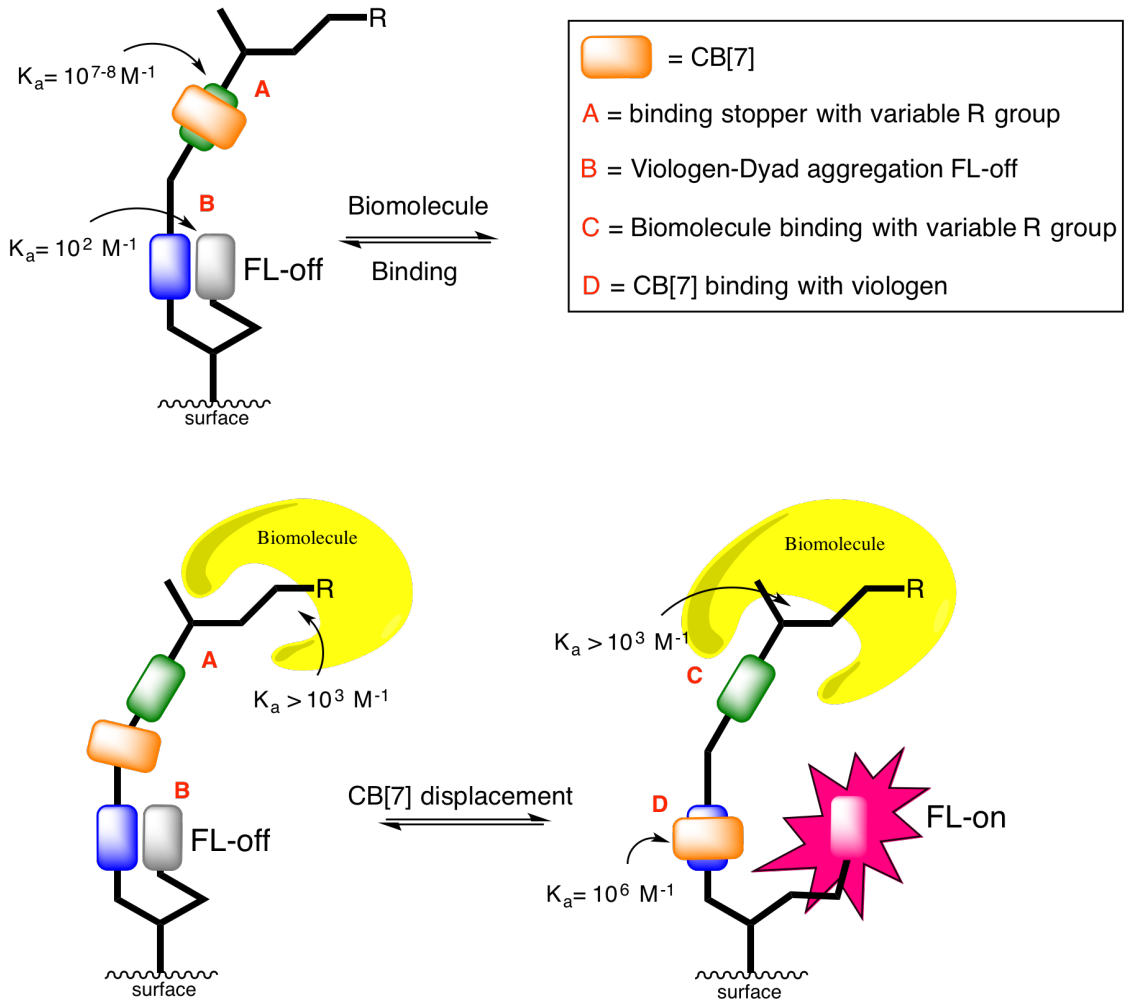

FL-on if biomolecule binding strong enough and close enough to displace CB[7]

Figure 4.2 Schematic of proposed surface-attached fluorescence-on sensor.

This verifies that CB[7] is docked near the unbound receptor unit a great extent of the time. Because CB[7] is bound with the receptor through equilibrium, and binding is not an "all-or-nothing" event, a small portion of CB[7] will shuttle across the axle to a weaker binding site, allowing the receptor to be exposed to fully sense any intended biomolecule. The steric bulk and electronic interactions between the biomolecule and receptor should diminish the binding affinity of CB[7] and receptor, and this factor should force CB[7] to bind with the weaker binding site where a fluorescence response

is initiated. The weaker binding site and fluorescent reporting unit have recently been established by Dr. Anuradha Singh in our group, and was determined to have a 1:1 binding constant with CB[7] ($K_a = 10^6$ M^{-1}). A rotaxane based on this scaffold would be the first of its kind and could be adapted for sensing different biomolecules for many potential biomedical applications. However the challenge of building the mechanical structure may not be easily overcome, and the focus of this chapter is on the assembly of the rotaxane and to resolve binding stopper effectiveness to prevent CB[7] from threading/dethreading.

4.2 Specific Aims

Before the above-proposed rotaxane (Figure 4.2) can be assembled, a model rotaxane needs to be established to fundamentally determine stopper efficiency against CB[7] threading/dethreading and shuttle activity. Methods for assembling a simple rotaxane have been previously discussed in Chapter 3 and we will explore combined methods of using an active metal and capping as our approach to assembling the rotaxane.

In order to form a full rotaxane, CB[7] will need to be precoordinated or prethreaded onto the axle and encapsulate the binding stopper through supramolecular interactions and then the axle end can be capped via copper(I)-catalyzed Azide-Alkyne cycloaddition (Cu-AAC) click chemistry. "Click chemistry" was promoted by K.B. Sharpless in 2001[12] and has gained popularity for its high efficiency and functional group tolerance in assembly of rotaxanes and other interlocked molecules under mild aqueous conditions.[13,14] This coupling reaction takes place by joining an unhindered

azide and terminal alkyne to form a 1,2,3 triazole through Cu-AAC as seen in Figure 4.3. For our initial study, we plan to use the alkyne stopper (Compound **2.3c**) from Chapter 2 and the benzyl bromide precursor from Chapter 3 to form the needed azide to optimize conditions for the cycloaddition reaction.

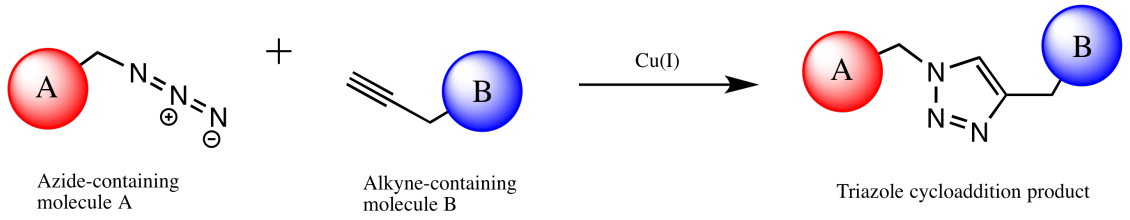

Figure 4.3 Synthetic scheme of copper(I)-catalyzed azide-alkyne cycloaddition (Cu-AAC).

This chapter presents the synthesis of a rotaxane-like molecule, containing two different stoppering groups, through the use of the CuAAC. The stoppering groups used for this simple rotaxane are the benzyl ammonium **2.3c** from Chapter 2 and 3,5 diisopropoxybenzyl-moiety from Chapter 3. Once formed, the rotaxane-like molecule will be analyzed as to its ability to sterically block CB[7] from "slipping" over the bulky stoppers. This will be done to specifically investigate if the diisopropylammonium stopper is sterically large enough to prevent CB[7] from threading or dethreading. If the benzyl ammonium stopper is large enough to block CB[7], it will be further investigated by incorporating it into a larger rotaxane with an additional docking group for CB[7] shuttling (Figure 4.4).

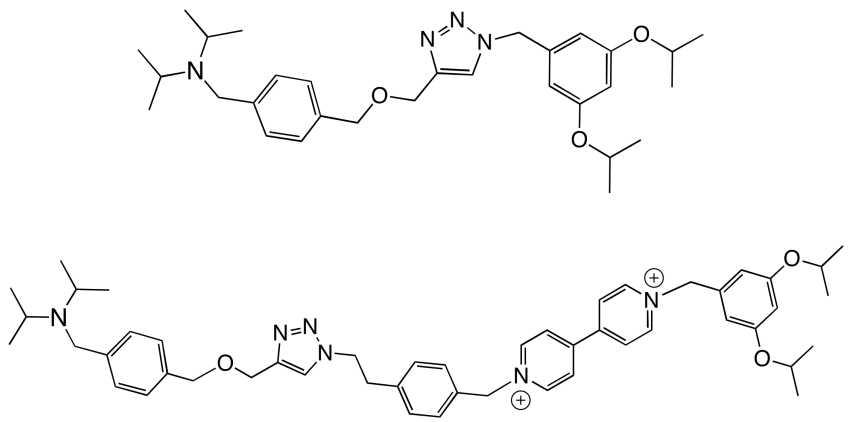

Figure 4.4 Proposed model rotaxane (top), model rotaxane with two docking sites for CB[7] shuttling (bottom).

Also presented in this chapter is the synthesis of two additional xylyl ammonium analog guest molecules. These xylyl ammonium guest molecules will serve as foundational data to determine if CB[7] is threading over the diisopropyl units, and their measurement of binding efficiency towards CB[7] in aqueous solutions using a competitive binder with NMR spectroscopy.

4.3 Synthesis

The rotaxane-like triazole **4.2b** 1-(3,5-diisopropoxybenzyl)-4-(4-((diisopropylamino)methyl)benzyloxymethyl)-1,2,3-triazole was synthesized as shown in Figure 4.5. First, 3,5-diisopropoxybenzyl bromide was prepared by the methods described in Chapter 3, followed by addition of sodium azide in DMF and stirred at 40 °C under nitrogen for 3 d. The crude mixture was extracted and the extract flushed through a plug of silica gel to remove any residual DMF to afford the 3,5-diisopropoxybenzyl azide **4.1a**. The additional precursor (propargyl **2.3c**) was prepared by the methods described in Chapter 2, and was combined with azide **4.1a**, copper(I)

iodide, and sodium ascorbate in 1:1 t-butyl alcohol:water and heated to 40 °C and allowed to stir for 2 d. The crude mixture was extracted and purified by column chromatography using 5% methanol in dichloromethane as an eluent to provide triazole **4.2b**.

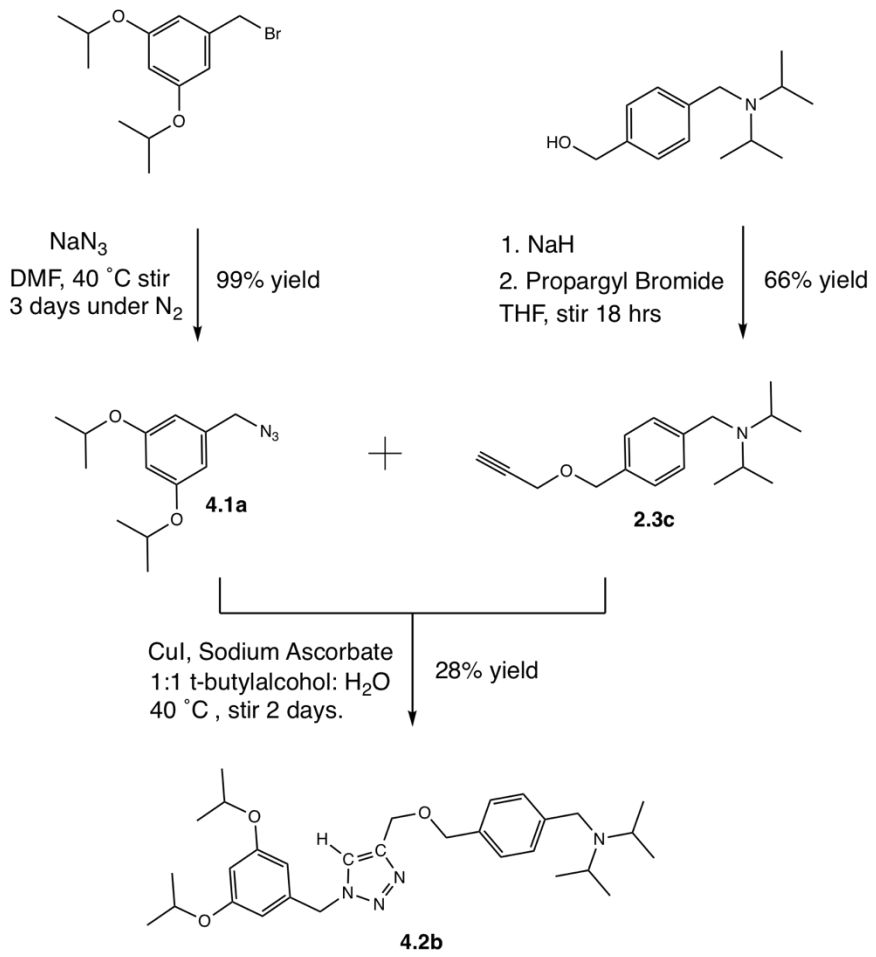

Figure 4.5 Synthetic scheme of 1-(3,5-diisopropoxybenzyl)-4-(4-((diisopropylamino)methyl)benzyloxymethyl)-1,2,3-triazole **4.2b**.

The two guests, *p*-bis(isopropylaminomethyl)benzene **4.3c** and *p*-bis-(diisopropylaminomethyl)benzene **4.4d,** were synthesized as shown in the following scheme (Figure 4.6). In each case α-α'-dibromo-p-xylene was combined with a 6-10

fold excess of amine in dichloromethane and the mixture was heated to reflux under nitrogen for 24 h. The solvent and excess amine was first evaporated, and the crude mixture was extracted to remove any starting materials. The extract was evaporated to provide xylydiamines **4.3c**, **4.4d**.

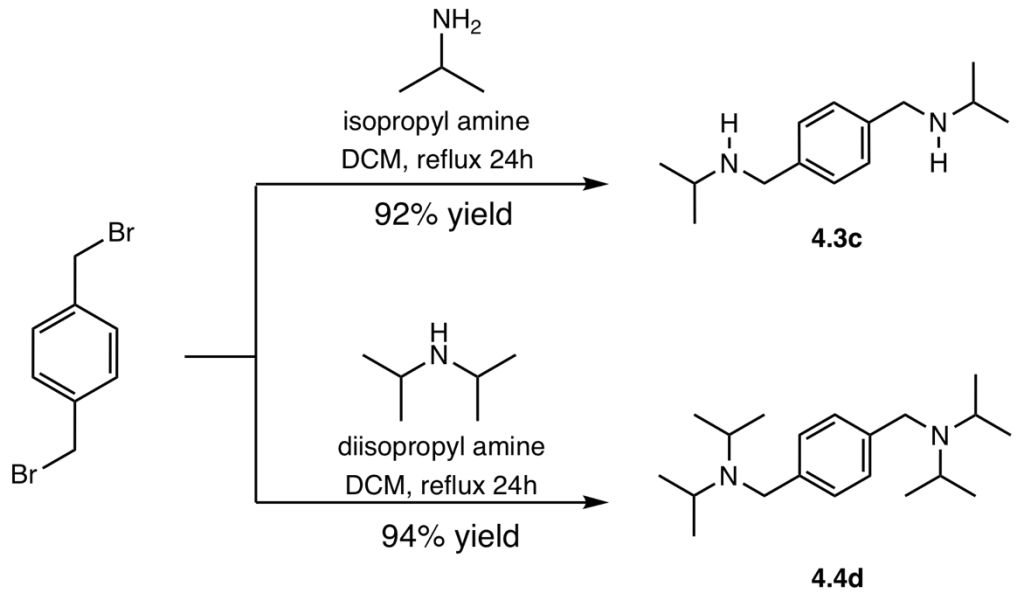

Figure 4.6 Synthetic scheme *p*-bis(isopropylaminomethyl)benzene **4.3c**, and *p*-bis-(diisopropylaminomethyl)benzene **4.4d**.

4.4 Results and Discussion

As previously discussed in Chapter 2, the diisopropyl groups on the benzyl amine binding stopper need to be examined to determine if they are bulky enough to prevent CB[7] from dethreading when incorporated into a rotaxane. In order to form a full rotaxane, we had initially envisioned prethreading CB[7] onto the 4-((diisopropylamino)methyl)benzyl propargyl ether **2.3c** and then joining the alkyne with azide **4.1a** through 1,3 dipolar cycloaddition using CuAAC. However, due to the previous concerns mentioned of the propargyl tail being either internal or external of

prethreaded CB[7], which could potentially impede reactivity of the 1,3 dipolar cycloaddition, the rotaxane-like triazole was synthesized without the prethreaded CB[7]. By forming the triazole first, the CuAAC conditions can be optimized and established, this also allows for conservation of CB[7] without the need for prethreading. Once the triazole was synthesized and its structure confirmed by NMR spectroscopy, we investigated rotaxane formation with CB[7] by the slipping method. Usually in the slipping method of rotaxane formation, applying higher temperatures or refluxing the macrocyclic host and dumbbell for a period of time is carried out to ensure that rotaxane formation has occurred, provided that rotaxane formation is slow at room temperature. We have already established in Chapter 3 that the 3,5-diisopropoxybenzyl moiety was bulky enough to prevent CB[7] from slipping over the end groups. Therefore the only possible way for rotaxane formation with CB[7] and the triazole **4.2b** would be to slip over the diisopropyl groups of the benzyl amine moiety.

4.4.1 Spectroscopic Investigations of 1-(3,5-diisopropoxybenzyl)-4-(4-((diisopropylamino)methyl)benzyloxymethyl)-1,2,3-triazole with Cucurbit[7]uril

Triazole **4.2b** and CB[7] were combined in a 1:1 concentration in D_2O (pD = 4) at room temperature and analyzed by NMR spectroscopy. According to the NMR spectra (Figure 4.7) triazole **4.2b** and CB[7] formed a full inclusion complex within minutes of mixing. The aromatic protons on the benzyl amine moiety had a significant upfield shift from 7.34–7.30 ppm to 6.93–6.83 ppm. The upfield shifts give a strong indication that the benzene core is included within the CB[7] cavity. This alerted us of the concern that the diisopropyl groups of the benzyl amine are not bulky enough to

prevent threading of CB[7]. This discovery was perplexing as we did not anticipate this outcome, and we needed control data to compare our findings. There were only a few examples found in the literature from Macartney and others that studied similar benzyl/xylyl amine compounds complexing with CB[7] and the resulting aromatic proton shifts of the benzyl/xylyl amines were consistent with our 1:1 complexation data.[15] To the best of our knowledge no rotaxane-like compounds resembling triazole **4.2b** were found in the literature to compare data with. Therefore, this data lead us to investigate what we have called an "adamantylammonium trap", that will essentially trap any decomplexed CB[7] with **4.2b** to confirm that CB[7] is dethreading off of the diisopropylbenzylammonium group.

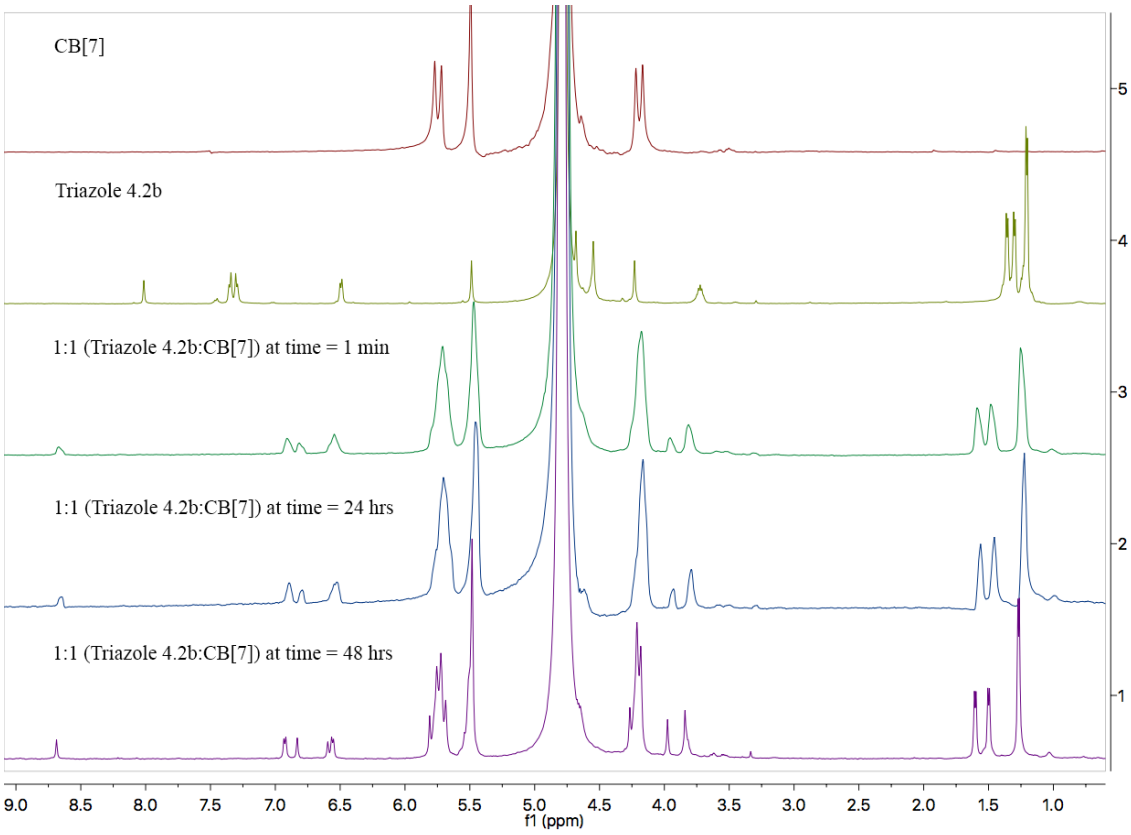

Figure 4.7 ^{1}H-NMR spectra of (500 MHz, D_2O) of 1-(3,5-diisopropoxybenzyl)-4-(4-((diisopropylamino)methyl)benzyloxymethyl)-1,2,3-triazole **4.2b** with CB[7] (0 to 1 equivalent at times 1 min to 48 h).

Follow up studies were conducted with the 1:1 complex of 1-(3,5-diisopropoxybenzyl)-4-(4-((diisopropylamino)methyl)benzyloxymethyl)-1,2,3-triazole **4.2b** and CB[7] with a titration of adamantylammonium in D_2O (pD = 4) at room temperature at 0, 0.5, and 1 equivalents (Figure 4.8). We determined that complexation with CB[7] was fast, but we wanted to know how fast CB[7] would dissociate; whether if it is minutes or hours when we added the stronger binding unit adamantylamine. Given that CB[7] threaded over the diisopropylammonium group, if any CB[7] were to dethread with triazole **4.2b** and generate any free CB[7], the macrocycle would prefer to bind with the stronger binding guest adamantylammonium. In other words the adamantylammonium would "trap" any CB[7] prohibiting any reverse equilibrium. From our results the spectra shows that upon mixing in 0.5 eq of adamantyl amine with the pre-formed CB[7]-diisopropylbenzylammonium complex, the aromatic benzylammonium **4.2b** showed two sets of aromatic proton shifts for unbound and bound, 7.39–7.35 ppm and 6.94–6.92 ppm respectively. Upon mixing the addition of 1 eq of adamantylamine to the preformed complex, the spectra showed full dissociation of CB[7] and compound **4.2b** and instead a complex of CB[7] with adamantylammonium was formed, this is seen by the apparent downfield shift of the aromatic protons of the benzene core and an upfield shift signals of the adamantyl group. It can be concluded that CB[7] has fast association with compound **4.2b** and fast dissociation when a more competitive binder is added. This also leads to the confirmation that the diisopropyl goups on the benzyl amine are not large enough to prevent threading and dethreading of CB[7]. Therefore, this data lead us to investigate two control compounds to further

deduce if the diisopropyl groups of the benzyl amine moiety in triazole **4.2b** were allowing slippage of CB[7].

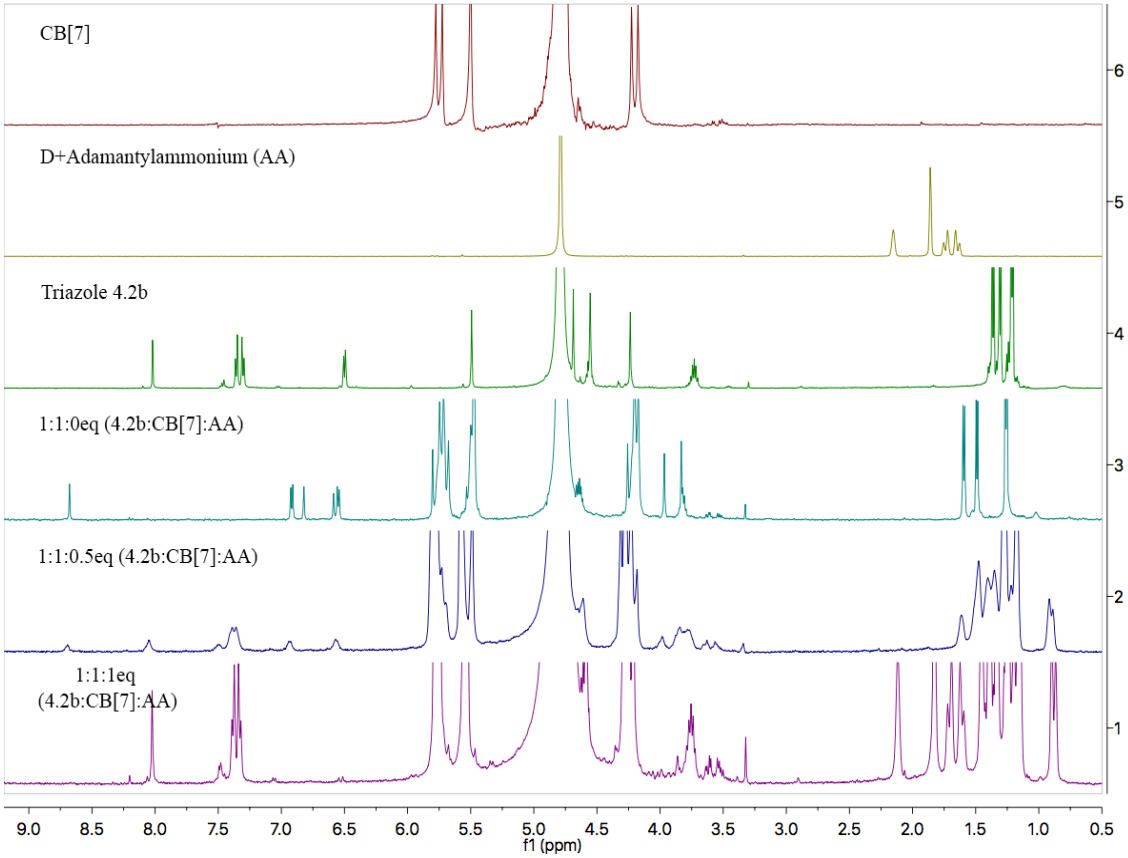

Figure 4.8 ^{1}H-NMR spectra of (500 MHz, D_2O) of 1-(3,5-diisopropoxybenzyl)-4-(4-((diisopropylamino)methyl)benzyloxymethyl)-1,2,3-triazole **4.2b** with CB[7] and adamantylammonium (0 to 1 equivalent).

4.4.2 Spectroscopic Investigations of *p*-Bis(isopropylaminomethyl)benzene with Cucurbit[7]uril

We had postulated that by incorporating single isopropyl groups at each end of the xylyldiamine **4.3c**, that CB[7] would slip over and form a full inclusion complex. This would allow us to specifically see the aromatic protons signature that the 1:1 complex gives in the NMR spectrum and use that as a foundation to compare with.

Compound **4.3c** and CB[7] were combined in the following titrations 1:0, 1:0.5, 1:1, 1:2 in D_2O (pD = 4) at room temperature and analyzed by ^{1}H NMR spectroscopy. According to the ^{1}H-NMR spectra (Figure 4.9) compound **4.3c** and CB[7] formed an inclusion complex within minutes of mixing. In the 1:0.5 eq mixture, the aromatic signals for the unbound and bound compound can be seen at 7.54 ppm and 6.63 ppm respectively. In the 1:1 eq mixture the compound formed a full inclusion complex with CB[7] and the aromatic protons on the benzene ring had a substantial upfield shift from 7.54 ppm (unbound) to 6.62 ppm (bound). The 1:2 eq mixture shows the same inclusion complex with upfield aromatic shifts. This indicates that the benzene core of *p*-bis(isopropylaminomethyl)benzene is encapsulated within the CB[7] host cavity. This data was consistent with Macartney's and others literature results, and also gives confirmation that the mono-isopropyl end groups are not bulky enough to prevent threading of the macrocyclic host. As we have established what the complexation looks like within the NMR spectra, we still needed to confirm slippage over the diisopropyl groups.

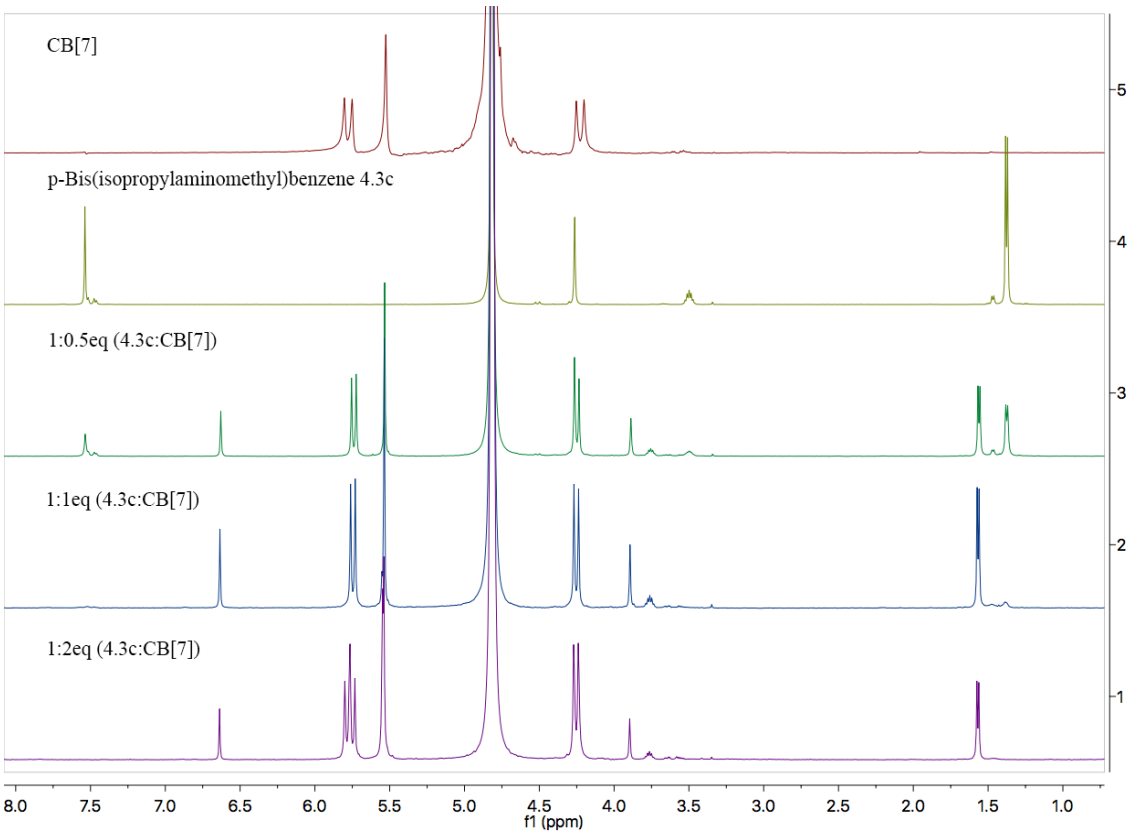

Figure 4.9 ^{1}H-NMR spectra of (500 MHz, D_2O) of *p*-bis(isopropylaminomethyl)benzene **4.3c** with CB[7] (0 to 2 equivalents).

4.4.3 Spectroscopic Investigations of *p*-Bis(diisopropylaminomethyl)benzene with Cucurbit[7]uril

The main aim of this experiment was to observe the probability of the sterically bulkier molecule **4.4d** fully complexed with CB[7], and use the results to compare to our previous experiments. Since we determined that CB[7] was fully complexed with *p*-bis(isopropylaminomethyl)benzene, installing an additional isopropyl group on the amine to give *p*-bis(diisopropylaminomethyl)benzene would give confirmation as to whether CB[7] was threading. Each end of the guest **4.4d** is essentially identical to that

of the benzyl amine moiety of the triazole **4.2b** and therefore CB[7] will have no preference which side to thread over if it were to establish a full complex at equilibrium.

Compound **4.4d** and CB[7] was combined in the following titrations 1:0, 1:0.5, 1:1, 1:2 in D_2O (pD = 4) at room temperature and analyzed by ^{1}H-NMR spectroscopy. According to the ^{1}H-NMR spectra (Figure 4.10) compound **4.4d** and CB[7] formed formed an inclusion complex within minutes of mixing. In the 1:0.5 eq mixture, the aromatic signals for the unbound and bound compound are broadened and can be seen at 7.45 ppm and 6.80 ppm respectively. In the 1:1 eq mixture the compound formed a full inclusion complex with CB[7] and the aromatic protons on the benzene ring had a substantial upfield shift from 7.55 ppm (unbound) to 6.80 ppm (bound). The 1:2 eq mixture shows the same inclusion complex with upfield aromatic shifts. This indicates that the benzene core of *p*-bis(diisopropylaminomethyl)benzene **4.4d** is encapsulated within the CB[7] host cavity, and that the bulkier diisopropyl end groups are not bulky enough to prevent threading of the macrocyclic host. These results confirm that CB[7] will thread over the diisopropyl units of the benzyl amine moiety in triazole **4.2b**.

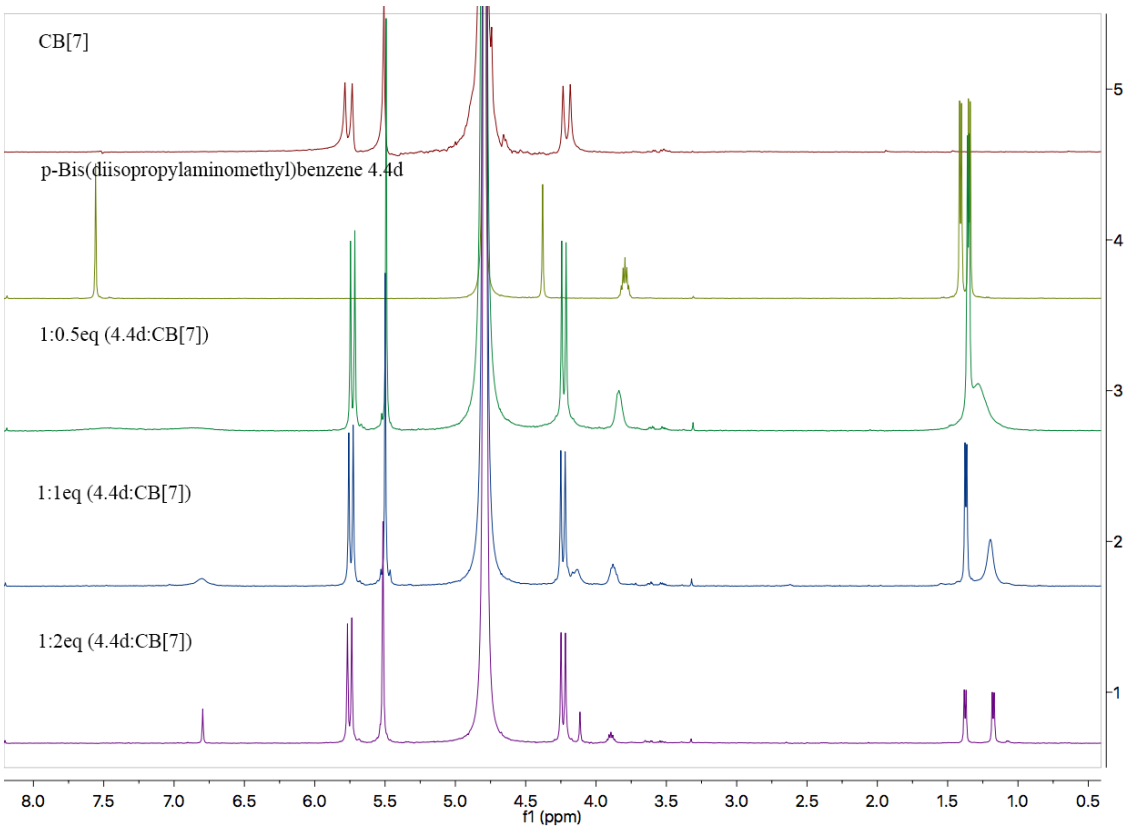

Figure 4.10 ^{1}H-NMR spectra of (500 MHz, D_2O) of *p*-bis(diisopropylaminomethyl)benzene **4.4d** with CB[7] (0 to 2 equivalents).

Follow up studies were conducted with the 1:1 complex of *p*-bis(diisopropyl-aminomethyl)benzene and CB[7] with a titration of adamantylammonium in D_2O (pD = 4) at room temperature at 0, 0.5, and 1 eq (Figure 4.11) to determine the rate of dissociation. We determined that complexation was fast, but we wanted to know how fast decomplexation or dissociation was if it were minutes or hours when we added the stronger binding unit adamantylamine. If any CB[7] had decomplexed with *p*-bis(diisopropylaminomethyl)benzene and generated any free CB[7], the macrocycle would prefer to bind with the stronger binding guest adamantylammonium. The adamantylammonium would trap any CB[7] prohibiting any reversal of binding with the initial *p*-bis(diisopropyl-aminomethyl)benzene. According to the spectra, upon

mixing in 0.5 eq of adamantylamine with the already formed CB[7]-xylyldiammonium complex, the xylyldiammonium **4.4d** showed two sets of signals for unbound and bound, 7.55 ppm and 6.83 ppm respectively. Upon mixing the addition of 1 eq of adamantyl amine to the complex, the spectra showed full dissociation of CB[7] and compound **4.4d** and instead a complexation of CB[7] with adamantylammonium was formed, this is seen by the apparent downfield shift of the aromatic protons of the benzene core and an upfield shift signals of the adamantyl group. It can be concluded that CB[7] has fast association with compound **4.4d** and fast dissociation when a more competitive binder is added. Due to the immediate results, the rate of dissociation was too fast to measure using standard NMR spectroscopy.

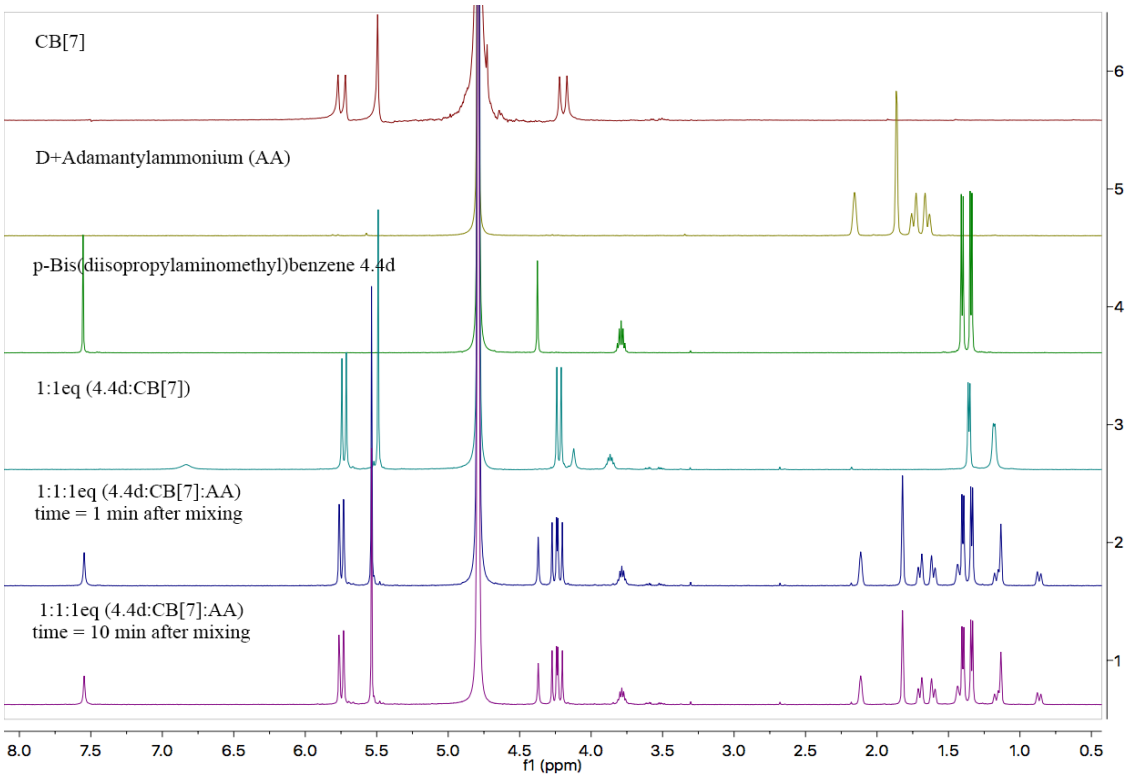

Figure 4.11 ^{1}H-NMR spectra of (500 MHz, D_2O) of *p*-bis(diisopropyl-aminomethyl)benzene **4.4d** with CB[7] and adamantylammonium (0 to 1 equivalent).

4.4.4 Determination of Binding Constants of Bis-(N-substituted)-xylenediamines

The main aim of this experiment was to determine binding of bulky N-substituted p-xylenediamine guests with CB[7] as there are limited bulky guests in the current literature. With the presence of host:guest inclusion complexes between CB[7] and the xylyl diamine guests previously confirmed by ^{1}H-NMR, the binding by CB[7] for each diamine was measured. The binding events between the xylyl diamine guests and CB[7] are driven by the ion dipole interactions of the positively charged ammonium cations of the guests and the carbonyl rims of the CB[7] macrocylic host.

In Chapter 2 we had established the method for determining binding constants through competitive binding using NMR spectroscopy. We followed the same general procedure for determining the equilibrium binding constants of the bis-monoisopropyl and bis-diisopropyl xylyldiamines. Issacs and co-workers had previously determined that p-xylenediamine had a 1:1 binding constant with CB[7] at $K_a = (1.84 \pm 0.34) \times 10^9$ M^{-1}, and based on these results we predicted that these two guests **4.3c** and **4.4d** would fall in the range of $10^8 - 10^9$ M^{-1}. Because p-xylenediamine and the guest are analogs and assigning the protons in the NMR spectrum would be challenging we opted to use a silane derivative reference compound to allow for a more thorough analysis of the spectra. The reference compound selected for this study was (trimethylsilyl)methylamine $(Me)_3SiCH_2NH_2$ **4.5e** (Figure 4.12) which has a binding constant of $K_a = (8.88 \pm 1.41) \times 10^8$ M^{-1}.[16]

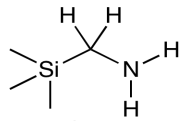 **4.5e**	$K_a = (8.88 \pm 1.41) \times 10^8$ M^{-1}

Figure 4.12 Line drawing of (trimethylsilyl)methylamine $(Me)_3SiCH_2NH_2$ **4.5e**.

Silane **4.5e** (TMSMA) has a ^{1}H-NMR shift at 0.0 ppm in its unbound state, and it has a shift at −0.7 ppm when bound to CB[7]. This compound demonstrates slow exchange on the ^{1}H-NMR timescale, therefore both peaks can be integrated to determine an accurate ratio of bound and unbound silane **4.5e**. As we began our study, we presumed that when the reference compound and an excess of our guest were allowed to compete for inclusion of a limiting quantity of CB[7] that the reference compound would be the stronger binder. However, we found that as we examined the initial NMR spectra that silane **4.5e** was completely unbound to CB[7], prompting us to increase the concentration of our reference compound and decreasing that of our guests, which indicates that our guests have stronger binding and would result in a higher binding constant.

Once the concentrations were optimized we proceeded with the competition binding experiments. Three solutions of 0.125 mM CB[7], 3.00 mM silane **4.5e**, and 0.300 mM (bis-isopropyl **4.3c**) were prepared in 50.0 mM Na(O_2CCD_3)-buffered D_2O (pD = 4.45). The bis-isopropyl **4.3c** guest and silane **4.5e** were allowed to compete for CB[7], and their resonances were examined. Silane **4.5e** showed slow exchange kinetics on the NMR time scale resulting in clear peaks for bound and unbound silane at −0.7 and 0.0 ppm respectively. The procedure was replicated for compound bis-diisopropyl **4.4d**. The integrations of the peaks for the bound and unbound silane **4.5e** allowed for a calculation of the K_{rel} for the competing guest, using the concentrations of all species in solution. Next, K_{rel} and the absolute binding constant of silane **4.5e** were used to calculate the absolute binding constant of the competing guest.

X = Competing Guest

Si = Known Binder (TMSMA)

$[Si]_{Total} = [Si]_{Free} + [CB_7 \cdot Si]_{Bound}$

$[CB_7]_{Total} = [CB_7 \cdot X]_{Bound} + [CB_7 \cdot Si]_{Bound}$

$[X]_{Total} = [X]_{Free} + [CB_7 \cdot X]_{Bound}$

$$CB_7 + Si \xrightleftharpoons{K_{Si}} CB_7 \cdot Si$$

$$CB_7 + X \xrightleftharpoons{K_X} CB_7 \cdot X$$

$$CB_7 \cdot Si + X \xrightleftharpoons{K_{Rel}} CB_7 \cdot X + Si$$

$$K_{rel} = \frac{[CB_7 \cdot X]\,[Si]}{[CB_7 \cdot Si]\,[X]}$$

$$K_X = (K_{Si})\,(K_{rel})$$

Figure 4.13 Equations outlining concentrations of bound and unbound guests with CB[7]. Using the concentrations of all species allow for calculationd of K_{rel} and the absolute K_a for the competing guest.

Table 4.1 1:1 Absolute binding constant values *(K_a)* for (Guest: CB[7]).

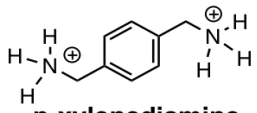 **p-xylenediamine**	$K_a = (1.84 \pm 0.34) \times 10^9\ M^{-1}$
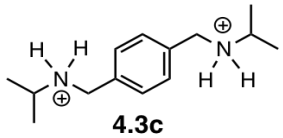 **4.3c**	$K_a = (6.03 \pm 1.21) \times 10^9\ M^{-1}$
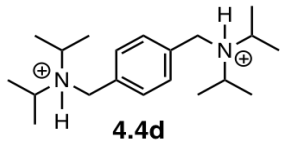 **4.4d**	$K_a = (4.83 \pm 0.93) \times 10^9\ M^{-1}$

Both diamine guests **4.3c** and **4.4d** showed surprisingly similar binding constants with CB[7] in the range of 10^9 M^{-1} as seen in Table 4.1. What was even more shocking was that each K_a value for guests **4.3c** and **4.4d** was stronger than p-xylenediamine $K_a = (1.84 \pm 0.34) \times 10^9$ M^{-1}. We presumed that CB[7] would form an inclusion complex with bis-isopropyl **4.3c** due to only having one isopropyl moiety at each nitrogen. We had also considered that the isopropyl groups might hinder the

binding and lower the binding efficiency. However, compound **4.3c** was determined to have the highest binding constant with CB[7] of $K_a = (6.03 \pm 1.21) \times 10^9\ M^{-1}$, which is 4.19×10^9 stronger binding than that of the p-xylenediamine. Compound **4.4d** was determined to have a binding constant with CB[7] of $K_a = (4.83 \pm 0.93) \times 10^9\ M^{-1}$, which is 2.99×10^9 stronger than that of p-xylenediamine. The stronger binding constants gives the indication that the presence of bulky alkyl groups on the amine has a greater effect on the binding efficiency of the xylyldiamines with CB[7].

4.5 Conclusion

This chapter described the need for and our efforts to develop a CB[7] shuttle rotaxane. We have shown the construction of a rotaxane-like molecule with bulky end groups under mild and favorable conditions by formation of a triazole using CuAAC Copper(I)-catalyzed azide-alkyne cycloaddition "click" reaction. The triazole compound, and two additional guest molecules were successfully synthesized and characterized by performing NMR spectroscopy and mass spectrometry experiments. The stopper efficacy of the benzyl ammonium moiety of **4.2b** upon the addition of CB[7] was studied. Additionally, equilibrium binding constants of bis-(N-substituted)-xylenediamines were studied.

Results from these studies provide evidence for the ability of CB[7] to thread over the N-substituted stopper end groups of the triazole **4.2b** forming a 1:1 full inclusion complex by ^{1}H-NMR experiments at room temperature. These results were further confirmed by comparison of ^{1}H-NMR titration experiments of 1:1 full inclusion complexes of bis-(N-substituted)-xylenediamines. Strong 1:1 host-guest complexation

($K_a = 10^9$ M^{-1}) for both xylenediamines was observed by competitive binding ^{1}H-NMR experiments. According to the data obtained I can conclude that CB[7] is threading over the ammonium stopper and therefore the proposed model rotaxane is considered to be a pseudorotaxane and not true rotaxane. These results provide fundamental information regarding the development of CB[7] shuttle rotaxanes, specifically with respect to ammonium binding stoppers. It is hopefull that these results will encourage additional studies of ammonium rotaxane stoppering groups and promote the continued development of a molecular sensing CB[7] shuttle rotaxane.

4.6 Future Directions

The largest issues that still needs to be addressed in future development of ammonium binding stoppers for their incorporation into CB[7] shuttle rotaxanes is the size of end groups on the ammonium stopper in addition to strengthening the binding efficiency. For the current design, increasing the steric bulk of one group of the ammonium stopper will decrease the probability of CB[7] threading/dethreading over the stopper and therefore achieving the desired full rotaxane. Although the diisopropyl groups are large, they are not large enough, but they give a foundation of where to start when considering "the next size up". The possbilities of determining the appropriate size of stoppering group is endless but should be considered carefully. If the group contains a larger substituents, i.e. benzyl, cyclohexyl, unintended binding competition with CB[7] between the binding group and the end groups may occur. Therefore, it is difficult to propose a suitable stoppering end group without further molecular modeling and synthetic experimentation. However, since we have fully determined in Chapter 3

that the 3,5-diisopropoxybenzyl- groups will prevent CB[7] slippage, this would be a favorable group to establish the next versions of ammonium rotaxane stoppers. Once this stoppering group is installed onto the ammonium binding unit, a prethreaded CB[7] rotaxane with a second docking site can be established.

There is also further work that needs to be investigated on the binding efficiency of a new ammonium stopper. In Chapter 2 we determined a binding range of $K_a = 10^5$ M^{-1} with only one ammonium moiety on the proposed stopper, and a binding range of $K_a = 10^9$ M^{-1} on a guest with two ammonium moieties in chapter 4. The ideal range for the binding unit should be in the range of $K_a = 10^7 - 10^9$ M^{-1}. A sterically bulky xylenediamine binding unit (with the 3,5-diisopropoxybenzyl group) should be tested to determine CB[7] shuttle mobility on a model rotaxane. It would also be interesting to determine the binding strength of the new ammonium stopper and compare that to our current results, and to that of the second binding viologen-dyad unit.

4.7 Experimental

Synthesis of CB[7]. CB[7] was synthesized using the same procedure from chapter two.

Synthesis of *p*-bis(isopropylaminomethyl)benzene.

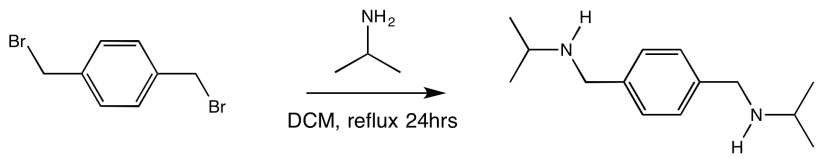

In a 250 mL reaction flask, α,α'-dibromo-p-xylene (790 mg, 3.0 mmol) was dissolved in dichloromethane (50 mL) and isopropylamine (3.0 mL, 35 mmol) was added. The mixture was heated at reflux for 24 h. The solution was washed with 1 M hydrochloric acid (20 mL x 3) and the layers were separated. To the acid solution, aqueous potassium hydroxide (4 M) was added there up to clearly basic, and the product was extracted with dichloromethane (25 mL x 3). The extract was washed with brine and dried over anhydrous Na_2SO_4 and filtered. The solvent was removed under reduced pressure to afford *p*-bis(isopropylaminomethyl)benzene (610 mg, 92 % yield) as a tan-yellow oil. ^{1}H NMR (500 MHz, D_2O DCl) δ 7.51 (s, 4H), 4.24 (s, 4H), 3.47 (s, 2H), 1.35 (d, J = 6.6 Hz, 12H). ^{13}C NMR (75 MHz, $CDCl_3$) δ 139.3, 128.2, 51.3, 47.9, 22.9. HRMS-ESI: m/z calculated for [$C_{14}H_{24}N_2$] 220.193; found 221.201 [M + H].

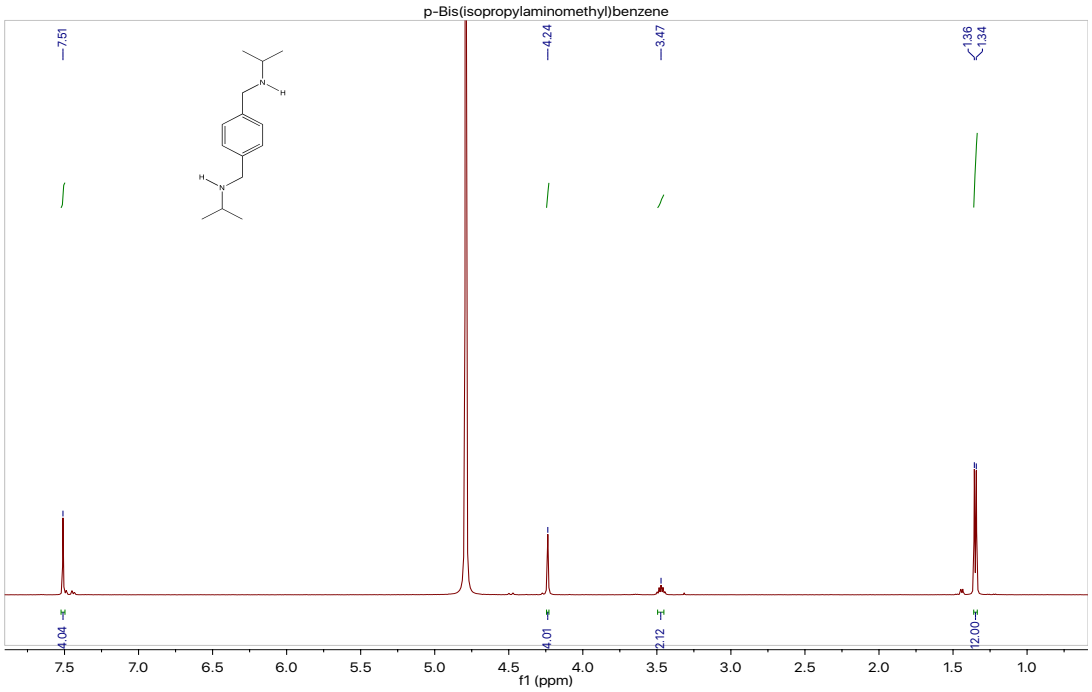

Figure 4.14 ^{1}H NMR (500 MHz, D_2O DCl) spectrum of *p*-bis(isopropylaminomethyl)-benzene.

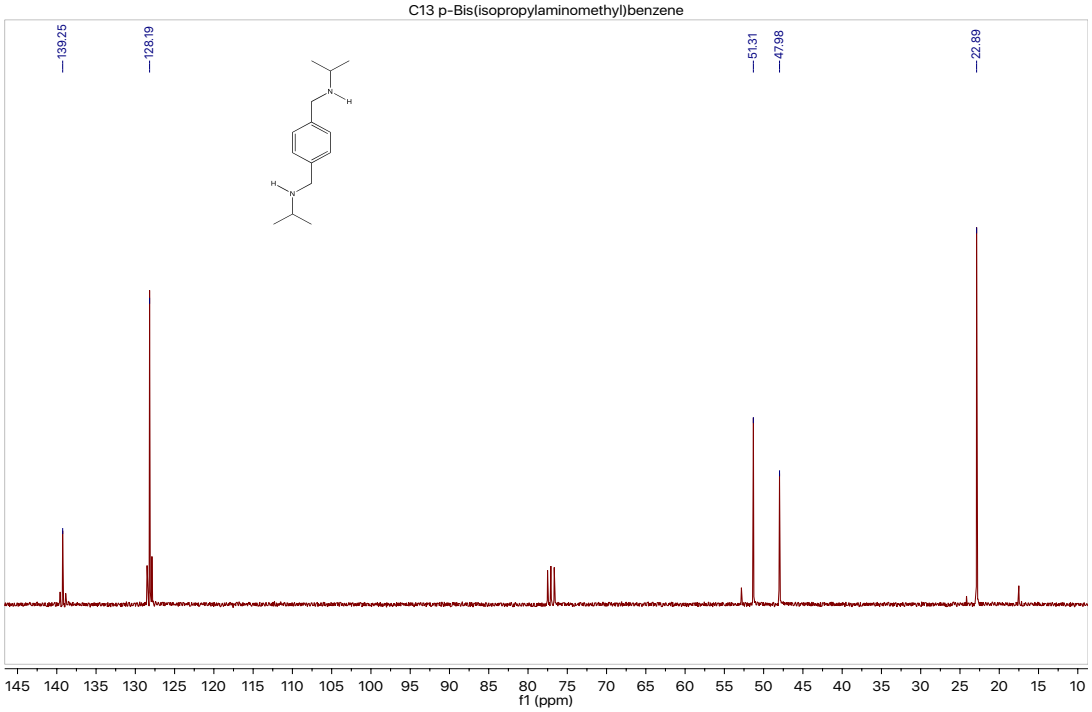

Figure 4.15 ^{13}C NMR (75 MHz, $CDCl_3$) spectrum of *p*-bis(isopropylaminomethyl)-benzene.

Synthesis of *p*-bis(diisopropylaminomethyl)benzene.

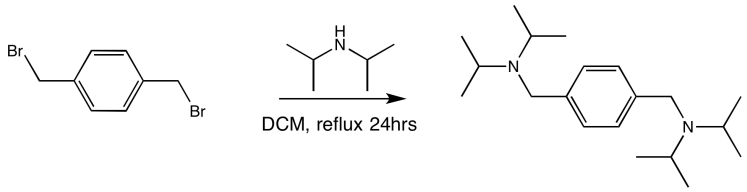

In a 250 mL reaction flask, α,α'-dibromo-p-xylene (790 mg, 3.0 mmol) was dissolved in dichloromethane (50 mL) and diisopropylamine (3.0 mL, 2.1 mmol) was added. The mixture was heated at reflux for 24 h. The solution was washed with 1 M hydrochloric acid (20 mL x 3) and the layers were separated. To the acid solution, aqueous potassium hydroxide was added there up to clearly basic, and the product was extracted with dichloromethane (25 mL x 3). The extract was washed with brine and dried over anhydrous Na_2SO_4 and filtered. The solvent was removed under reduced pressure to afford *p*-bis(diisopropylaminomethyl)benzene (865 mg, 94.5% yield) as an off-white solid. ^{1}H NMR (500 MHz, D_2O DCl) δ 7.55 (s, 4H), 4.37 (s, 4H), 3.81 – 3.76 (m, 4H), 1.40 (d, J = 6.7 Hz, 12H), 1.34 (d, J = 6.6 Hz, 12H). ^{13}C NMR (101 MHz, $CDCl_3$) δ 136.0, 127.5, 48.6, 47.6, 20.8. HRMS-ESI: m/z calculated for [$C_{20}H_{36}N_2$] 304.287; found 305.296 [M + H].

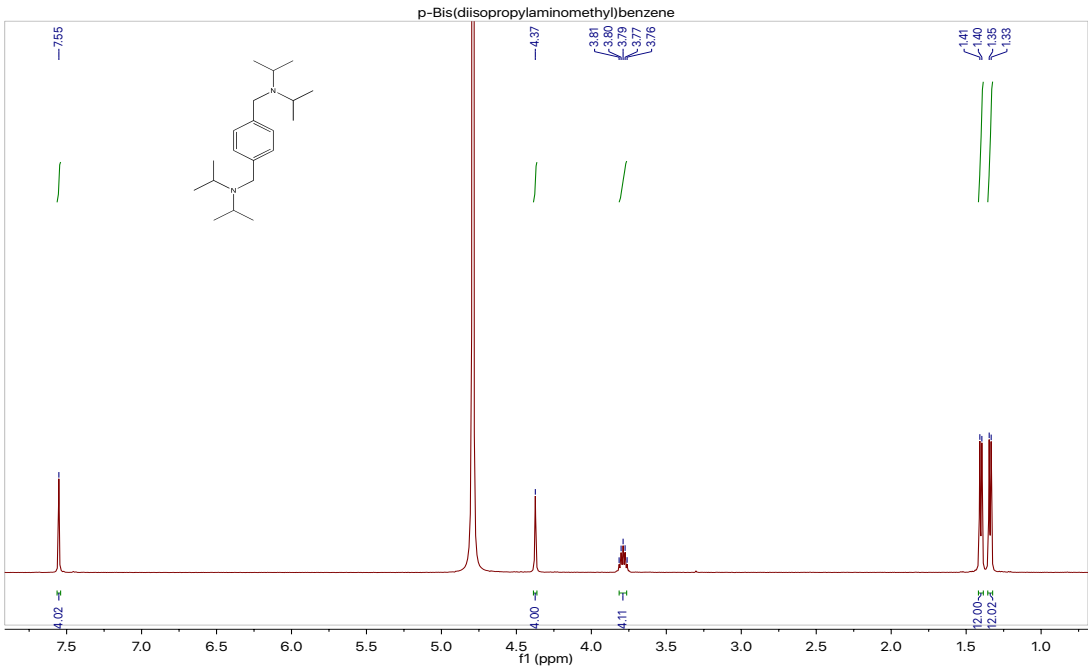

Figure 4.16 ^{1}H NMR (500 MHz, D_2O DCl) spectrum of *p*-Bis(diisopropylaminomethyl)-benzene.

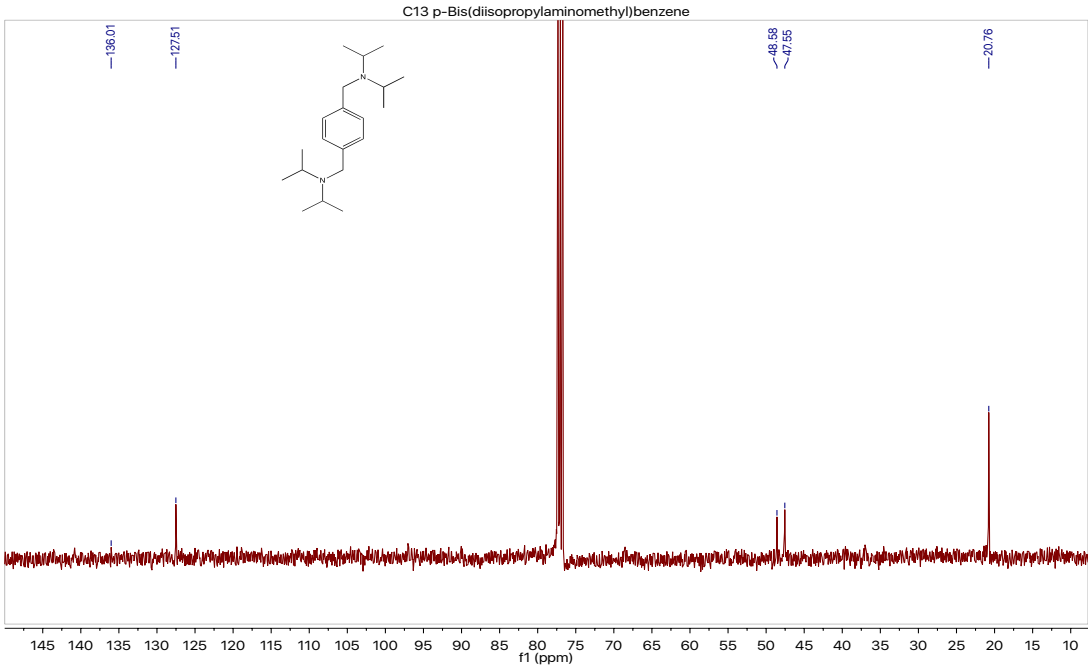

Figure 4.17 ^{13}C NMR (101 MHz, $CDCl_3$) spectrum of *p*-bis(diisopropylaminomethyl-benzene.

Synthesis of 3,5-diisopropoxybenzyl azide.

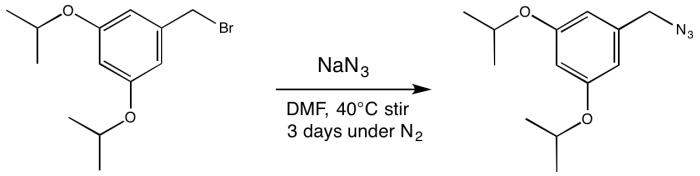

In a 250 mL reaction flask, 3,5-diisopropoxybenzyl bromide (1.08 g, 3.77 mmol) was dissolved in DMF (30 mL) and sodium azide (0.378 g, 5.80 mmol) was added. The solution was heated to 40 °C and allowed to stir under nitrogen for 3 days. The solution was diluted with ethyl acetate (100 mL) and washed with copious amounts of water and brine. The extract was dried over anhydrous $MgSO_4$ and filtered. The solvent was removed by reduced pressure to almost dryness, and the residue was diluted with dichloromethane (10 mL) and flushed through a silica plug to remove any residual DMF. The solvent was removed by reduced pressure to afford 3,5-diisopropoxybenzyl azide (0.939 g, 99.8 % yield) as an oil. ^{1}H NMR (400 MHz, $CDCl_3$) δ 6.41 (d, J = 2.2 Hz, 2H), 6.39 (t, J = 2.3 Hz, 1H), 4.55 – 4.48 (m, 2H), 4.23 (s, 2H), 1.32 (d, J = 6.1 Hz, 12H). ^{13}C NMR (101 MHz, $CDCl_3$) δ 159.4, 137.4, 107.7, 103.5, 69.9, 54.9, 22.0. HRMS-ESI: m/z calculated for [$C_{13}H_{19}N_3O_2$] 249.147; found 207.138 [M – N_3].

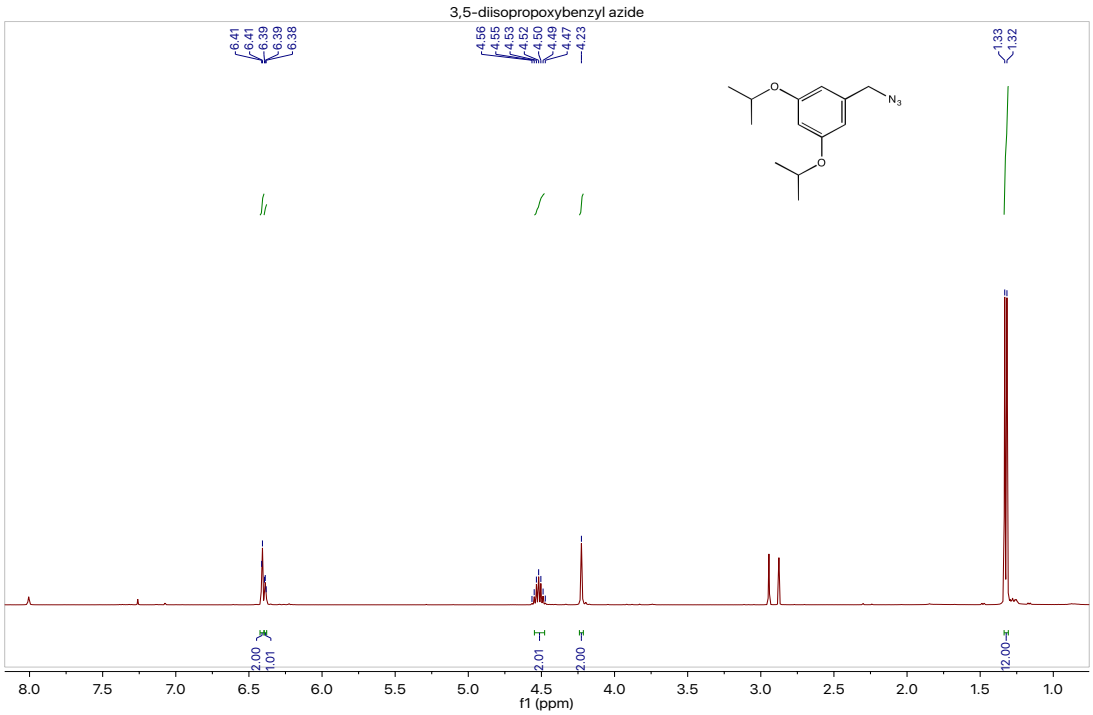

Figure 4.18 ^{1}H NMR (400 MHz, $CDCl_3$) spectrum of 3,5-diisopropoxybenzyl azide.

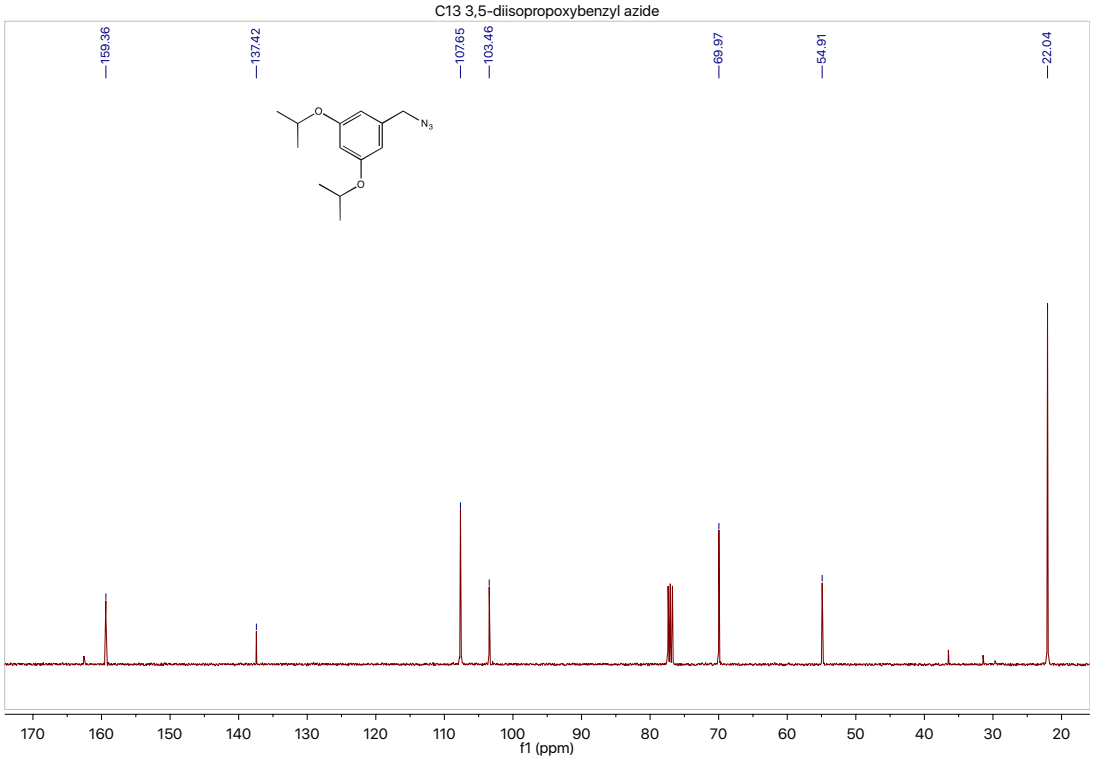

Figure 4.19 ^{13}C NMR (101 MHz, $CDCl_3$) spectrum of 3,5-diisopropoxybenzyl azide.

Synthesis of 1-(3,5-diisopropoxybenzyl)-4-(4-((diisopropylamino)methyl)-benzyloxymethyl)-1,2,3-triazole.

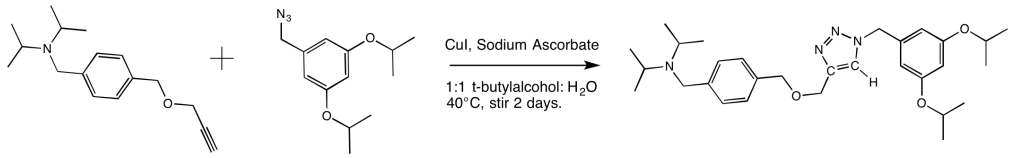

In a scintillation vial, 3,5-diisopropoxybenzyl azide (169 mg, 0.677 mmol), 4-((diisopropylamino)methyl)benzyl propargyl ether (159 mg, 0.613 mmol), CuI (30.8 mg 0.162 mmol), sodium ascorbate (48.8 mg, 0.246 mmol) was added to a 1:1 t-butyl alcohol:water (5 mL) solution. The suspension was heated to 40 °C and allowed to stir for 2 d. The solution was diluted with ethyl acetate and washed with water and brine. The solvent was dried over anhydrous $MgSO_4$ and filtered. The solvent was removed by reduced pressure to almost dryness, and the crude residue was purified by column chromatography (SiO_2, 5% methanol in dichloromethane) to provide 1-(3,5-diisopropoxybenzyl)-4-(4-((diisopropylamino)methyl)benzyloxymethyl)-1,2,3-triazole (88 mg, 28 % yield) as light tan oil. ^{1}H NMR (500 MHz, $CDCl_3$) δ 7.48 (s, 1H), 7.34 (d, *J* = 7.9 Hz, 2H), 7.24 (d, *J* = 7.9 Hz, 2H), 6.38 (t, *J* = 2.2 Hz, 1H), 6.35 (d, *J* = 2.3 Hz, 2H), 5.39 (s, 2H), 4.65 (s, 2H), 4.54 (s, 2H), 4.49 – 4.45 (m, 2H), 3.62 (s, 2H), 3.00 (p, *J* = 6.6 Hz, 2H), 1.29 (d, *J* = 6.1 Hz, 12H), 1.00 (d, *J* = 6.7 Hz, 12H). ^{13}C NMR (126 MHz, $CDCl_3$) δ 159.7, 145.8, 142.9, 136.6, 135.6, 128.0, 127.9, 122.5, 107.7, 103.6, 72.6, 70.1, 63.7, 54.4, 48.8, 47.9, 22.1, 20.8. HRMS-ESI: m/z calculated for [$C_{30}H_{44}N_4O_3$] 508.341; found 509.349 [M + H].

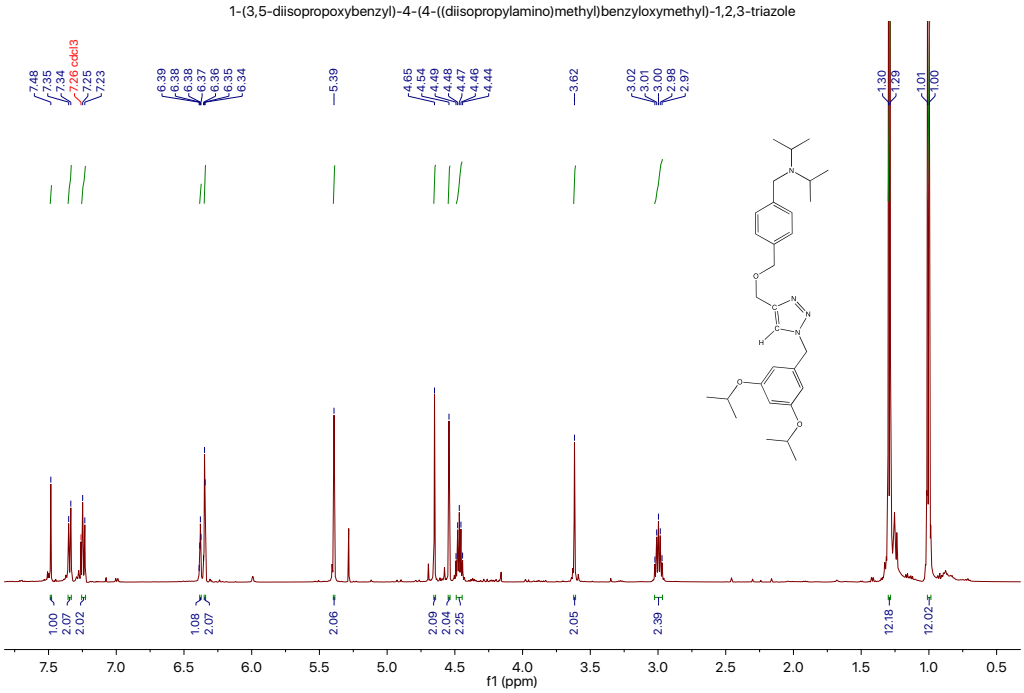

Figure 4.20 ^{1}H NMR (500 MHz, $CDCl_3$) spectrum of 1-(3,5-diisopropoxybenzyl)-4-(4-((diisopropylamino)methyl)benzyloxymethyl)-1,2,3-triazole.

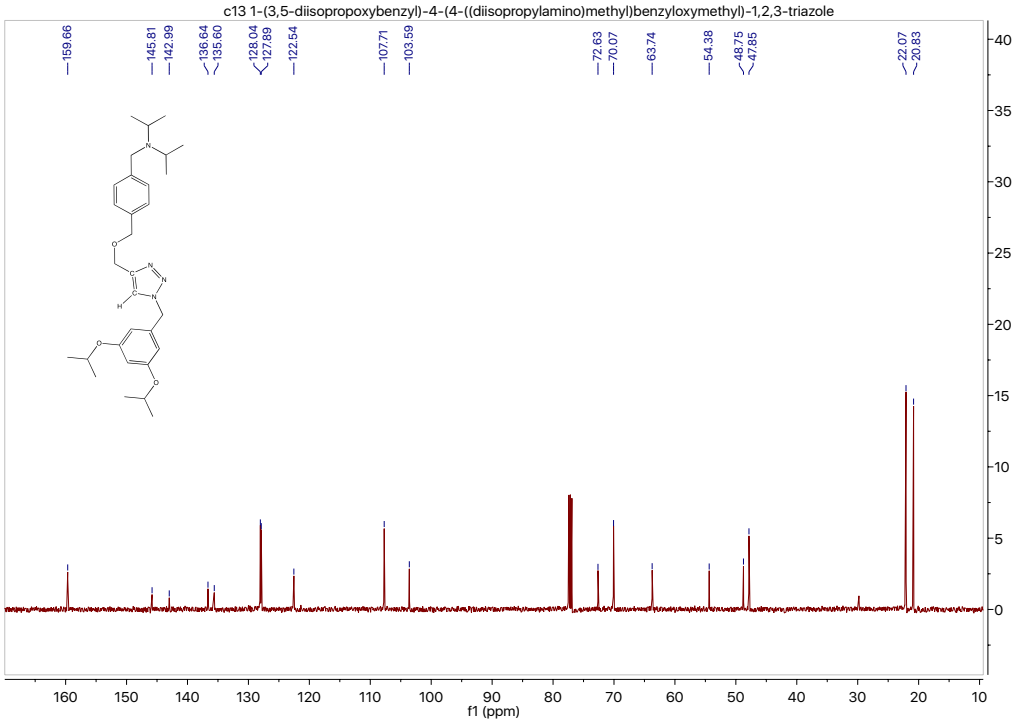

Figure 4.21 ^{13}C NMR (126 MHz, $CDCl_3$) spectrum of 1-(3,5-diisopropoxybenzyl)-4-(4-((diisopropylamino)methyl)benzyloxymethyl)-1,2,3-triazole.

^{1}H-NMR stability study of (*p*-Bis(isopropylaminomethyl)benzene).

The equilibrium constant of compound bis-isopropyl **4.3c** with cucurbit[7]uril was determined by analyzing the competitive binding of bis-isopropyl **4.3c** compared to that of the reference compound $(Me)_3SiCH_2NH_2$ (TMSMA) **4.5e** using ^{1}H-NMR spectroscopy (500 MHz). The stability constant of the 1:1 adduct of CB[7] and silane **4.5e** is $K_a = (8.88 \pm 1.41) \times 10^8$ M^{-1}. The procedure followed was developed by Mock and Isaacs.[16] Three solutions of 0.125 mM CB[7], 3.00 mM silane **4.5e**, and 0.300 mM bis-isopropyl **4.3c** were prepared in 50.0 mM $Na(O_2CCD_3)$-buffered D_2O (pD = 4.45). Silane **4.5e** demonstrated slow exchange kinetics on the NMR time scale resulting in clear peaks for bound and unbound silane **4.5e** –0.7 and 0.0 ppm respectively. From the average of ratios of the bound and unbound silane **4.5e** of the three solutions (which was determined with a ±6.2% std. dev.), we determined the binding constant of bis-isopropyl **4.3c**:CB[7] (1:1) to be $K_a = (6.03 \pm 1.21) \times 10^9$ M^{-1}. Error analysis was carried out according to literature.[16]

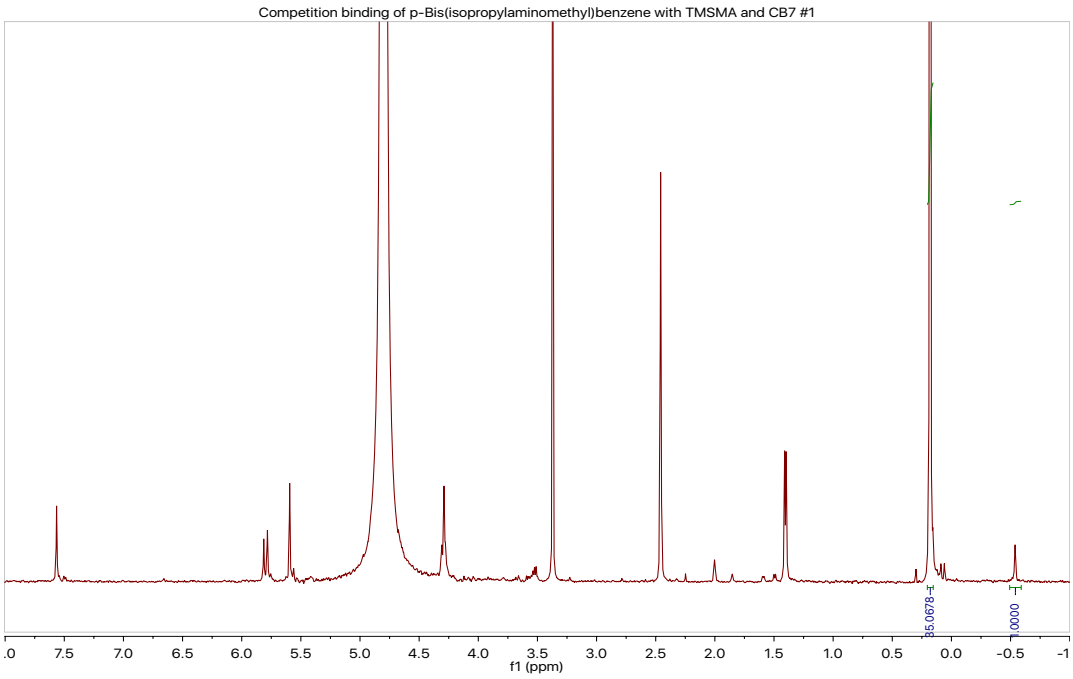

Figure 4.22 ^{1}H NMR (500 MHz, Na(O_2CCD_3)-buffered D_2O (pD = 4.45)) spectrum 1 of competitive binding of **4.3c**, **4.5e**, and CB[7].

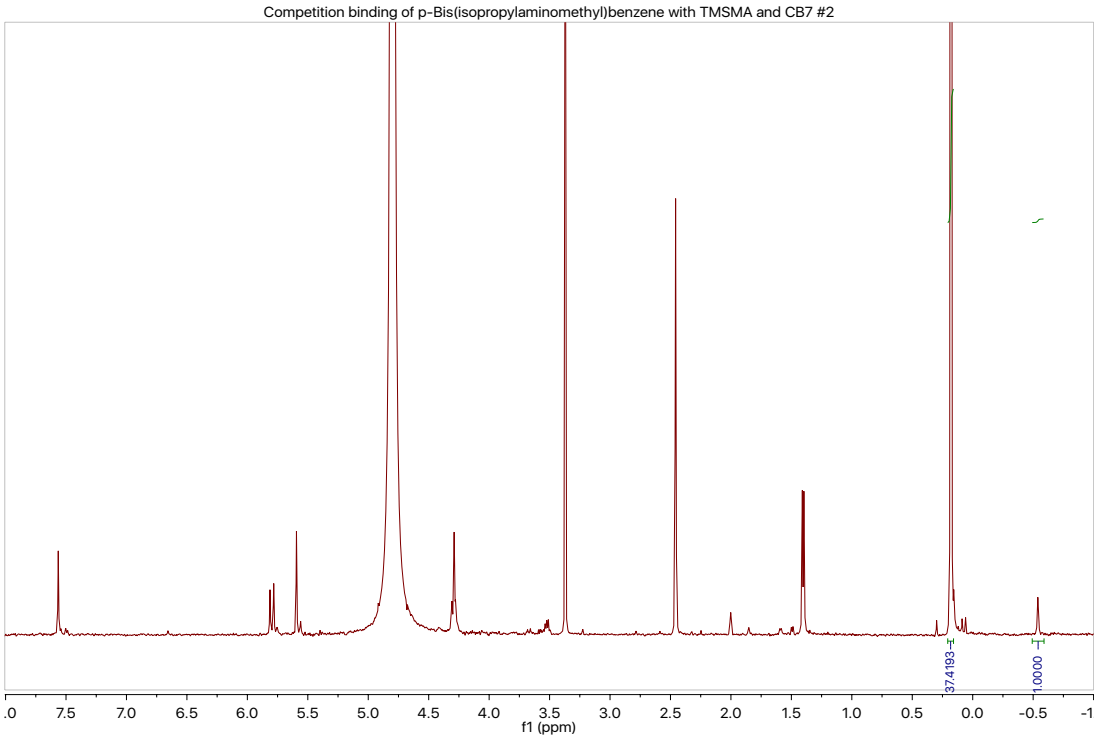

Figure 4.23 ^{1}H NMR (500 MHz, Na(O_2CCD_3)-buffered D_2O (pD = 4.45)) spectrum 2 of competitive binding of **4.3c**, **4.5e**, and CB[7].

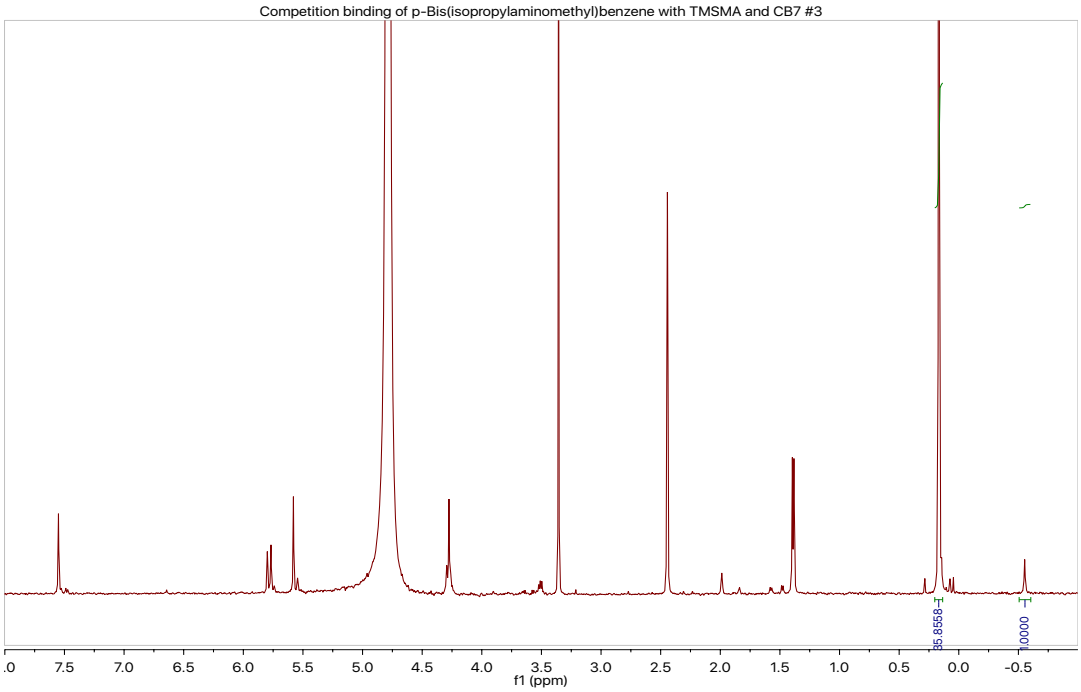

Figure 4.24 ^{1}H NMR (500 MHz, Na(O_2CCD_3)-buffered D_2O (pD = 4.45)) spectrum 3 of competitive binding of **4.3c**, **4.5e**, and CB[7].

^{1}H-NMR stability study of (*p*-Bis(diisopropylaminomethyl)benzene).

The equilibrium constant of compound bis-diisopropyl **4.4d** with cucurbit[7]uril was determined by analyzing the competitive binding of bis-diisopropyl **4.4d** compared to that of the reference compound $(Me)_3SiCH_2NH_2$ (TMSMA) **4.5e** using ^{1}H-NMR spectroscopy (500 MHz). The stability constant of the 1:1 adduct of CB[7] and silane **4.5e** is $K_a = (8.88 \pm 1.41) \times 10^8$ M^{-1}. The procedure followed was developed by Mock and Isaacs.[16] Three solutions of 0.125 mM CB[7], 3.00 mM silane **4.5e**, and 0.300 mM bis-diisopropyl **4.4d** were prepared in 50.0 mM $Na(O_2CCD_3)$-buffered D_2O (pD = 4.45). Silane **4.5e** demonstrated slow exchange kinetics on the NMR time scale resulting in clear peaks for bound and unbound silane **4.5e** –0.7 and 0.0 ppm respectively. From the average of ratios of the bound and unbound silane **4.5e** of the three solutions (which was determined with a ±5.4% std. dev.), we determined the binding constant of bis-diisopropyl **4.4d**:CB[7] (1:1) to be $K_a = (4.83 \pm 0.93) \times 10^9$ M^{-1}. Error analysis was carried out according to literature.[16]

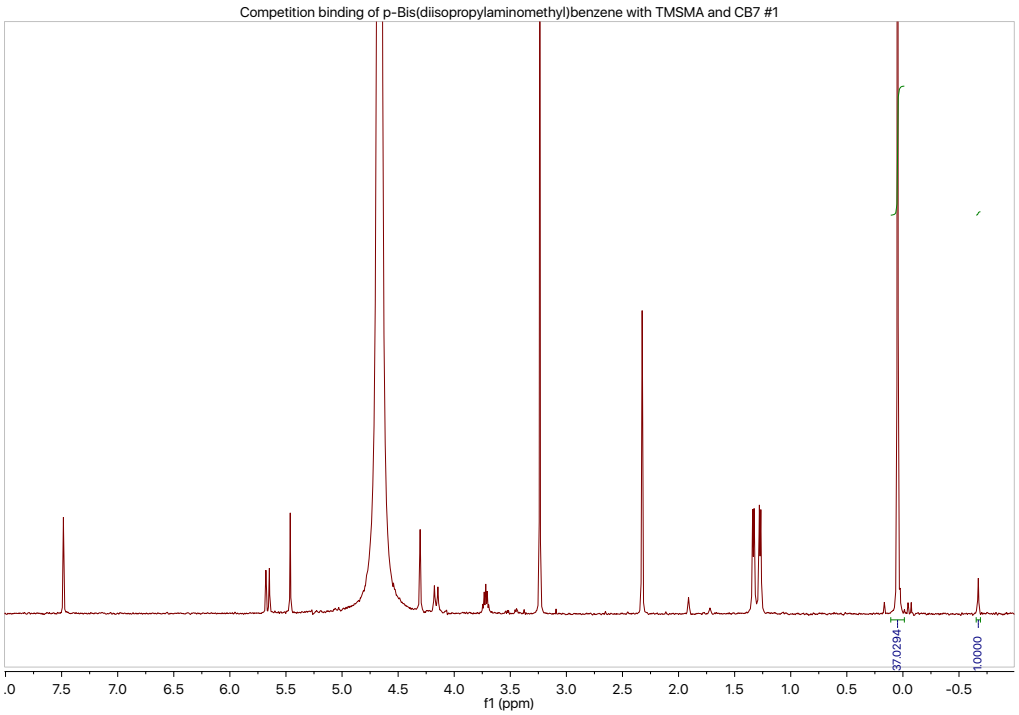

Figure 4.25 ^{1}H NMR (500 MHz, Na(O_2CCD_3)-buffered D_2O (pD = 4.45)) spectrum 1 of competitive binding of **4.4d**, **4.5e**, and CB[7].

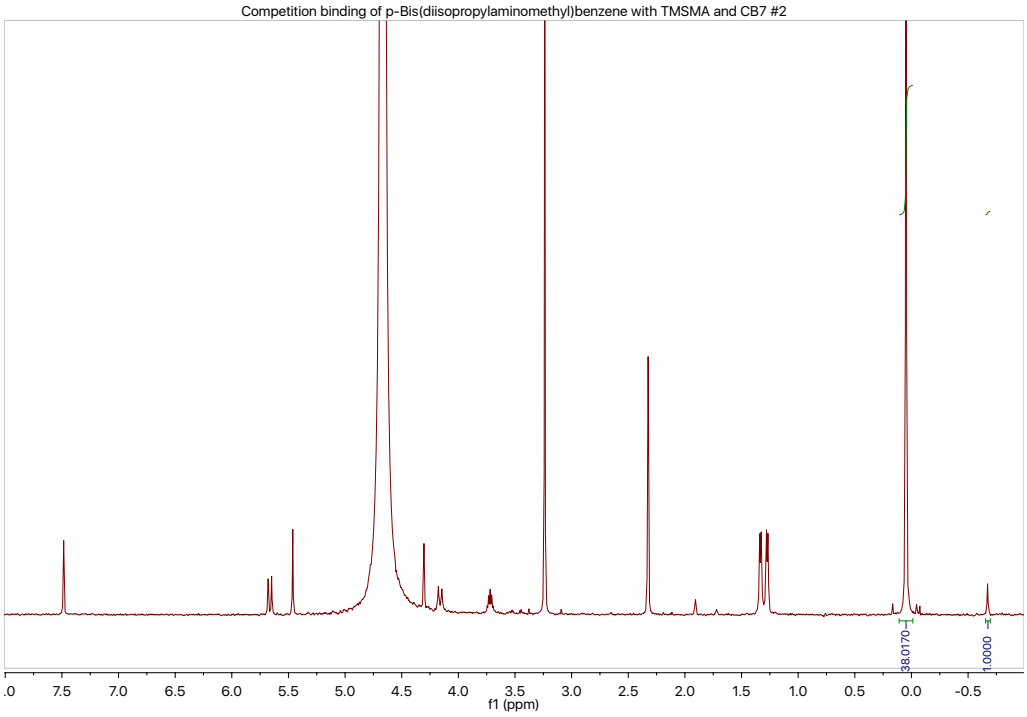

Figure 4.26 ^{1}H NMR (500 MHz, Na(O_2CCD_3)-buffered D_2O (pD = 4.45)) spectrum 2 of competitive binding of **4.4d**, **4.5e**, and CB[7].

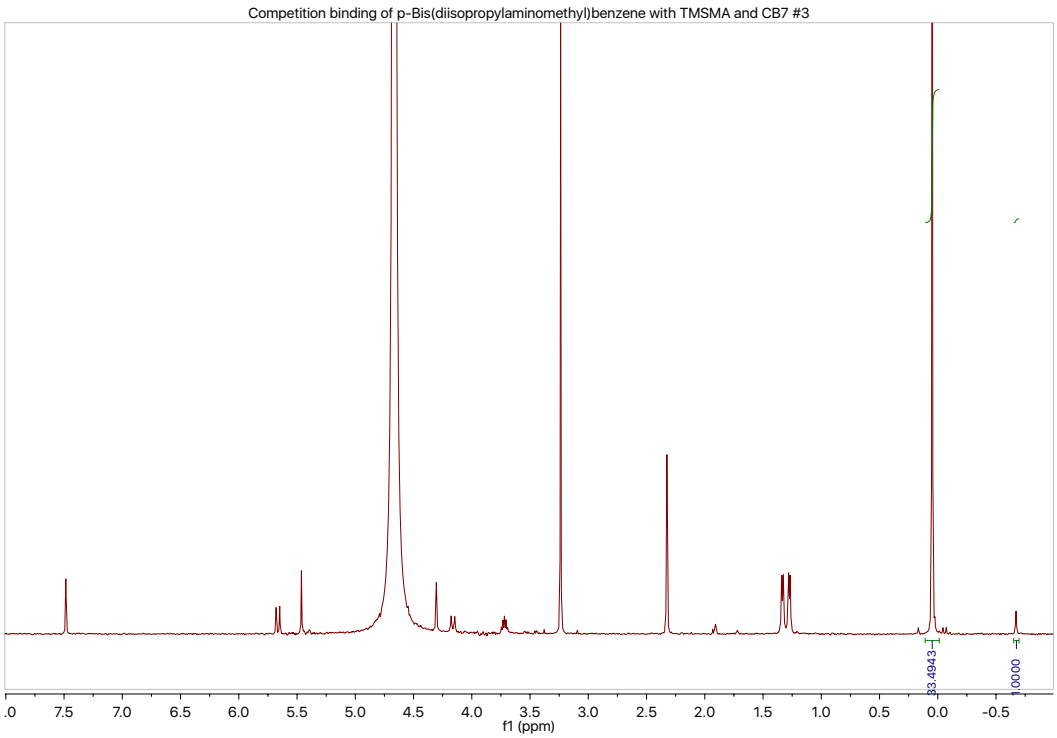

Figure 4.27 ^{1}H NMR (500 MHz, Na(O_2CCD_3)-buffered D_2O (pD = 4.45)) spectrum 3 of competitive binding of **4.4d**, **4.5e**, and CB[7].

Procedure for ^{1}H NMR docking studies.

Synthesis of CB[7]. CB[7] was synthesized using the same procedure from chapter two.

Stock solution of CB[7]. A CB[7] stock solution (4.0 mM) was prepared by dissolving CB[7] (23 mg, 0.020 mmol) in D_2O (5 mL).

Stock solution of 1-(3,5-diisopropoxybenzyl)-4-(4-((diisopropylamino)methyl)-benzyloxymethyl)-1,2,3-triazole. A 1-(3,5-diisopropoxybenzyl)-4-(4-((diisopropyl-amino)methyl)-benzyloxymethyl)-1,2,3-triazole stock solution (4.0 mM) was prepared by dissolving 1-(3,5-diisopropoxybenzyl)-4-(4-((diisopropylamino)methyl)benzyloxy-

methyl)-1,2,3-triazole (10 mg, 0.020 mmol) in D_2O (5 mL) and DCl was added until pD = 4.

Stock solution of *p*-bis(isopropylaminomethyl) benzene. A *p*-bis(isopropylaminomethyl) benzene stock solution (4.0 mM) was prepared by dissolving *p*-bis(isopropylaminomethyl) benzene (4.5 mg, 0.020 mmol) in D_2O (5 mL) and DCl was added until pD = 4.0.

Stock solution of *p*-bis(diisopropylaminomethyl) benzene. A *p*-bis(diisopropylaminomethyl) benzene stock solution (4.0 mM) was prepared by dissolving *p*-bis(diisopropylaminomethyl) benzene (6.1 mg, 0.020 mmol) in D_2O (5 mL) and DCl was added until pD = 4.0.

Stock solution of Adamantylammonium An adamantylammonium stock solution (16 mM) was prepared by dissolving 1-adamantylamine (12 mg, 0.080 mmol) in D_2O (5 mL) and DCl was added until pD = 4. A portion of the stock solution (50 μL) was taken in a 5 mL volumetric flask and diluted up to 5 mL with D_2O to prepare 4.0 mM solution.

Complexation measurement of 1-(3,5-diisopropoxybenzyl)-4-(4-((diisopropyl-amino)methyl)benzyloxymethyl)-1,2,3-triazole with CB[7]. To an NMR tube, portions of 1-(3,5-diisopropoxybenzyl)-4-(4-((diisopropyl-amino)methyl)benzyloxy-methyl)-1,2,3-triazole stock solution (4.0 mM, 250 μL) and of CB[7] stock solution (4.0 mM, 250 μL) were added respectively and mixed well. For the measurement of NMR

spectroscopy, after the solutions were added to the NMR tube, measurements were carried out on a 500 MHz NMR instrument at r.t. at times 1 min to 48 h (Figure 4.7).

Decomplexation measurement of 1-(3,5-diisopropoxybenzyl)-4-(4-((diisopropyl-amino)methyl)benzyloxymethyl)-1,2,3-triazole and CB[7] with adamantly-ammonium. To a vial, portions of 1-(3,5-diisopropoxybenzyl)-4-(4-((diisopropyl-amino)methyl)benzyloxy-methyl)-1,2,3-triazole stock solution (4.0 mM, 250 μL) and of CB[7] stock solution (4.0 mM, 250 μL) were added respectively and mixed well to allow for complexation. The CB[7] complexed solution (500 μL) was added to an NMR tube and 0.5 eq of adamantylammonium was (125 μL) added. A second NMR tube was prepared using the same method with the CB[7] complexed solution and 1 eq of adamantylammonium. For the measurement of NMR spectroscopy, after the solutions were added to the NMR tube, measurements were carried out on a 500 MHz NMR instrument at r.t. (Figure 4.8).

Complexation measurement of *p*-bis(isopropylaminomethyl) benzene with CB[7]. To an NMR tube, portions of *p*-bis(isopropylaminomethyl) benzene stock solution (4.0 mM, 250 μL) and of CB[7] stock solution (4.0 mM, 250 μL) were added 1:1 respectively and mixed well. To a second NMR tube, portions of *p*-bis(isopropylaminomethyl) benzene stock solution (200 μL) and of CB[7] stock solution (400 μL) were added 1:2 respectively and mixed well. For the measurement of NMR spectroscopy, after the solutions were added to the NMR tube, measurements were carried out on a 500 MHz NMR instrument at r.t. (Figure 4.9).

Complexation measurement of *p*-bis(diisopropylaminomethyl) benzene with CB[7]. To an NMR tube, portions of *p*-bis(diisopropylaminomethyl) benzene stock solution (4.0 mM, 250 μL) and of CB[7] stock solution (4.0 mM, 250 μL) were added 1:1 respectively and mixed well. To a second NMR tube, portions of *p*-bis(diisopropylaminomethyl) benzene stock solution (200 μL) and of CB[7] stock solution (400 μL) were added 1:2 respectively and mixed well. For the measurement of NMR spectroscopy, after the solutions were added to the NMR tube, measurements were carried out on a 500 MHz NMR instrument at r.t. (Figure 4.10).

Decomplexation measurement of *p*-bis(diisopropylaminomethyl) benzene and CB[7] with adamantylammonium. To a vial, portions of *p*-bis(diisopropylaminomethyl) benzene stock solution (4.0 mM, 250 μL) and of CB[7] stock solution (4.0 mM, 250 μL) were added respectively and mixed well to allow for complexation. The CB[7] complexed solution (500 μL) was added to an NMR tube and 0.5 eq of adamantylammonium was (125 μL) added. A second NMR tube was prepared using the same method with the CB[7] complexed solution and 1 eq of adamantlyammonium. For the measurement of NMR spectroscopy, after the solutions were added to the NMR tube, measurements were carried out on a 500 MHz NMR instrument at r.t. (Figure 4.11).

4.8 References

1. Bajaj, A.; Miranda, O.R.; Kim, I.B.; Phillips, R.L.; Jerry, D.J.; Bunz, U.H.F.; Rotello, V.M. *Proc. Natl. Acad. Sci. USA.* **2009**, *106*, 10912–10916. (b) Umali, A.P.; Anslyn, E.V. *Curr. Opin. Chem. Biol.* **2010**, *14*, 685–692.; (b) ; (c) Bajaj, A.; Miranda, O.R.; Phillips, R.; Kim, I.B.; Jerry, D.J.; Bunz, U.H.F.; Rotello, V.M. *J. Am. Chem. Soc.* **2010**, *132*, 1018–1022.; (d) El-Boubbou,; Zhu, K. D.C.; Vasileiou, C.; Borhan, B.; Prosperi, D.; Li, W.; Huang, X.F. *J. Am. Chem. Soc.* **2010**, *132*, 4490–4499.; (e) Bajaj, A.; Rana, S.; Miranda, O.R.; Yawe, J C.; Jerry, D.J.; Bunz, U.H.F.; Rotello, V.M. *Chem. Sci.* **2010**, *1*, 134–138.; (f) Scott, M.D.; Dutta, R.; Haldar, M.K.; Guo, B.; Friesner, D.L.; Mallik, S. *Anal. Chem.* **2012**, *84*, 17–20.
2. Skvara, H.; Teban, L.; Fiebiger, M.; Binder, M.; Kittler, H. *Arch. Dermatol.* **2005**, *141*, 155–160.
3. Gao XH, Cui YY, Levenson RM, Chung LWK, Nie SM. *Nat. Biotechnol.* **2004**, *22*, 969–976.
4. (a) Wiskur, S. L.; Floriano, P. N., Anslyn, E. V.; McDevitt, J. T. *Angew. Chem. Int. Ed.* **2003**, *42*, 2070-2072.; (b) Lavigne, J. J.; Savoy, S. M.; Clevenger, M. B.; Ritchie, J. E.; McDoniel, B.; Yoo, S. J.; Anslyn, E. V.; McDevitt, J. T.; Shear, J. B.; Neikirk, D. P. *J. Am. Chem. Soc.* **1998**, *120*, 6429-6430.; (c) Curey, T. E.; Goodey, A.; Tsao, A.; Lavigne, J. J.; Sohn, Y.; McDevitt, J. T.; Anslyn, E. V.; Neikirk, D.; Shear, J. B. *Anal. Biochem.* **2001**, *293*, 178-184.; (d) McCleskey, S. C.; Griffin, M. J.; Schneider, S. E.; McDevitt, J. T.; Anslyn, E. V. *J. Am. Chem. Soc.* **2003**, *125*, 1114-1115.
5. Greene, N. T.; Shimizu, K. D. *J. Am. Chem. Soc.* **2005**, *127*, 5695-5700.

6. Peng, G.; Tisch, U.; Adams, O. *Nat. Nanotech.* **2009**, *4*, 669–673.

7. Folmer-Andersen, J. F.; Kitamura, M.; Anslyn, E. V. *J. Am. Chem. Soc.* **2006**, *128*, 5652–5653.

8. De. M.; Rana, S.; Akpinar, H. *Nat. Chem.* **2009**, *1*, 461–465.

9. Wright, A. T.; Zhong, Z. L.; Anslyn, E. V. *Angew. Chem. Intl. Ed.* **2005**, *44*, 5679–5682.

10. Liu, S.; Ruspic, C.; Mukhopadhyay, P.; Chakrabarti, S.; Zavalij, P. Y.; Isaacs, L. *J. Am. Chem. Soc.* **2005**, *127*, 15959-15967

11. Barrow, S. J.; Kasera, S.; Rowland, M. J.; Barrio, J.; Scherman, O. R. *Chem. Rev.* **2015**, *115*, 12320-12406.

12. Kolb, H. C.; Finn, M. G.; Sharpless, K. B. *Angew. Chem., Int. Ed.* **2001**, *40*, 2004.

13. (a) Miljanić, O. Š.; . Dichtel, W. R; Mortezaei, S.; Stoddart, J. F. *Org. Lett.* **2006**, *8*, 4835.; (b) Dichtel, W. R.; Miljanić, O. Š.; Spruell, J. M.; Heath, J. R.; Stoddart, J. F. *J. Am. Chem. Soc.* **2006**, *128*, 10388-10390.; (c) Tuncel, D.; Özsar, O.; Tiftik, H. B.; Salih, B. *Chem. Commun.* **2007**, 1369-1371.; (d) Aprahamian, I.; Miljanić, O. Š.; Dichtel, W. R.; Isoda, K.; Yasuda, T.; Kato, T.; Stoddart, J. F. *Bull. Chem. Soc. Jpn.* **2007**, *80*, 1856-1869.; (e) Miljanić, O. Š.; Dichtel, W. R.; Khan, S. I.; Mortezaei, S.; Heath, J. R.; Stoddart, J. F. *J. Am. Chem. Soc.* **2007,** *129*, 8236-8246.; (f) Miljanić, O. Š.; Dichtel, W. R.; Aprahamian, I.; Rohde, R. D.; Agnew, H. D.; Heath, J. R.; Stoddart, J. F. *QSAR Comb. Sci.* **2007**, *26*, 1165-1174.; (g) Aprahamian, I.; Dichtel, W. R.; Ikeda, T.; Heath, J. R.; Stoddart, J. F. *Org. Lett.* **2007**, *9*, 1287-1290.

14. (a) Braunschweig, A. B.; Dichtel, W. R.; Miljanić, O. Š.; Olson, M. A.; Spruell, J. M.; Khan, S. I.; Heath, J. R.; Stoddart, J. F. *Chem. Asian J.* **2007**, *2*, 634.;

(b) Tuncel, D.; Katterle, M. *Chem. Eur. J.* **2008**, *14*, 41140-4116.; (c) Wang, J.-Y.; Han, J.-M.; Yan, J.; Ma, Y.; Pei, J. *Chem. Eur. J.* **2009**, *15*, 3585-3594.; (d) Hänni, K. D.; Leigh, D. A. *Chem. Soc. Rev.* **2010**, *39*, 1240-1251.; (e) Tuncel, D.; Ünal, Ö.; Artar, M. *Isr. J. Chem.* **2011**, *51*, 525-532.; (f) Barin, G.; Coskun, A.; Fouda, M. M. G.; Stoddart, J. F. *ChemPlusChem.* **2012**, *77*, 159-185.; (g) Pasini, D. *Molecules* **2013**, *18*, 9512-9530. (h) Cao, Z.-Q.; Miao, Q.; Zhang, Q.; Li, H.; Qui, D.-H.; Tian, H. *Chem. Commun.* **2015**, *51*, 4973-4976.

15. (a) Sindelar, V.; Moon, K.; Kaifer, A. E. *Org. Lett.* **2004**, *6*, 2665-2668.; (b) Wang, R.; Yuan, L.; Macartney, D. H. *Chem. Commun.* **2006**, 2908-2910.; (c) Wyman, I. W.; Macartney, D. H. *Org. Biomol. Chem.* **2010**, *8*, 253-260.; (d) Logsdon, L. A.; Schardon, C. L.; Ramalingam, V.; Kwee, S. K.; Urbach, A. R. *J. Am. Chem. Soc.* **2011**, *133*, 17087-17092.; (e) Li, S.; Wyman, I. W.; Wang, C.; Wang, Y.; Macartney, D. H.; Wang, R. *J. Org. Chem.* **2016**, *81*, 9494-9498.; (f) Ling, X.; Saretz, S.; Xiao, L.; Francescon, J.; Masson, E. *Chem. Sci.* **2016**, *7*, 3569-3573.

16. Liu, S.; Ruspic, C.; Mukhopadhyay, P.; Chakrabarti, S.; Zavalij, P. Y.; Isaacs, L. *J. Am. Chem. Soc.* **2005**, *127*, 15959-15967.